Characterization of genes affecting the adaptation of *Mucor lusitanicus* for environmental changes

PhD Thesis

Sandugash Ibragimova

Supervisors:
Prof. Dr. Tamás Papp
Dr. Gábor Nagy

Doctoral School of Biology

Department of Microbiology
Faculty of Science and Informatics
University of Szeged

Szeged
2024

TABLE OF CONTENTS

LIST OF ABBREVIATIONS

AmB	Amphotericin B
Arf	ADP-ribosylation factor
ATCC	American Type Culture Collection
Cas9	CRISPR associated protein 9
cAMP	Cyclic adenosine 3',5'-monophosphate
CBS	Centraalbureau voor Schimmelcultures, Utrecht, Netherlands
CE2	Control element 2
Cer	Ceramide
CFW	Calcofluor White
CnaA	Calcineurin catalytic A subunit
CnaB	Calcineurin catalytic B subunit
CnaC	Calcineurin catalytic C subunit
CnbR	Calcineurin regulatory R subunit
CR	Congo Red
CRISPR	Clustered, regularly interspaced, short palindromic repeat
crRNA	CRISPR RNA
CTA	Carboxy-terminal transactivation domain
DBD	DNA binding domain
DEGs	Differentially expressed genes
DG	Diglyceride
DHA1	Drug:H^+ antiporter 1
DHA2	Drug:H^+ antiporter 2
Fen2	Pantothenate:H+ symporter
FLU	Fluconazole
GlcCer	Glucosylceramide
gRNA	Guide RNA
HDR	Homology driven repair
HRA	Heptad repeats A
HRB	Heptad repeats B
HSE	Heat shock elements
Hsf1	Heat shock factor protein 1
Hsf2	Heat shock factor protein 2

ISA	Isavuconazole
ITR	Itraconazole
KET	Ketoconazole
LB	Lysogeny broth
LZ	Leucine zipper
MEA	Malt extract agar
MFS	Major facilitator superfamily
MIC	Minimal inhibitory concentration
MIP2C	Mannosyl-di-(inositolphosphoryl)-ceramide
MOPS	3-(N-morpholino)-propanesulfonic acid
NCBI	National Center for Biotechnology Information
NTA	N-terminal transactivation domain
NUDIX	Nucleoside diphosphate linked moiety X
PAM	Protospacer adjacent motif
PBS	Phosphate buffered saline
PC	Phosphatidylcholine
PE	Phosphatidylethanolamine
PEG	Polyethylene glycol
Pho84	Inorganic phosphate uptake porter
PI	Phosphatidylinositol
PKA	Protein kinase A
PKAC	Catalytic subunit of protein kinase A
PKAR	Regulatory subunit of protein kinase A
PMC	PEG-sorbitol-MOPS-calcium chloride buffer
POS	Posaconazole
PS	Phosphatidylserine
Qdr2	Quinidine resistance protein
RAV	Ravuconazole
RD	Regulatory domain
SMC	Sorbitol-MOPS-calcium chloride buffer
SZMC	Szeged Microbiology Collection, Hungary
TAE	Tris acetic acid-disodium EDTA buffer
TG	Triglycerides

TMS	Transmembrane spans
TRIS	Tris (hydroxymethyl) aminomethane
TX100	Triton X-100
VOR	Voriconazole
YEG	Yeast extract-glucose medium
YNB	Yeast nitrogen base
YPD	Yeast extract-peptone-dextrose medium
YPG	Yeast extract-peptone-glucose broth

Mucor lusitanicus strains, genes, and encoded proteins

MS12	*M. lusitanicus* auxotrophic mutant (*leuA*- and *pyrG*-)
MS12+*pyrG*	MS12 containing a functional *pyrG* complement
MS12+*Δhsf1*	*hsf1* disruption mutant
MS12+*Δhsf2*	*hsf2* disruption mutant
MS12+*Δqdr2a*	*qdr2a* disruption mutant
MS12+*Δqdr2b*	*qdr2b* disruption mutant
MS12+*Δqdr2c*	*qdr2c* disruption mutant
MS12+*Δqdr2d*	*qdr2d* disruption mutant
pyrG	Gene encoding orotidine-5-monophosphate decarboxylase
fen2	Gene encoding pantothenate:H+ symporter
hsf1	Gene encoding heat shock factor protein 1
hsf2	Gene encoding heat shock factor protein 2
nudix	Gene encoding nucleoside diphosphate-linked moiety X
pho84	Gene encoding inorganic phosphate (Pi) uptake porter
qdr2a	Gene encoding quinidine resistance protein 2a
qdr2b	Gene encoding quinidine resistance protein 2b
qdr2c	Gene encoding quinidine resistance protein 2c
qdr2d	Gene encoding quinidine resistance protein 2d

1. INTRODUCTION

1.1 General characterization of *Mucor lusitanicus*

Mucor lusitanicus (formerly known as – *M. circinelloides* f. *lusitanicus*) belongs to the Kingdom Fungi, Phylum Mucoromycota, Order Mucorales and the Family Mucoraceae (**Spatafora et al., 2016**). It is a ubiquitous saprotrophic fungus widely distributed in soil, decaying plant material and organic debris (**Richardson, 2009; Binder et al., 2018; Elkhateeb and Daba, 2022**). *M. lusitanicus* is a dimorphic fungus and exhibits hyphal growth in aerobic conditions or multi-budded yeast growth under anaerobic conditions with high hexose concentration (**Orlowski, 1991; Serrano et al., 2001; McIntyre et al., 2002; Wolff et al., 2002; Lübbehüsen et al., 2004**). Its complete genome of the size 36.6 Mb has been known and available since 2010 (**https://mycocosm.jgi.doe.gov/Mucci2/Mucci2.home.html**) (**Corrochano et al., 2016**). Life cycle of *M. lusitanicus* is shown in **Figure 1**.

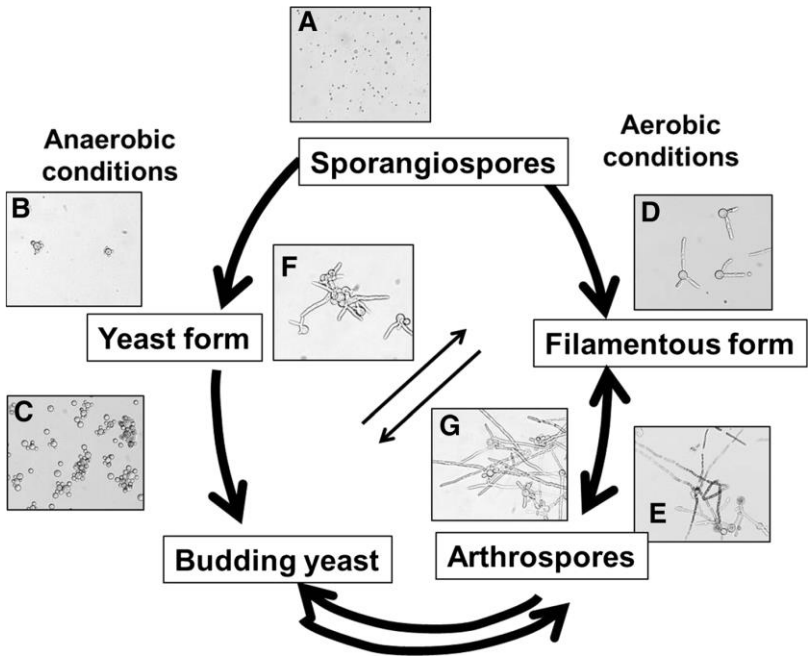

Figure 1. Anaerobic and aerobic stages of *Mucor lusitanicus* (Moriwaki-Takano et al., 2021). Sporangiospores (A) develop into a filamentous (D) or yeast form (B) under aerobic or anaerobic conditions, respectively. During the exponential growth phase mycelia are elongating from the filamentous form to arthrospores (E), while budding yeasts (C) are increasing. Changing the conditions of environment causes the dimorphic shift. Changing from anaerobic to aerobic condition triggers yeast to filamentous form (F) and opposite changing of gas atmosphere leads to yeast form from filamentous (G).

The asexual reproductive cycle is more preferred culture method to maintain this fungus under laboratory conditions because mycelia develop fast and sporangia contain multinucleate sporangiospores (**Navarro-Mendoza et al., 2019**). *M. lusitanicus* can produce three types of spores: zygospores, sporangiospores and arthrospores. Zygospores considering to be dormant are generated in the sexual life cycle by fusing hyphae of two opposite mating types designated as (+) and (-). Sporangiospores are multinucleate asexual spores involving in dissemination. They are produced within sporangia at the apices of aerial hyphae that formed from complex mycelia on solid substrate. Arthrospores are formed through hyphal fragmentation under unfavorable stress conditions or in submerged cultures after the exponential growth (**Orlowski, 1991; Botha and du Preez, 1999; McIntyre et al., 2002; Morin-Sardin et al., 2017; Patiño-Medina et al., 2019a; Walther et al., 2019**). Sporangiospores are produced in different sizes depending on the mating type variant. Strains with (-) mating type produce larger sporangiospores in a higher number than those with the (+) mating type. Larger sporangiospores were reported as more virulent than the smaller ones and can lyse mammalian macrophages (**Li et al., 2011; Muszewska et al., 2014)**.

M. lusitanicus also can act as a human and animal pathogen causing an opportunistic infection in immunocompromised patients known as mucormycosis (**Pérez-Arques et al., 2019**). The most important underlying conditions predisposing to mucormycosis are neutropenia, poorly controlled diabetes mellitus with hyperglycemia and ketoacidosis, organ transplantation, hematological diseases, treatment with corticosteroids, deferoxamine therapy in patients receiving hemodialysis, major trauma and burns, cancer, AIDS and currently COVID-19 **(Roden et al., 2005; Chayakulkeeree et al., 2006; Petrikkos et al., 2012; Ibrahim and Kontoyiannis, 2013; Watkins et al., 2018; Hussain et al., 2023)**. There are different forms of mucormycosis, i.e.: rhinocerebral, pulmonary, cutaneous, gastrointestinal, and disseminated infection (**Brown, 2005; Bulent Ertugrul and Arikan-Akdagli, 2014**). Despite the aggressive surgery, antifungal treatment and correction of risk factors, the overall mortality rate of mucormycosis remains high, ranging from 50% and up to 90% depending on the infection form and underlying condition of the patient. Angioinvasion, vessel thrombosis, and necrosis lead to a poor penetration of antifungal drugs to affected areas and a restricted access of phagocytic effector cells **(Ibrahim et al., 2005; Spellberg et al., 2005; Katragkou et al., 2014; Kennedy et al., 2016; Skiada et al., 2018; Hassan & Voigt, 2019; Jeong et al., 2019; Jestin et al., 2021; Muthu et al., 2021**).

Mucor and other mucormycosis causing fungi are inherently resistant to nearly all routinely used antifungal agents including most azoles (**Almyroudis et al., 2007; Drogari-Apiranthitou et al., 2012; Riley et al., 2016; Chang and Heitman, 2019**). Mucormycosis is difficult to cure due to less knowledge or poor understanding on host-fungus interactions, pathogenetic mechanisms of the infection, the role of specific virulence factors, and greater difficulties in early diagnosis (**Morace and Borghi, 2012; Katragkou et al., 2014**). Therefore, researchers investigate different virulence factors and genes of mucormycosis causing fungi to identify potential targets for the development of future antifungals (**Trieu et al., 2017; López-Fernández et al., 2018; Navarro-Mendoza et al., 2018; Lax et al., 2020**).

Development of molecular tools like plasmid transformation, protoplast formation, RNA interference induction, genetic complementation, directed mutagenesis, gene tagging, CRISPR-Cas9 system (**Nicolás et al., 2003; Trieu et al., 2015; Nagy et al., 2017; Trieu et al., 2017; Navarro-Mendoza et al., 2019**) has allowed to carry out genetic manipulation of *M. lusitanicus* to investigate response to light: carotene biosynthesis, phototropism, photoperiodism, etc. (**Navarro et al., 2001; Silva et al., 2006; Nicolás et al., 2008; Silva et al., 2008; Zhang et al., 2016**), RNA interference mechanisms (**Torres-Martínez & Ruiz-Vázquez, 2016**), virulence (**Trieu et al., 2017; Navarro-Mendoza et al., 2018**), lipid production (**Vicente et al., 2009; Rodríguez-Frómeta et al., 2013; Zhao et al., 2016),** centromere structure **(Navarro-Mendoza et al., 2019**), and dimorphism (**Lee et al., 2013; Torres-Martínez et al., 2016**).

In addition to its role as a saprophyte, *M. lusitanicus* has also been found to have potential applications in biotechnology due to its ability to produce a variety of enzymes (**Shimonaka et al., 2006; Huang et al., 2014**) and metabolites, such as carotenoids (**Naz et al., 2020**). *M. lusitanicus* has the ability to degrade various pollutants and contaminants, making it a potential candidate for bioremediation of contaminated sites. Its ability to accumulate a range of substrates such as polyphosphates (**Ye et al., 2015; He et al., 2019**) and the heavy metal sorption capability (**Cui et al., 2017; Zhang et al., 2017**) make it a promising organism for bioremediation applications (**Sankaran et al., 2010**) as well. *M. lusitanicus* produces an array of enzymes such as lipases (**Szczęsna-Antczak et al., 2006; Carvalho et al., 2015; Szczęsna-Antczak et al., 2016; Zan et al., 2016a; Zan et al., 2016b**), amylases (**Thanh et al., 2008)**, proteases (**Andrade et al., 2002; Sathya et al., 2009**) and cellulases (**Takano and Hoshino, 2012; Dotsenko et al., 2018**), which can be used in various industrial processes such as food processing,

detergent production, and pharmaceutical production. *M. lusitanicus* produces significant amounts of biomass, which can be used as a source of food for aquaculture and animal feed (**Mitra et al., 2012**).

1.2 Dimorphism in *Mucor lusitanicus*

Regulation of dimorphism in *M. lusitanicus* is a complex process. Studies have identified several key regulators of dimorphism, including cyclic AMP (cAMP)-dependent protein kinase (Pka) pathway (**Borges-Walmsley and Walmsley, 2000; Harris, 2006; Ocampo et al., 2009; Ocampo et al., 2012**), calcineurin pathway (**Lee et al., 2013; Lee et al., 2015**), heterotrimeric G proteins (**Valle-Maldonado et al., 2015; Patiño-Medina, et al., 2019a; Valle-Maldonado et al., 2020**) and ADP-ribosylation factors (**Patiño-Medina, et al. 2018; Patiño-Medina, et al., 2019b)**. Filamentous form of *M. lusitanicus* is involved in virulence and the yeast-like form is less pathogenic (**Lee et al., 2013; Tahiri et al., 2023**). Hence, the analysis of genes involving in the process of dimorphism can improve the knowledge about the pathogenicity of *M. lusitanicus*.

1.2.1 Cyclic AMP dependent protein kinase A pathway

cAMP-dependent Pka has a key role in dimorphic transition in fungi (**Borges-Walmsley and Walmsley, 2000; Harris, 2006**). The exogenous addition of cAMP to *M. lusitanicus* promotes yeast growth (**Kubo and Mihara, 2007**). The Pka of *M. lusitanicus* is a tetrameric holoenzyme that has two regulatory (PkaR) and two catalytic (PkaC) subunits (**Rinaldi et al., 2008**; **Ocampo et al., 2009**). cAMP is a second messenger that regulates activity of Pka by constructing cAMP-PkaR complex. It binds to the PkaR and releases PkaC from the tetrameric inactive holoenzyme to initiate a phosphorylation cascade regulating the morphological change (**Taylor et al., 1992**; **Wolff et al., 2002)**.

There are four genes coding the regulatory subunits of Pka in *M. lusitanicus*: *pkaR1*, *pkaR2*, *pkaR3*, and *pkaR4.* Three of them are implicated in the dimorphism. *PkaR1* and *pkaR2* show highest expression level and expressed during both aerobic and anaerobic growth. *pkaR3* is expressed in spores, while *pkaR4* is expressed during the mycelial growth (**Ocampo et al., 2009**). Overexpression of *pkaR1* promotes mycelial growth and its deletion causes defects in the yeast-mycelium transition. PkaR2 works as a repressor of the yeast-hyphae transition. PkaR4 is essential for the viability of this fungus and involved in dimorphism (**Moriwaki-Takano et al., 2021)**. **Moriwaki-**

Takano et al. (2021) suggested hypothesis on the regulation of morphological change of *Mucor* under anaerobic condition via the cAMP pathway (**Figure 2**).

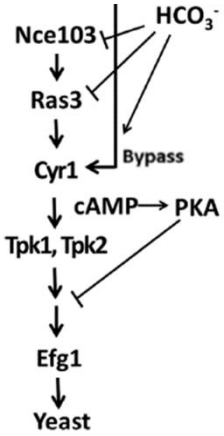

Figure 2. Morphological change pathway of *M. lusitanicus* via cAMP under anaerobic condition (Moriwaki-Takano et al., 2021). *Nce103* – gene encoding carbonic anhydrase; *Ras3* – gene encoding GTPase; *Cyr1* – gene encoding adenylate cyclase; cAMP – cyclic adenosine monophosphate; PKA – protein kinase A; *Tpk1* – gene encoding thiamin phosphokinase 1; *Tpk2* – gene encoding thiamin phosphokinase 2; *Efg1* – gene encoding elongation factor G1. Under anaerobic conditions in liquid medium, CO_2 is spontaneously converted to HCO_3^- by carbonic anhydrase in the fungal cells. High concentration of the ion triggers suppression of *nce103* encoding carbonic anhydrase and *ras3* encoding GTPase and upregulation of *cyr1* encoding adenylate cyclase. It leads to the synthesis and accumulation of cAMP activating PKA. High PKA activity suppresses the expression of *efg1* encoding elongation factor G1 that causes inhibition of hyphae elongation.

1.2.2 Calcineurin pathway

The calcineurin pathway plays a critical role in regulating dimorphism in *M. lusitanicus*. Calcineurin is a serine/threonine-specific protein phosphatase. This pathway is activated by an increase in intracellular calcium levels and involves the activation of the calcineurin phosphatase enzyme. When the calcineurin pathway is activated, it leads to the induction of filamentous growth. Conversely, when the pathway is inhibited, it results in the induction of yeast growth (**Lee et al., 2013**). Several genes involved in the calcineurin pathway have been identified in *M. lusitanicus*, including the genes of three calcineurin catalytic A subunits (*cnaA, cnaB,* and *cnaC*) with phosphatase activity and

one calcineurin regulatory B subunit (*cnbR*) that binds to calcium (**Lee et al. 2013; Baberwal et al., 2022; Madhavan et al., 2022**).

Mutations in the *cnbR* and in the FKBP12-FK506 binding domain of *cnaA* result in hyphal growth in the presence of FK506 (immunosuppressant targeting calcineurin function) (**Dumont, 2000)**. *cnbR* is necessary for calcineurin activity. Δ*cnbR* mutants are locked in perpetual yeast growth. They are less virulent than the wild-type strain. Δ*cnaA* mutants are hypersensitive to calcineurin inhibitors and have a defect of hyphal polarity (**Lee et al. 2013)**.

Inhibition of calcineurin by FK506 or its mutation leads to yeast growth of *M. lusitanicus*. The sensitivity of Δ*cnaA* mutants to sodium dodecyl sulphate (SDS) suggested that calcineurin has a role in maintaining cell wall integrity. These mutants generated larger spores compared to the wild type, indicating that calcineurin is involved in the regulation of *Mucor* spore size. Phagosomes can maturate with *Mucor* yeast form but not with spores (**Lee et al., 2015**) (**Figure 3**). These findings suggest that calcineurin can be used as a therapeutic target for developing new approaches to treat mucormycosis (**Juvvadi et al., 2017**; **Vellanki et al., 2020**).

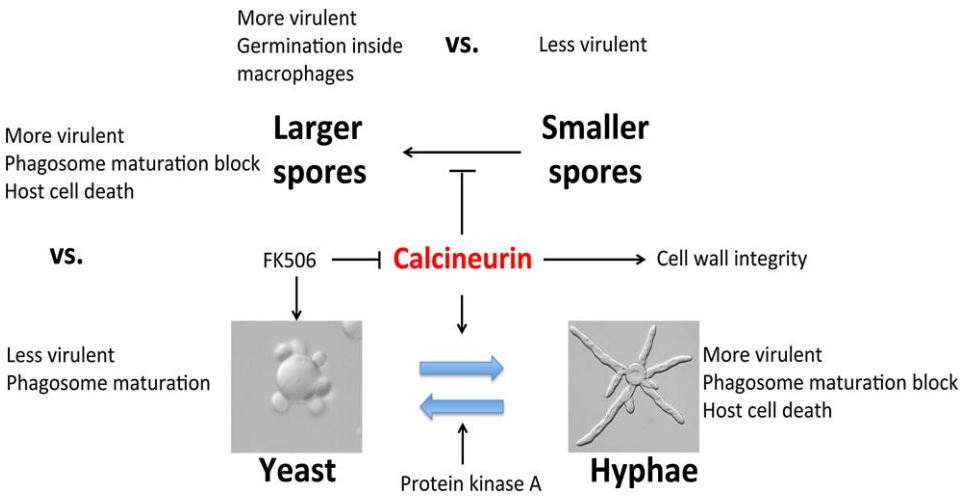

Figure 3. Roles of calcineurin in the dimorphism, virulence, and host-pathogen interactions (Lee et al., 2015).

1.2.3 Heterotrimeric G proteins

Heterotrimeric G proteins are signaling proteins involved in various cellular processes including growth, differentiation, and response to environmental stimuli. *M. lusitanicus* possesses three primary G protein subunits: Gα, Gβ, and Gγ. Its genome has

multiple genes encoding putative heterotrimeric G protein subunits: 12 Gα (Gpa1-12), 3 Gβ (Gpb1-3), and 3 Gγ (Gpg1-3) (**Valle-Maldonado et al., 2015**). Gpb1 is functionally associated with PkaR1 and upregulates virulence. *pkaR1* and *gpb1* deletion mutants have similar phenotypes. Defects of the Δ*gpb1* mutant can be genetically suppressed by *pkaR1* overexpression. In *M. lusitanicus*, the PKA pathway is controlled by *gpb1* (**Figure 4)**.

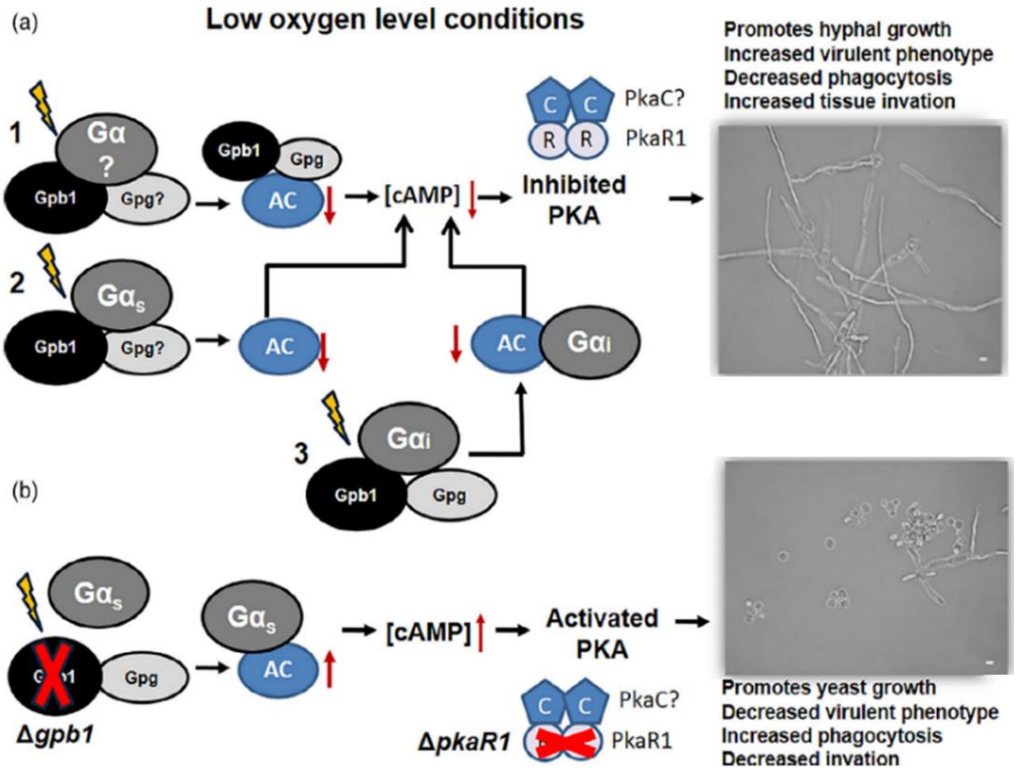

Figure 4. Possible models of the role of Gpb1 in *M. lusitanicus* growth regulation under low oxygen growth conditions (Valle-Maldonado et al., 2020). (a) Gpb1 is a putative regulator of adenylyl cyclase (AC) activity under low oxygen levels. 1) Gpb1 is part of an activated Gβγ heterodimer directly inhibiting the activity of AC. 2) Gβγ antagonistically binds the Gα stimulatory (Gαs) subunit, inhibiting indirectly the AC. 3) Gβγ binds to Gα inhibitory (Gαi) subunit, the unknown signal releases the Gβγ and the Gαi which inhibits the AC. Decreased levels of cAMP by AC do not cause the PkaR and PkaC dissociation. Hence, hyphal growth with an increased virulent phenotype is promoted. (b) Lack of Gpb1 or PkaR1 increases yeast growth with a reduced virulence phenotype. Deletion of Gpb1 or PkaR1 affects cAMP levels and PKA activity. The lack of Gpb1 leads to the incorrect formation of the heterotrimer, resulting in impairment of signaling. AC is activated and the level of cAMP is increased. This leads to the PKA pathway activation. PkaC is released in the absence of *pkaR1*.

Morphological changes induce differential accumulation of transcripts encoding heterotrimeric G proteins. *gpg1* shows low expression during the whole development, and other genes show differential expression during dimorphic growth. *gpb3* (Gβ) and *gpg2* (Gγ) have similar patterns during mycelium development. *gpa1*, *gpb2*, and *gpg2* are co-expressed during yeast growth. Among all Gβ subunits, *gpb1* is highly expressed during mycelial growth compared to spore or yeast growth (**Valle-Maldonado et al., 2015**).

1.2.4 ADP-ribosylation factors

ADP-ribosylation factors (Arfs) are small G proteins of the Ras superfamily involved in vesicular biogenesis and membrane trafficking. They are molecular switches, cycling between an inactive GDP-bound and an active GTP-bound states. Once activated, Arfs interact with downstream effectors to regulate various cellular functions. Four *arf* genes were identified in *M. lusitanicus* (**Corrochano et al., 2016**). Arfs are involved in the regulation of morphological transition of *M. lusitanicus* (**Jones et al., 1999; Kahn et al., 2006**). A model of the role of *M. lusitanicus* Arfs is shown in **Figure 5**.

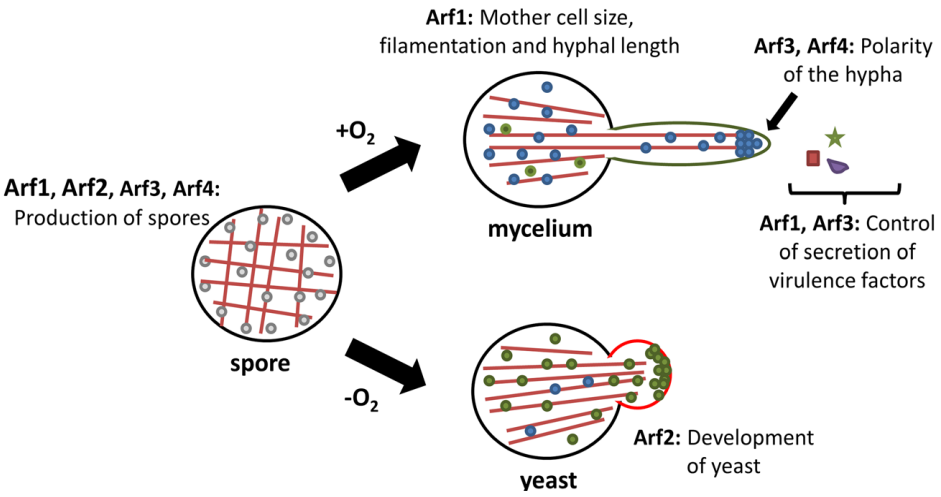

Figure 5. A model of the role of Arf proteins in morphology and virulence of *M. lusitanicus* (Patiño-Medina et al., 2018). The cell wall in hyphae (green) or yeast cells (red) must be synthesized to promote cell growth. Red lines – the cytoskeleton. Blue and green circles – specific vesicles involved in hyphal and yeast growth, respectively. Stars, squares, and triangles – secreted molecules.

arf1-arf3 were differentially expressed during dimorphism, while expression of *arf4* was not affected. Spore production is mainly controlled by Arf1 and Arf2, although

the absence of Arf3 and Arf4 also moderately reduces sporulation. Under aerobic conditions, the lack of Arf1 causes enlarging the mother cells size, increasing the number of hyphae per mother cell, and decreasing the hyphal length. Arf3 and Arf4 participate in the maintenance of the hyphal tip polarity. Under anaerobic condition, Arf2 has a critical role in the development of yeast cells. Arf1 and Arf3 are involved in the secretion of virulence factors (**Patiño-Medina et al., 2018**). Hence, Arfs can be viable targets for mucormycosis diagnosis during the dimorphism stage.

1.3 Heat shock factor (HSF)-type transcription factor 1

Adaptation to stress is essential for all living organisms as well as for fungal pathogens. Sensing the temperature of environment is important for surveillance and virulence. Eukaryotic heat shock response involves an activation of heat shock transcription factor 1 (Hsf1). Hsf1 plays a crucial role in regulating the expression of genes involved in cellular stress responses, including heat shock response. Hsf1 is conserved across all eukaryotes (**Nover et al., 2001; Pirkkala et al., 2001; Nicholls et al., 2009; Nicholls et al., 2011; Barna et al., 2018; Gomez-Pastor et al., 2018**). The structure of yeast Hsf1 is shown in **Figure 6**.

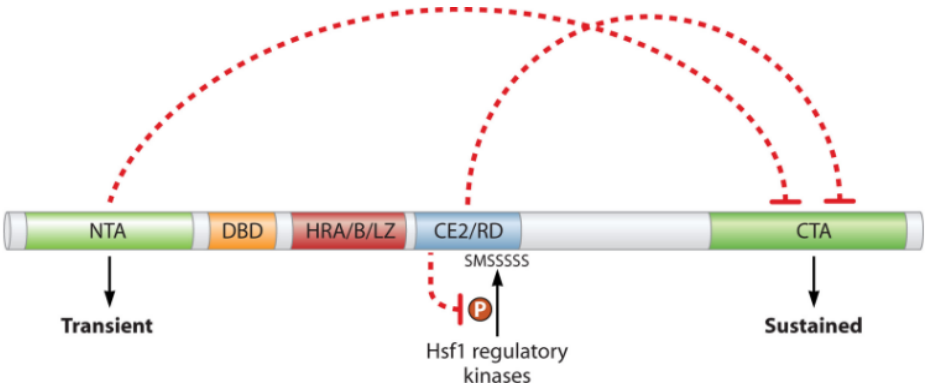

Figure 6. Structure of yeast Hsf1 (Verghese et al., 2012). Dashed lines – regulatory relationships between the NTA (N-terminal transactivation domain) and the CE2 (control element 2) in RD (regulatory domain) on the CTA (carboxy-terminal transactivation domain). NTA and CE2 are unique features of the yeast protein. The serine-rich region within the RD is phosphorylated to promote the repression of the CTA through CE2. NTA promotes a transient transcriptional response. CTA is essential for sustained responses. DBD – DNA-binding domain; HRA/B/LZ – heptad repeats A and B, also called the leucine zipper; P – phosphorylation.

Hsf1 plays a crucial role in the activation of genes involved in the production of chaperones that help other proteins fold properly and prevent them from aggregating during stress conditions. Fungal Hsf1 also controls basal expression of chaperones (**Solís et al., 2016**). It is constitutively trimerized and expressed under normal conditions and under stress **(Verghese et al., 2012; Neef et al. 2014; Pincus et al., 2018)**. During the heat shock stress Hsf1 is hyperphosphorylated and translocates to the nucleus. Hsf1 activates heat shock proteins (Hsp90 and/or Hsp70) by binding to canonical heat shock elements (HSEs) in their promoter regions (**Yamamoto et al., 2005; Nicholls et al., 2009; Nicholls et al., 2011; Leach and Cowen, 2013; Hossain et al., 2021)**. Hsp70 is the main titrating Hsf1 chaperone (**Neef et al., 2014; Masser et al., 2020**) (**Figure 7**).

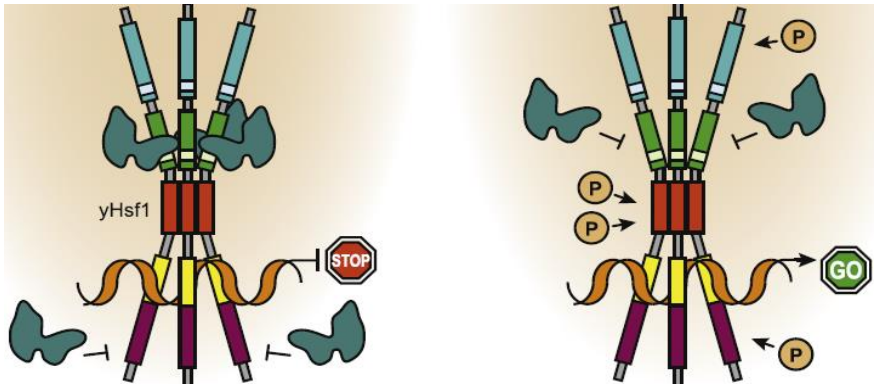

Figure 7. **Regulation of yeast Hsf1 DNA-binding and transactivation (Masser et al., 2020).** Purple – N-terminal transactivation domain (NTA); yellow – DNA-binding domain; red - three leucine zippers (HR-A/B); green – regulatory domain (RD) containing a control element 2 (CE2) in RD; blue – carboxy-terminal transactivation domain (CTA) containing a fourth leucine zippers (HR-C); turquoise – heat shock protein 70 (Hsp70); P – phosphorylation events. DNA-binding is regulated by Hsp70 binding to the NTA. Hsp70 represses transactivation by binding to the CE2 domain. Phosphorylation events promote transactivation of Hsp70 liberated Hsf1.

DNA-binding domain recognizes HSEs, which consist of inverted nGAAn sequence motifs (**Jaeger et al., 2016; Neudegger et al., 2016**). HSPs activate chaperons restoring protein homeostasis (**Feder and Hofmann, 1999; Leach et al., 2012a; Leach et al., 2012b; Tiwari et al., 2015; Zheng et al., 2016)**. Carboxy-terminal transactivation domain is essential for transcription activation. Upon heat shock the concentration of

unfolded proteins exceeds the capacity of Hsp70. Molecules of Hsp70 are released from Hsf1. So, the released molecules of Hsf1 induce more Hsp70. After protein homeostasis restoring Hsp70 inactivates Hsf1 by binding to it **(Masser et al., 2020)**.

In *Saccharomyces cerevisiae*, Hsf1 regulates gene transcription in response to heat shock, oxidative stress, glucose starvation, heavy metal and proteotoxic stress (**Sugiyama et al., 2000; Zähringer et al., 2000; Hahn and Thiele, 2004; Albrecht et al., 2010; Brandman et al., 2012; Sueiro-Olivares et al., 2015; Gomez-Pastor et al., 2018**).

In *Candida albicans,* in addition to heat shock response Hsf1 also controls expression of genes essential for filamentation, pathogenesis, adhesion, and biofilm formation under the elevated temperature. Cells of *C. albicans* that were exposed to high temperatures caused more damage to host cells and are associated with a higher mortality of infection model organisms such as zebrafish (*Danio rerio*) and wax moth (*Galleria mellonella*) in infection models (**Leach et al., 2016**). Lack of *hsf1* resulted in dysfunctional mitochondria, increased susceptibility towards oxidative stress, disturbed cell wall integrity and defect in hyphal development, reduced virulence, and decreased resistance to antifungal drugs **(Nair et al., 2017)**.

The main function of Hsf1 in *Aspergillus fumigatus* is regulation of the heat shock response and expression of Hsps. Hsf1 increases heat resistance by regulating cell wall biosynthesis and remodeling and expression of lipid homeostasis genes (**Fabri et al., 2021; Xiao et al., 2022**).

Cryptococcus neoformans hsf1 does not regulate its own expression. Hsf1 was found to regulate the expression of genes involved in the adaptation of *C. neoformans*. Hsf1 is transiently phosphorylated during the exposure to enhanced temperature and promotes thermotolerance by regulating temperature-responsive genes. While its expression is induced upon oxidative stress. However, Hsf1 represses resistance to oxidative stresses. Therefore, Hsf1 likely functions both as a transcriptional activator and repressor for thermotolerance and oxidative stress responses in *C. neoformans* (**Yang et al., 2017**).

1.4 Qdr2 multidrug transporter

Quinidine drug resistance protein 2 (Qdr2) is a major facilitator superfamily (MFS) multidrug transporter that is located in the plasma membrane. It exports different compounds like quinidine and barban across the cell membrane (**Vargas et al., 2004)**. It is also involved in the resistance to the anticancer agents like cisplatin and bleomycin

(**Nunes et al., 2001; Tenreiro et al., 2005**), as well as to polyamines (**Teixeira et al., 2011**).

There are two subfamilies of MFS transporters: DHA1 (drug:H^+ antiporter 1 with 12 transmembrane segments) and DHA2 (with 14 transmembrane segments) (**Paulsen et al., 1996; Gbelska et al., 2006; Law et al., 2008; Costa et al, 2014**). Qdr2 is a member of the DHA1 subfamily. DHA1 family transporters have a cytoplasmic loop between transmembrane segments. DHA1 subfamily transporters are strictly conserved within fungi (**Costa et al., 2014; Galocha et al., 2020)**. DHA1 transporters are energized by the electrochemical proton motive force consisting of an electrical potential ($\Delta\psi$) and a chemical proton gradient ($\Delta pH = pH_{external} - pH_{internal}$) (**Cannon et al., 2009; Sá-Correia et al., 2009)** (**Figure 8**).

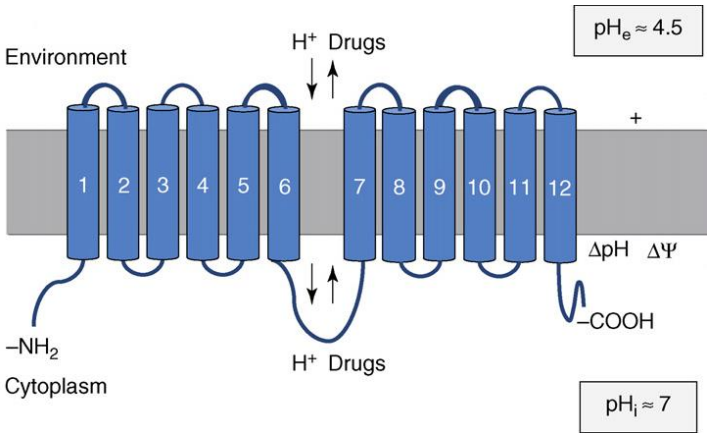

Figure 8. Depiction of representative yeast 12-spanner DHA1 family transporters (Sá-Correia et al., 2009).

In *S. cerevisiae*, Qdr2 can transport monovalent and divalent cations including potassium (K^+) and copper (Cu^{2+}). It has an important role in the potassium and copper homeostasis. Qdr2 helps to keep physiological levels of potassium under potassium-limited growth and in the presence of quinidine that can decrease potassium accumulation and uptake rate. Qdr2 also acts as an alternative K^+ transporter (**Ríos et al., 2013**). Copper is essential for yeasts because it is a substrate for many redox reactions (**Bleackley and MacGillivray, 2011**). *qdr2* expression is involved in amino acid homeostasis in *S. cerevisiae*. Its transcription is activated under nitrogen (NH_4^+) limitation or leucine limitation (**Vargas et al., 2007)**. It also has been associated to the uptake of tunicamycin (**Lanthaler et al., 2011)**.

In *Candida glabrata,* Qdr2 is associated to resistance to quinidine and antifungal drugs such as imidazole, miconazole, tioconazole, clotrimazole, and ketoconazole (**Nunes et al., 2001; Vargas et al., 2004; Tenreiro et al., 2005; Costa et al., 2013**). Lack of Qdr2 leads to improper intracellular pH regulation that affects cell growth, cell metabolism, biofilm formation, oxidative stress response and drug susceptibility (**Widiasih Widiyanto et al., 2019; Santos et al., 2020**).

In *C. albicans*, a Qdr2 transporter is not directly involved in antifungal resistance. It seems to play role in pathogenicity (**Redhu et al., 2016)**. In *C. albicans*, there are three Qdr proteins: Qdr1, Qdr2 and Qdr3. Disruption of *qdr* genes individually or collectively leads to upregulation of glucose transport genes (i.e., *HGT*s), elevating glucose and glycerol accumulation and enhanced hyphal network (**Figure 9**).

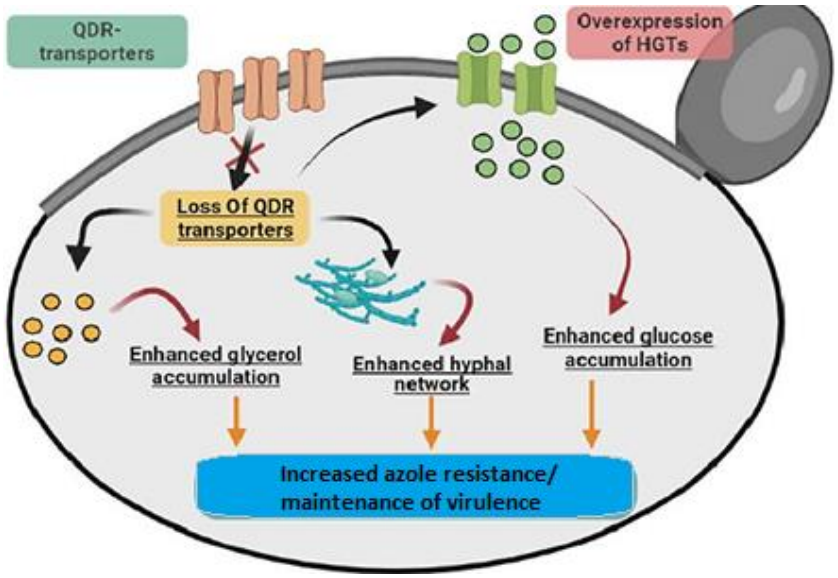

Figure 9. The impact of the deletion of *qdr* transporter genes on *C. albicans* (Qadri et al., 2022).

The crosstalk between these two classes of MFS-transporters is also reflected in enhanced hyphal morphogenesis, glycerol accumulation, etc., collectively leading to increased azole drug resistance and possibly maintaining virulence/pathogenicity (**Rodaki et al., 2009; Dikicioglu et al., 2014**). Qdr2 transporter has also been involved in cellular lipid homeostasis in *C. albicans* and *C. glabrata*. Lack of Qdr2 leads to the accumulation of phosphatidylinositol, phosphatidyl serine and sphingolipids (**Shah et al., 2014; Cavalheiro et al., 2018)**.

2. AIMS

Mucor lusitanicus is a human opportunistic fungal pathogen with ability to switch between yeast and filamentous growth in response to environmental changes. It has multi-budded yeast growth form in the presence of a fermentable hexose under anaerobic conditions, while filamentous growth is triggered under aerobic conditions or upon nutrient limitation. This adaptation complicates the treatment for mucormycosis infections. Till these days information about genes involving in the adaptation of *M. lusitanicus* to unfavorable conditions is limited. Characterization of these genes can broaden the knowledge about the adaptation mechanisms of Mucoralean fungi.

The aim of the study was to identify and characterize differentially expressed genes in *M. lusitanicus* under anaerobic conditions, determine their functions, and investigate their role in yeast morphology, antifungal resistance, and pathogenicity.

Therefore, objectives of the presented research were the following:

1. Identification of differentially expressed genes under anaerobiosis in *M. lusitanicus* via transcriptomic analysis.
2. Validation and selection of genes for further characterization based on transcription analysis under various cultivation conditions, such as oxygen tension, cultivation time, different temperatures, and antifungal treatments.
3. Functional characterization of the selected genes:
    a) Disruption of the selected genes by using a plasmid-free CRISPR-Cas9 method.
    b) Morphological and physiological characterization of the disruption mutants (growth under different conditions, pathogenicity test).

3. MATERIALS AND METHODS

3.1 Strains used in the experiments

The *M. lusitanicus* (SZMC 12082) double auxotrophic strain MS12 (*leuA*$^-$ and *pyrG*$^-$), a derivative of the wild-type strain CBS 277.49, was used during the transformation experiments (**Nagy et al., 2014**). MS12+*pyrG* strain with the complemented uracil auxotrophy expressing the functional *pyrG* gene was used as a control for the morphological and physiological studies. Plasmid construction and propagation were performed in *Escherichia coli* DH5α$^-$. For the antifungal susceptibility test, *Candida krusei* ATCC 6258 was used as a reference strain.

3.2 Composition of the applied media

YNB (yeast nitrogen base) minimal medium: 1% (w/V) D-glucose, 0.15% (w/V) ammonium sulphate, 0.15% (w/V) sodium L-glutamate, 0.05% (w/V) YNB without amino acids (Sigma-Aldrich) supplemented with 0.05% (w/V) uracil and/or 0.05% leucine (w/V), if required. For solid medium 2% (w/V) agar was added.

Malt extract agar (MEA): 1% (w/V) D-glucose, 0.5% (w/V) yeast extract, 1% (V/V) malt extract, 2% (w/V) agar.

Yeast extract-glucose medium (YEG): 1% (w/V) D-glucose, 0.5% (w/V) yeast extract, 2% (w/V) agar for protoplast formation.

Yeast extract-peptone-dextrose medium (YPD): 2% (w/V) dextrose, 1% (w/V) yeast extract, 2% (w/V) peptone, 2% (w/V) agar (optional, for making solid medium).

Luria-Bertani (LB) medium: 1% (w/V) sodium chloride, 1% (w/V) tryptone, 0.5% (w/V) yeast extract (w/v) (pH 7.0) supplemented with 2% (w/V) agar for making solid medium. For selecting *E. coli* transformants, LB medium was supplemented with 50 μg/ml ampicillin (Sigma Aldrich).

Roswell Park Memorial Institute 1640 (RPMI-1640) (pH 7.0): 1.04% (w/V) RPMI-1640 medium powder (Sigma Aldrich), 3.453% (w/V) of 3-(N-morpholino) propanesulfonic acid (MOPS), 0.1% (w/V) L-glutamine (30 mg/ml; w/V), supplemented with 0.05% (w/V) uracil and/or 0.05% leucine (w/V), if required.

3.3 Growth conditions and strain maintenance

To test the mitotic stability of the mutants after transformation experiment, malt extract agar was used as a complete, i.e., non-selective medium. When the effect of different cultivation conditions on the gene transcription was investigated the *M.*

lusitanicus MS12 strain was cultivated on solid YNB plates and grown for 4 days under continuous daylight illumination at 25 °C. The inoculum size was 10^4 sporangiospores/plate. Occasionally, the cultivation was performed in 10 ml YNB liquid medium; the inoculum size was 10^4 sporangiospores/ml.

To examine the effect of the temperature on the growth of the mutants, fungal strains were cultivated on solid YNB at 15, 20, 25, 30 and 35 °C and the number of the plated spores was 10^4 sporangiospores/ml. To check the effect of various cell wall stressors and detergents on fungal strains, YNB containing 0.1% (V/V) of Triton X-100, 0.004 % (w/V) sodium dodecyl sulphate (SDS), 0.001 % (w/V) calcofluor white (CFW), or 0.002 % (w/V) Congo red (CR) was used. To test the effect of the different salts and H_2O_2 on the growth of fungal strains YNB medium was supplemented with NaCl, $FeSO_4$, $ZnSO_4$, $CuSO_4$ and H_2O_2.

To test the effect of different antifungals on the gene expression, 10^4 spores/ml of MS12 strain were grown in 10 ml of liquid RPMI-1640 medium supplemented with leucine and uracil for 24 h at 25 °C. After spores were treated with the corresponding antifungal agent and incubated for another 16 h before the RNA extraction. Itraconazole (Across Organics), isavuconazole (Sigma Aldrich), ravuconazole (Sigma Aldrich), fluconazole (Alfa Aesar), and ketoconazole (Alfa Aesar) were applied at a final concentration of 8 μg/ml, while posaconazole (Sigma Aldrich) was applied at a final concentration of 1 μg/ml, and amphotericin B (Sigma Aldrich) at a final concentration of 0.5 μg/ml.

Anaerobic growth was performed in 50 ml liquid YNB or RPMI-1640 media supplemented with leucine and uracil in a BBL GasPak Anaerobic System (Becton Dickinson) at 25°C.

3.4 Extraction of fungal genomic DNA

Genomic DNA of the fungal strains was purified using the Quick-DNA™ Fungal/Bacterial Miniprep Kit (Zymo Research) according to the manufacturer's instructions.

3.5 DNA/RNA agarose gel electrophoresis

For agarose gel electrophoresis, 0.8-2% (w/v) agarose was dissolved in TAE (Tris acetic acid-disodium EDTA) buffer (40 mM Tris-acetic acid (pH: 7.6); 1 mM Sodium EDTA). DNA was stained with 0.5 mg/ml ethidium bromide (Sigma Aldrich) from 10

mg/ml stock solution, dissolved in distilled water. 1-X DNA loading dye (Thermo Scientific) was used as the sample buffer. GeneRuler 1 kb DNA ladder: distilled water – molecular marker – 6-X DNA loading dye (4:1:1) (Thermo Scientific) was used to determine the size of the bands. The electrophoretic separation was carried out in TAE buffer, with current of 80V for 1 hour. Visualization of the DNA was done by exposing the agarose gel to UV light.

3.6 Isolation of DNA from agarose gel

To isolate the DNA fragments from the 0.8% agarose gel, the appropriate DNA band was cut from the gel using a sterile scalpel under UV light. The DNA was then purified from the gel using the Zymoclean^{TM} Large Fragment DNA recovery Kit (Zymo Research) according to manufacturer's instructions.

3.7 PCR amplification for gene cloning

For gene fragments amplification from genomic DNA PCR reactions were carried out in the ProFlex PCR system (Applied biosystems). Details of the applied primers used in the study are shown in **Table S1**. Primers were synthesized with Integrated DNA Technologies (IDT). Phusion Flash High-Fidelity PCR Master Mix (Thermo Scientific) was used in the PCR experiments according to the manufacturer's recommendations.

The reactions were prepared in a final volume of 20 µl as follows: 10-100 ng template DNA, 10 µM specific primers, 2X Phusion High Fidelity DNA Polymerase Master mix, Molecular water (RNAse and DNAse free). Amplification conditions were as follows: 98 °C for 10 s, 98 °C for 1 s, 60 °C for 5 s, 72 °C for 15 s – 1 min, repeat for 30 cycles, 72 °C for 1 min. The extension time was modified according to the length of the expected amplicon.

3.8 Design and construction of the guide RNA (gRNA) and the template DNA for CRISPR-Cas9 gene disruption

Nucleotide sequences of *M. lusitanicus* genes used in the current study were obtained from **https://mycocosm.jgi.doe.gov/Mucci2/Mucci2.home.html** (**Corrochano et al., 2016**). Protospacer sequences designed to target the DNA cleavage in the *hsf1, hsf2, qdr2a, qdr2b, qdr2c,* and *qdr2d* genes were as follows, 5'–GTGCGTCAACTAAACATGTA–3'; 5'–GATGAAACCAATAAACTGTA–3'; 5'–CTTCTGGTAAAGTAATGGAC–3', 5'–ATCCAACACCAATGCAAGCC–3'; 5'–

CTTCCTCTACTTGTTTGAGA–3’; and 5’–GCCATCACTCTGATCTTTAG–3’ respectively, which correspond to the fragments of the nucleotide positions between 132 and 152 downstream from the start codon of the *hsf1* gene, between the positions 180 and 200 downstream from the start codon of *hsf2*, between the positions 1267 and 1287 downstream from the start codon of *qdr2a*, between the positions 901 and 921 downstream from the start codon of *qdr2b*, between the positions 885 and 905 downstream from the start codon of *qdr2c*, between the positions 1098 and 1118 downstream from the start codon of *qdr2d*, respectively. Using these sequences, the Alt-R CRISPR crRNA and Alt-R CRISPR-Cas9 tracrRNA molecules were designed and purchased from Integrated DNA Technologies (IDT). To form the crRNA: tracrRNA duplexes (i.e., the gRNAs), the Nuclease-Free Duplex Buffer (IDT) was used according to the instructions of the manufacturer. Homology driven repair (HDR) was applied for all gene disruptions following the strategy described previously (**Nagy et al., 2017**). Disruption cassettes functioning also as the template DNA for the HDR were constructed by PCR using the Phusion Flash High-Fidelity PCR Master Mix (Thermo Scientific). Gene disruption strategy and the template DNA is presented in **Figure 10**.

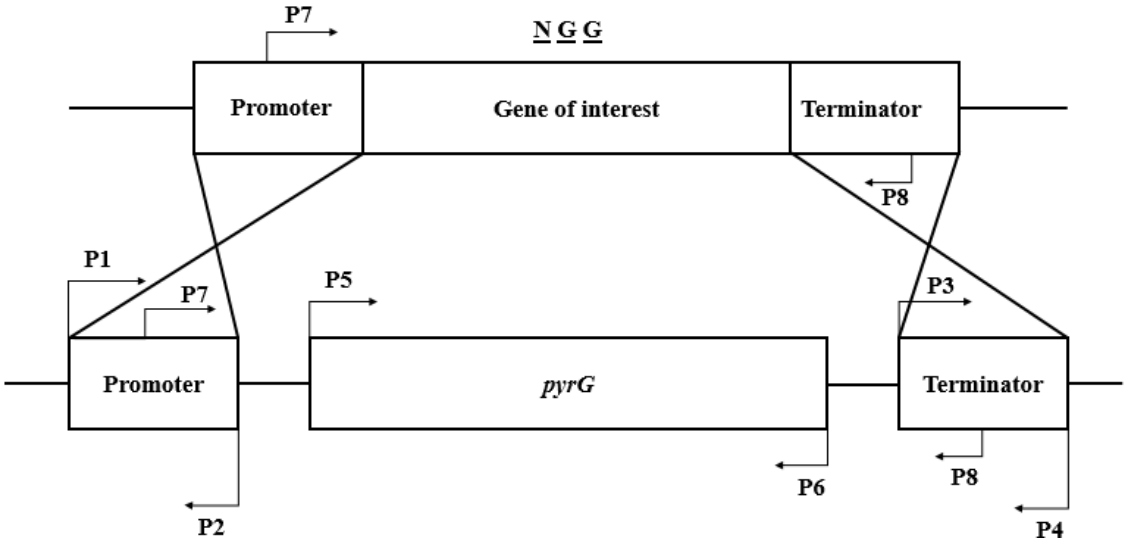

Figure 10. Strategy designed to disrupt the *hsf1, hsf2, qdr2a, qdr2b, qdr2c,* and *qdr2d* genes of *M. lusitanicus* using the CRISPR-Cas9 method. NGG indicates the PAM (Protospacer adjacent motif) sequence. The arrows show the orientations of the primers. P1-P2 – primers used to amplify the promoter sequence; P5-P6 – primers used to amplify the *pyrG* sequence; P3-P4 – primers used to amplify the terminator sequence; P7-P8 – nested primers used to amplify the Phusion PCR product (i.e., disruption cassette).

In case of the *hsf1* gene, at first, two fragments being 2135 and 2127 nucleotides upstream and downstream from the protospacer sequence and the *M. lusitanicus pyrG* gene (CBS277.49v2.0 genome database ID: Mucci1.e_gw1.3.865.1) along with its promoter and terminator sequences were amplified using the primers listed in **Table S1**. The amplified fragments were fused in a subsequent PCR using the nested primers Mc123815P7 and Mc123815P8.

Disruption of *hsf2* using the *pyrG* gene was carried out in the same way as follows: two fragments, which were 1686 and 1626 nucleotides upstream and downstream from the protospacer sequence, respectively, were fused with the *pyrG* gene by PCR using the nested primers Mc125667P7 and Mc125667P8 (**Table S1**).

In case of *qdr2a*, two fragments, 2770 and 2148 nucleotides upstream and downstream from the protospacer sequence, respectively, were fused with the *pyrG* using the nested primers Mc42380P7 and Mc42380P8 (**Table S1**).

Disruption of *qdr2b* using the *pyrG* gene was carried out in the same way as follows: two fragments, which were 2404 and 2720 nucleotides upstream and downstream from the protospacer sequence, respectively, were fused with the *pyrG* gene by PCR using the nested primers Mc138979P7 and Mc138979P8 (**Table S1**).

In case of *qdr2c*, two fragments, 2388 and 2189 nucleotides upstream and downstream from the protospacer sequence, respectively, were fused with the *pyrG* using the nested primers Mc152822P7 and Mc152822P8 (**Table S1**).

Disruption of *qdr2d* using the *pyrG* gene was carried out in the same way as follows: two fragments, which were 2601 and 2286 nucleotides upstream and downstream from the protospacer sequence, respectively, were fused with the *pyrG* gene by PCR using the nested primers Mc160673P7 and Mc160673P8 (**Table S1**).

3.9 PEG mediated protoplast transformation of *M. lusitanicus*

For the CRISPR-Cas9-mediated gene disruption a modified version of the PEG-mediated protoplast transformation method described by **van Heeswijck and Roncero (1984)** was used. Sporangiospores of the MS12 strain were washed with 5 ml of distilled water from YNB plate that was inoculated 4 days before. Spore suspension was inoculated by using a microbiological replicator onto 20 YEG plates covered with cellophanes. Plates were incubated at 25 °C for 16 hours (**Nagy et al., 2017**).

Snail enzyme mix (30 ml: 17 ml sterile distilled water, 3 ml sodium-phosphate buffer pH 6.4 (100 mM sodium phosphate buffer: 25 mM Na_2HPO_4 and 75 mM

NaH_2PO_4), 10 ml of 2.4 M sorbitol and 0.45 g snail enzyme) was centrifuged for 10 minutes at 8064 g at 4 °C. Then snail enzyme mix was filtered through a 0.45 µm pore size filter by using a vacuum pump.

Young colonies were washed from the 10 cellophanes into the 30 ml snail enzyme mix and incubated for 3 hours at room temperature with gentle shaking. The developed protoplasts were filtered through a sterile gauze with 5 ml SMC (50ml: 2.5 ml 1 M $CaCl_2$, 1 ml 0.5 M MOPS, 16.65 ml 2.4 M sorbitol, 38.5 ml distilled water). Then protoplasts were centrifuged for 10 minutes at 2162 g at 4 °C to get pellets. The pelleted protoplasts were resuspended again in 5 ml SMC buffer and pulled into one tube. Then protoplasts were centrifuged under the same conditions.

For CRISPR-Cas9 mutagenesis of the gene of interest, 200 µl SMC, 45 µl template DNA (i.e., the gene disruption cassette), 20 µl 2.4 M sorbitol, 20 µl PMC (20 ml: 13.33 ml PEG, 400 µl MOPS (3-(N-morpholino) propanesulfonic acid), 6.6 ml 2.4 M sorbitol, 1 ml $CaCl_2$), 1.5 µl 10 nM gRNA (IDT), 1.1 µl 10 nM Cas9 enzyme (IDT) were added to the protoplasts and gently resuspended.

After incubation the tube on ice for 30 minutes, 5 ml of PMC was added to the protoplasts, that were incubated at room temperature for 30 minutes. Then 20 ml SMC was added to the tube and the mix was centrifuged at 2162 x g 10 minutes at 4 °C. Supernatants were discarded after centrifuging. Protoplasts were resuspended in hand warm YNB containing 1% agar (top) and spread onto YNB containing 2% agar (bottom) supplemented with 0.8 M sorbitol and 0.05% leucine. Plates were covered with aluminum foil to protect fungal protoplasts from the light and incubated at 25 °C for 2-4 days.

3.10 RNA isolation

Total RNA samples were purified from mycelia using the Direct-zol™ RNA MiniPrep kit (Zymo Research) by following the manufacturer's instructions. The quality of each RNA samples was checked in 2% agarose gel. Concentration of RNA samples was checked by using Colibri (Titertek Berthold) and were stored at -80 °C until use.

3.11 cDNA preparation

cDNA synthesis was performed by using either the Maxima H Minus First Strand cDNA Synthesis Kit (Thermo Scientific) or RevertAid H Minus First Strand cDNA Synthesis Kit (Thermo Scientific). Oligo (dT)18 and random hexamer primers were used in the reaction mixture according to manufacturer's instructions.

3.12 Quantitative real-time reverse transcription PCR (qRT-PCR)

The qRT-PCR experiments were performed in a CFX96 real-time PCR detection system (Bio-Rad) using the Maxima SYBR Green qPCR Master Mix (Thermo Scientific). Used primers are showed in **Table S1**. The gene expression was carried out by the $2^{-\Delta\Delta Ct}$ method (**Livak and Schmittgen, 2001**) using the actin gene (scaffold_07: 2052804-2054242; *M. lusitanicus* CBS277.49v2.0 genome database; http://genome.jgi-psf.org/Mucci2/Mucci2.home.html) of *M. lusitanicus* (**Corrochano et al., 2016**) as a reference. The reactions were measured in 20 µl on 96-well plates: 20-50 ng cDNA, 0.4 µM - 0.4 µM specific primer **(Table S1**), 1-X Maxima SYBR Green qPCR Master Mix. The amplification conditions for the qRT-PCR were as follows: 95 °C for 3 min (initial denaturation), (95 °C for 15 sec, 60 °C for 30 sec, 72 °C for 30 sec was carried out for 40 cycles). Melting curve analysis was performed at 65-95 °C, with a 0.5 °C increment. In all experiments, appropriate negative controls containing no template cDNA were subjected to the same procedure to exclude or detect any possible contaminations or carryover. Experiments were performed in biological and technical triplicates.

3.13 Restriction digestion and ligation

Restriction digestions and ligations were performed according to the commonly used methods and following the manufacturer's instructions with optimization to the particular experimental conditions (**Sambrook and Russel, 2001**). DNA fragments were ligated into pJET1.2/blunt cloning vector (CloneJET PCR Cloning Kit, Thermo Scientific). The ligation reaction consisted of 2X reaction buffer, PCR product, 50 ng pJET1.2/blunt cloning vector and 5U T4 DNA ligase. Total volume was 20 µL. The ligation mixture was vortexed briefly and centrifuged for 3-5 seconds. The ligation mixture was incubated at 4 °C for 16 hours.

3.14 Transformation of competent *Escherichia coli* cells

2 µL plasmid, 100 µL DH5α^{-} competent cells along with 80 µl Tris-calcium chloride-magnesium chloride (TCM) buffer (10mM Tris, 10mM $CaCl_2$ and 10mM $MgCl_2$; pH: 7.5) were combined in one tube. The tube was gently tapped and incubated on ice for 30 min. Then the mixture was kept at 42 °C for 2 min (heat shock). Then cells were incubated at room temperature for 10 min. 30, 50 and 100 µl of the cell mixtures were inoculated onto the surface of LB plates supplemented with ampicillin (50 µg/ml) and incubated at 37 °C for 16 h.

3.15 Plasmid DNA purification

For plasmid DNA purification from *E. coli* Zyppy™ Plasmid Miniprep Kit (Zymo Research) was used following the instructions of the manufacturer.

3.16 RNA sequencing

For RNA purification, the 30 mL cultures were filtered through 0.45 nm MCE membrane filters (Millipore, Burlington, MA, USA) and the extraction was performed by using the Direct-zol™ RNA MiniPrep Kit (Zymo Research), following the recommendations of the manufacturer. The samples were kept at -80 °C until their use. The quality of total RNA samples was analyzed by capillary gel electrophoresis in an Agilent 2100 Bioanalyzer using Agilent RNA 6000 Nano Kit and only samples with RIN > 9 were processed further. RNA sequencing was carried out by Dr. L. Bodai and his group at the Department of Biochemistry and Molecular Biology, Faculty of Science and Informatics, University of Szeged. RNA-seq libraries were prepared from three biological and two technical replicates per treatment condition (i.e., six samples per treatment were used in total). Thus, six libraries were generated and all of them were sequenced. Libraries were pooled before sequencing, but since these were indexed, libraries sequence reads belonging to different samples could be demultiplexed (separated to different files) after sequencing. From 800 ng total RNA samples, polyA-RNA was isolated using NEBNext Poly(A) mRNA Magnetic Isolation Module (New England Biolabs), then indexed; strand-specific sequencing libraries were prepared using NEBNext Ultra II Directional RNA Library Prep Kit (New England Biolabs) following the protocol of the manufacturer. Sequencing libraries were validated and quantitated with an Agilent 2100 Bioanalyzer using Agilent DNA 1000 Kit; the average fragment length of the libraries was in the range of 271–289 bp. Libraries were pooled in equimolar concentrations, and after denaturing, the library pool was loaded at 15 pM concentration with 1% PhiX Control V3 (Illumina) in a MiSeq Reagent Kit v3 (150-cycle) kit and sequenced in an Illumina MiSeq instrument producing 2 X 75 bp paired-end reads.

3.17 Analysis of the RNA-Seq Data

Transcriptome data analysis was carried out by Dr. L. Bodai and his group at the Department of Biochemistry and Molecular Biology and Dr. M. Homa at the Department of Microbiology, Faculty of Science and Informatics, University of Szeged. FASTQ files were generated with the GenerateFASTQ 1.1.0.64 application on Illumina BaseSpace.

Sequence quality checks and adapter trimming were performed using TrimGalore/Cutadapt. Sequence reads were aligned to the *M. lusitanicus* CBS 277.49 v2.0 reference genome assembly available from the Joint Genome Institute (JGI) website (https://genome.jgi.doe.gov/Mucci2/Mucci2.home.html (**Corrochano et al., 2016**) using HISAT2 (parameters: –max-intronlen 45000, –rna-strandness RF). From the generated binary alignment files, gene specific read counts were calculated in R using the summarizeOverlaps (parameters: ignore.strand = FALSE, singleEnd = FALSE, fragments = TRUE, preprocess.reads = invertStrand) Bioconductor package with a TxDb transcript metadata object generated from the transcript annotation available from JGI using the makeTxDbFromGFF function of the GenomicFeatures Bioconductor package. Differential gene expression analysis was performed with DESeq2 parameter: $p < 0.05$, and a cpm > 1 read count filter. Gene Ontology analysis was performed with the topGO Bioconductor package (parameters: algorithm = "classic", statistic = "fisher"). A gene was considered differentially expressed if the absolute $\log_2$ fold-change was greater than or equal to 3. Differentially expressed genes (DEGs) were functionally classified into KOG categories and subcategories based on the manual curation of the results from the InterProScan analysis using InterProScan version 5.47–82.0 (**Homa et al., 2022**).

3.18 Sporulation assay

Sporangiospores of *M. lusitanicus* disruption mutants were collected on the 7th day of cultivation on solid YNB plates supplemented with leucine at 25 °C. To check the sporulation capacity, spores with final concentration of 5×10^4 sporangiospores/ml were inoculated into MEA medium and incubated at 25 °C for 4 days. Then produced spores were washed with 5 ml of sterile distilled water and counted using a Bürker chamber.

3.19 Germination assay

Sporangiospores of *M. lusitanicus* disruption mutants were collected on the 7th day of cultivation on solid YNB plates supplemented with leucine at 25 °C. Spores were stored in liquid YNB medium at 4 °C for 16 hours to synchronize their physiological state. To examine the germination ability, 10^7 spores were inoculated into 10 ml liquid YNB medium and incubated at 25 °C under continuous shaking (180 rpm). Germination of the spores was examined by using Leica DMI 4000 B automated inverted research microscope at 2, 4, and 6 h post-inoculation, by using 10 µl of spore suspension in a glass

slide and taking microscopic pictures for 10 focus areas. The number of ungerminated and germinated spores were counted by using the ImageJ software version 1.54d.

3.20 Susceptibility test

Sensitivity of the fungal strains to different antifungal agents, hydrogen peroxide, osmotic stressors, and metal stressors was examined in a 96-well microtiter plate assay. Microtiter plates were incubated for 48 hours at 25 °C. The final amount of the sporangiospores in the wells was 10^4. All experiments were performed in biological and technical triplicates.

The susceptibility tests were performed according to a microdilution technique (CLSI M38-A2) (**Clinical and Laboratory Standards Institute, 2008**). Amphotericin B (Sigma Aldrich), itraconazole (Across Organics), isavuconazole (Sigma Aldrich), ravuconazole (Sigma Aldrich), posaconazole (Sigma Aldrich), voriconazole (Sigma Aldrich), fluconazole (Alfa Aesar), and ketoconazole (Alfa Aesar) were dissolved in dimethylsulfoxide (DMSO) to prepare stock solutions: 10 mg/ml for amphotericin B and itraconazole, 25 mg/ml for isavuconazole, ravuconazole, and posaconazole, and 50 mg/ml for voriconazole, fluconazole, and ketoconazole. These stocks were then diluted with liquid RPMI-1640 medium. Final concentrations of ketoconazole, itraconazole, fluconazole in the wells ranged from 0.125 to 64 μg/ml, while those of ravuconazole, isavuconazole and voriconazole ranged from 0.125 to 16 μg/ml. In the case of posaconazole and amphotericin B, the range was from 0.125 to 8 μg/ml.

Hydrogen peroxide (Sigma Aldrich) was diluted in liquid YNB medium supplemented with leucine to get a stock solution of 100 mM. Final concentrations of the hydrogen peroxide in the wells ranged from 0 to10 mM. Inocula were prepared and diluted in liquid YNB medium supplemented with leucine.

Final concentrations of $FeSO_4$, $CuSO_4$, $ZnSO_4$, D-sorbitol and NaCl in the wells were 1-10 mM, 0.5-5 mM, 0.5-10 mM, 1-3 M, and 0.5-2.5 M, respectively.

Quinidine (Sigma Aldrich) and bleomycin sulfate (Sigma Aldrich) were dissolved in DMSO, cisplatin (Sigma Aldrich) was dissolved in 0.9% NaCl to prepare the stocks. These stocks were then diluted with liquid RPMI-1640 medium. Final concentrations of quinidine in the wells ranged from 1 to 10 mg/ml, while those of bleomycin sulfate ranged from 10 to 100 μg/ml. In case of cisplatin the range was from 0.1 to 1 mg/ml.

MIC90 (minimum inhibitory concentration) was defined as the lowest drug concentration leading to at least 90% reduction in growth of the test isolate.

3.21 *In vivo* interaction with *Galleria mellonella*

Spores were resuspended in an insect physiological saline (IPS, 200 ml: 150 mM NaCl, 5 mM KCl, 10 mM EDTA, 30 mM Na-citrate, 0.1 M Tris-HCl, pH 6.9). Larvae of wax moth (*G. mellonella*; BioSystem Technology, TruLarv), in groups of 20, were injected through the last right or left pro-leg into the hemocoel with $5x10^6$ spores in a volume of 20 µl using a sterile insulin syringe U-100 (BD Micro-Fine) and incubated at 25 °C in the dark. Untouched larvae and larvae injected with sterile IPS served as controls. Survival was determined every 24 hours over a period of 6 days. For each test group 20 larvae were used, experiments were repeated three times.

3.22 Lipid extraction and analysis

The experiment was carried out in three biological parallel experiments. For the lipid extraction strains were inoculated on solid YNB medium. Strains were incubated at 25 °C for four days. Mycelia were collected and grinded with liquid nitrogen. After that mycelia were lyophilized and stored at -20°C until lipid extraction. 5-6 mg of lyophilized mycelium of each strain was used for lipid extraction. Lipid extraction was performed in one step using ethyl acetate/2-propanol/water (60/30/10) according to **Bielawski et al. (2009)**, with some modifications as described. After addition of 80 µl water to 20 mg freeze-dried mycelium, lipides were extracted with 1 ml of the triphasic solvent system by sonication for 10 min followed by centrifugation at 20.000 x g for 10 min. The supernatant was removed, and the extraction was repeated once in a similar way. The combined supernatants were evaporated to dryness under nitrogen and the residue was dissolved in 200 µl of HPLC mobile phase „B". LC-HRMS measurements were performed by Dr. M. Varga at the Department of Microbiology using a DionexUltimate 3000 UHPLC system (Thermo Scientific) coupled to a Q Exactive Plus hybrid quadrupole-Orbitrap mass spectrometer (Thermo Scientific) operating with a heated electrospray interface (HESI). Metabolites were separated on an Discovery HS C-18 (150 x 2.1mm, 3µm) column (Supelco) termostated at 45 °C. Mobile phase A consisted of 5 mM of ammonium-acetate containing 0.1% acetic acid, while methanol/2-propanol (1/1) containing 5mM of ammonium-acetate and 0.1% acetic acid served as mobile phase B. Gradient elution program was applied as follows: 0-3 min: 75% B, 3-38 min: 100% B, 38-53 min: 100% B, 53-54 min: 75% B, 54-60 min: 75% B. The flow rate was kept at 0.2 mL/min, and the injection volume was 5 µL. All samples were analyzed in both positive and negative ionization mode using the following ion source settings: the temperature of

the probe heater and ion transfer capillary, spray voltage, sheath gas flow rate, auxiliary gas flow rate and S-lens RF level were set to 300 °C, 350 °C, 3.75 kV, 35 arbitrary unit, 10 arbitrary unit and 50 arbitrary unit, respectively. For data acquisition full-scan/data-dependent MS/MS method (Full MS/ddMS2) was applied, where the full scan MS spectra were acquired at a resolution of 70,000 from m/z 100 to 1200 with a maximum injection time of 100 ms. For every full scan, 10 ddMS2-scans were carried out with a resolution of 17,500 and a minimum automatic gain control target of 1.00×105. Isolation window was 1 m/z. Instrument control and data collection were carried out using Trace Finder 4.0 (Thermo Scientific) software. The raw data files were processed by Compound Discoverer 2.1 software for chromatographic alignment, compound detection, and accurate mass determination. Lipids were identified based on their exact mass and MS/MS fragmentation patterns.

3.23 Statistical analysis

All experiments were performed on three independent occasions. Values expressed as the mean ± standard deviation (SD) for the technical and biological replicates. Significance was calculated and assessed by unpaired t-test, paired t-test, one-way and two-way ANOVA using GraphPad Prism software version 8.00 and Microsoft excel software of the Microsoft Office package for Windows. Differences were considered significant at $p \leq 0.05$. Survival rates were evaluated by using Kaplan-Meier survival curves and analyzed with the log rank Gehan-Breslow-Wilcoxon test.

4. RESULTS AND DISCUSSION

4.1 Transcriptomic analysis

RNA-sequencing detected transcriptional changes in *M. lusitanicus* after cultivating it either aerobically or anaerobically (**Homa et al., 2022**). A total of 539 genes were differentially expressed (DEGs), of which 190 were upregulated (**Figure S1**) and 349 were downregulated (**Figure S2**) in anaerobic environment compared to aerobic environment. Our research was focused on the studying genes involved in the adaptive responses of *M. lusitanicus* to different stresses, including temperature stress, antifungal resistance, and those differentially expressed under anaerobiosis. *hsf1* and *hsf2*, encoding a heat shock factor protein 1 and 2; *nudix*, encoding nucleoside diphosphate-linked moiety X; *pho84*, encoding inorganic phosphate (Pi) uptake porter; *fen2*, encoding pantothenate:H+ symporter; *qdr2d*, encoding quinidine resistance protein 2d were selected for further studies. *hsf1*, *hsf2*, *nudix*, and *qdr2d* were upregulated, and *fen2* and *pho84* were downregulated under anaerobiosis (log2 fold-changes are shown in **Table 1**).

Table 1. List and description of differentially expressed genes (DEGs) of *M. lusitanicus* selected for further studies. KOG – Eukaryotic Orthologous Group.

log2 fold-change	Protein ID	Gene ID	Name in this study	KOG	KOG class	Description
5.967190113	123815	gw1.01.1197.1	*hsf1*	Information storage and processing	Transcription	Heat shock transcription factor
3.766593287	125667	gw1.01.1486.1	*hsf2*			
4.956521239	154932	fgenesh1_kg.01_#_279_	*nudix*	Cellular processes and signaling	Signal transduction mechanisms	Diadenosine and diphosphoinositol polyphosphate phosphohydrolase
-5.198111244	155237	fgenesh1_kg.02_#_110_#_306_1_CCIA_CCIB_EXTA	*pho84*	Metabolism	Inorganic ion transport and metabolism	Inorganic phosphate transporter
-6.147876616	156313	fgenesh1_kg.04_#_355_#_1734_1_CCIA_CCIB_EXTA	*fen2*	Metabolism	Carbohydrate transport and metabolism	Permease of the major facilitator superfamily
5.853890338	160673	fgenesh1_pg.02_#_1277	*qdr2d*	Poorly characterized	General function prediction only	Predicted major facilitator superfamily transporter

4.2 qRT-PCR validation of RNA-Seq analysis

4.2.1 Transcription of the selected genes under aerobic and anaerobic conditions

To validate the results of RNA-Seq analysis, transcription of selected differentially expressed genes (i.e., *hsf1*, *hsf2*, *nudix*, *pho84*, *fen2* and *qdr2d)* were assayed by qRT-PCR. New samples of *M. lusitanicus* were exposed to the same test (anaerobic) conditions as the samples used in RNA-seq. Results of qRT-PCR analysis confirmed data obtained in RNA-Seq analysis (**Figure 11**).

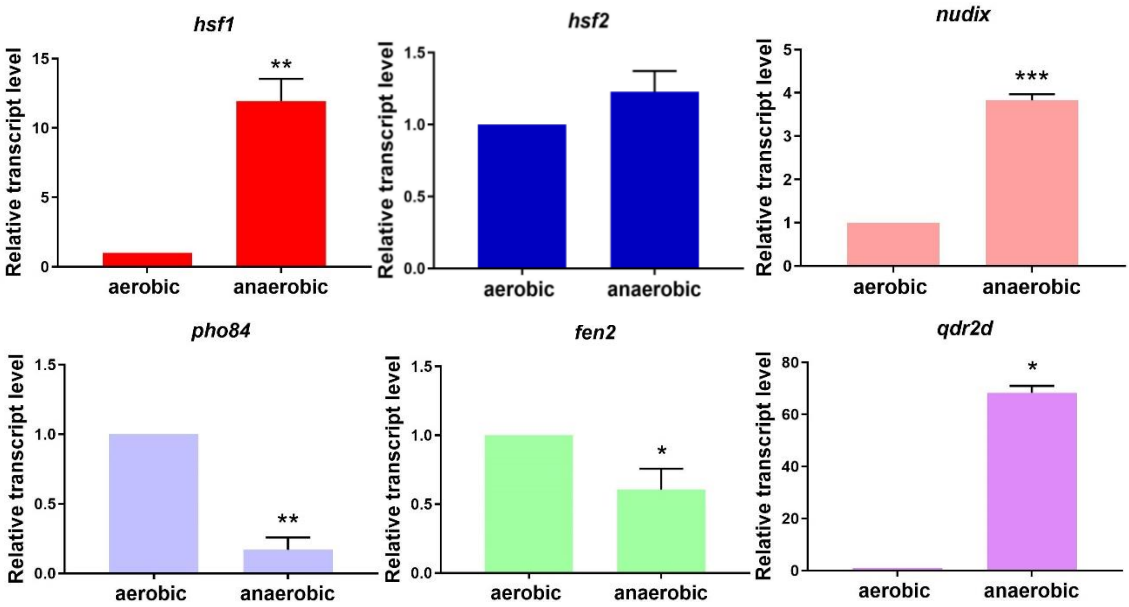

Figure 11. Relative transcript levels of the *hsf1, nudix, pho84, fen2* and *qdr2d* genes under anaerobic condition. MS12 was grown in YNB broth at 25 °C under aerobic or anaerobic conditions respectively for 4 days. Transcript level of each gene measured after aerobic cultivation was taken as 1. The presented values are averages of three independent experiments; error bars indicate standard deviation. Values indicated by asterisks significantly differed from the value taken as 1 according to the statistical method paired t-test (* $p < 0.05$; ** $p < 0.01$; *** $p < 0.01$).

The differential expression of *hsf1*, *nudix*, *qdr2d*, *fen2*, and *pho84* highlights the plasticity of the fungal transcriptome in response to environmental cues. Our study revealed significant changes in the expression levels of tested genes when *M. lusitanicus* was subjected to anaerobic conditions. Notably, the relative transcript levels of *hsf1*, *nudix*, and *qdr2d* showed a significant increase under oxygen-limited conditions. While

fen2 and *pho84* were significantly downregulated in response to the same condition. These findings suggest that *M. lusitanicus* adapts to oxygen limitation by modulating the expression of specific genes involved in various cellular processes. It is worth noting that there is a paucity of research concerning the expression of *hsf1*, *hsf2*, *nudix*, *pho84*, *fen2*, and *qdr2d* under oxygen limitation in *M. lusitanicus*. To contextualize our findings, we refer to related studies conducted in other fungal species.

In *Aspergillus nidulans*, transcription of *nudix hydrolase A* (*ndxA*) was found to be upregulated under oxygen limitation (**Shimizu et al., 2012; Shimizu and Takaya, 2013**). Additionally, in the well-studied yeast species *S. cerevisiae*, the *pho84* gene was reported to be downregulated under anaerobic conditions (**Rintala et al., 2011**). *Lichtheimia corymbifera* genome contains 24 *hsf* genes, aligning with its established tolerance to elevated temperatures (**Schwartze et al., 2014**). This expansion of the *hsf* gene family appears to be a common feature among all Mucorales.

In *M. lusitanicus*, *hsf1* and *hsf2* genes exhibited increased activity under hypoxic conditions, suggesting that various members of the *hsf* family serve additional roles in responding to diverse stressors and environmental growth conditions.

4.2.2 Relative transcript levels of the *hsf1* and *hsf2* genes of *M. lusitanicus* at different temperatures

Expression of *hsf* genes has a crucial role in temperature-dependent responses of opportunistic human fungal pathogens, such as *C. albicans*, *C. neoformans* and *A. fumigatus* (**Veri et al., 2018**). Hsfs are structurally and functionally conserved proteins that respond to diverse cellular and environmental signals, ultimately regulating gene expression and aiding in stress adaptation (**Morano et al., 1999; Sakurai and Enoki, 2010**).

The genome of *M. lusitanicus* contains a total of 20 *hsf* genes. In our research, we investigated two of them, *hsf1* (ID:123815) and *hsf2* (ID:125667) based on their differential expression after aerobic and anaerobic growth. Expression of *hsf1* and *hsf2* in response to various temperatures (i.e., 20, 25, 30 and 35 °C) and oxygen levels during continuous cultivation for four days were checked. The results revealed distinct temperature-related expression patterns for *hsf1* and *hsf2*. Under continuous aerobic conditions, *hsf1* exhibited significant upregulation at 20 and 30 °C compared to its transcriptional activity at 25 °C. In contrast, *hsf2* demonstrated a significantly higher relative transcript level at 35 °C under aerobic conditions. Under anaerobic conditions,

hsf1 was significantly upregulated at 20 °C, while *hsf2* showed upregulation at 35 °C (**Figure 12**). These findings suggest that *hsf1* and *hsf2* are both responsive to changes in temperature and oxygen levels in *M. lusitanicus*.

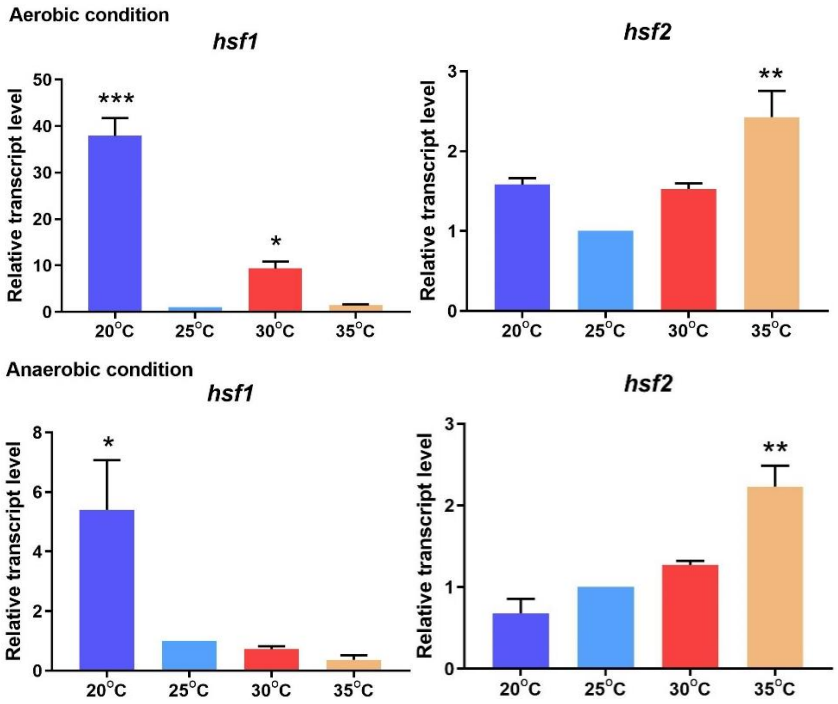

Figure 12. Relative transcript levels of the *hsf1* and *hsf2* genes of *M. lusitanicus* at different cultivation temperatures under aerobic and anaerobic conditions. MS12 was grown in YNB liquid medium; transcript level of each gene measured at 25 °C was taken as 1. The presented values are averages of three independent experiments; error bars indicate standard deviation. Values indicated by asterisks significantly differed from the value taken as 1 according to the statistical method unpaired t-test (* $p < 0.05$; ** $p < 0.01$; *** $p < 0.001$).

Genome of *C. neoformans* encodes three *hsf* genes – *hsf1*, *hsf2* and *hsf3*. When exposed to a temperature upshift from 25 °C to 42 °C, *hsf1* undergoes downregulation, while *hsf2* and *hsf3* are induced in expression. Loss of *hsf3* in *C. neoformans* leads to a decreased rate of cell survival under lethal temperature conditions (**Yang et al., 2017; Gao et al., 2022**). In *C. albicans*, *hsf1* gene was upregulated as the temperature increased to 42°C (**Leach and Cowen, 2014**).

The temperature-related expression patterns of *hsf1* and *hsf2* genes in *M. lusitanicus* imply their potential roles in regulating cellular processes related to cold and

heat stresses. These genes' responsiveness to both temperature and oxygen levels makes them intriguing candidates for further characterization.

4.2.3 Relative transcript levels of *nudix*, *pho84*, *fen2* and *qdr2d* genes after amphotericin B treatment

nudix, *pho84*, *fen2* and *qdr2d* genes have been identified as playing a role in the susceptibility of different fungal pathogens to antifungal drugs. They are all involved in different aspects of cellular functions related to drug resistance (**Stolz and Sauer, 1999; Costa et al., 2013; Lee et al., 2014; Jakab et al., 2021**). Since amphotericin B is the most active drug that is used against Mucorales (**Skiada et al., 2018; Borman et al., 2021; Smith and Lee, 2022**) we analyzed the relative transcript level of these genes in *M. lusitanicus* in response to this antifungal agent. Among the tested genes only *qdr2d* was significantly upregulated in response to amphotericin B treatment under aerobic and anaerobic conditions (**Figure 13 and Figure 14**).

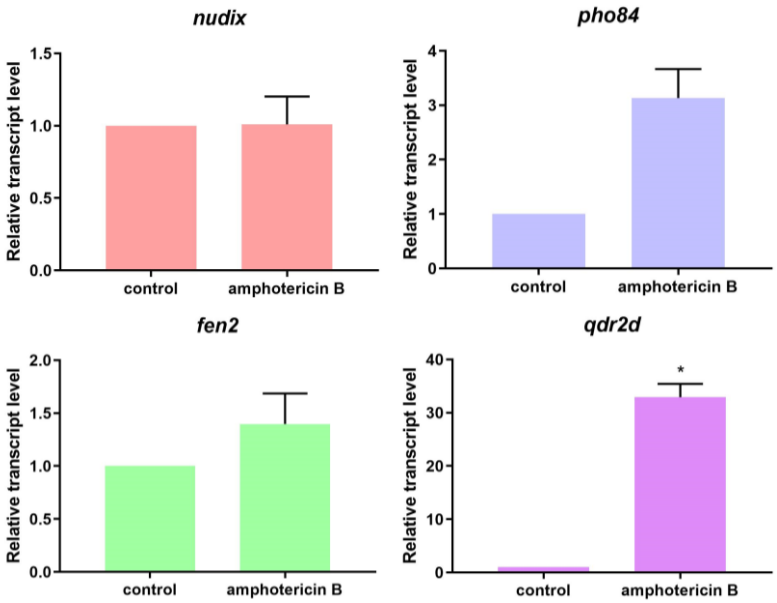

Figure 13. Relative transcript levels of the *nudix*, *pho84*, *fen2* and *qdr2d* genes after amphotericin B treatment under aerobic condition. MS12 was grown in RPMI-1640 liquid medium at 25 °C; Transcript level of each gene measured in the untreated control was taken as 1. The presented values are averages of three independent experiments; error bars indicate standard deviation. Relative transcript values followed by asterisk significantly different from the untreated control according to the paired t-test (* $p < 0.05$).

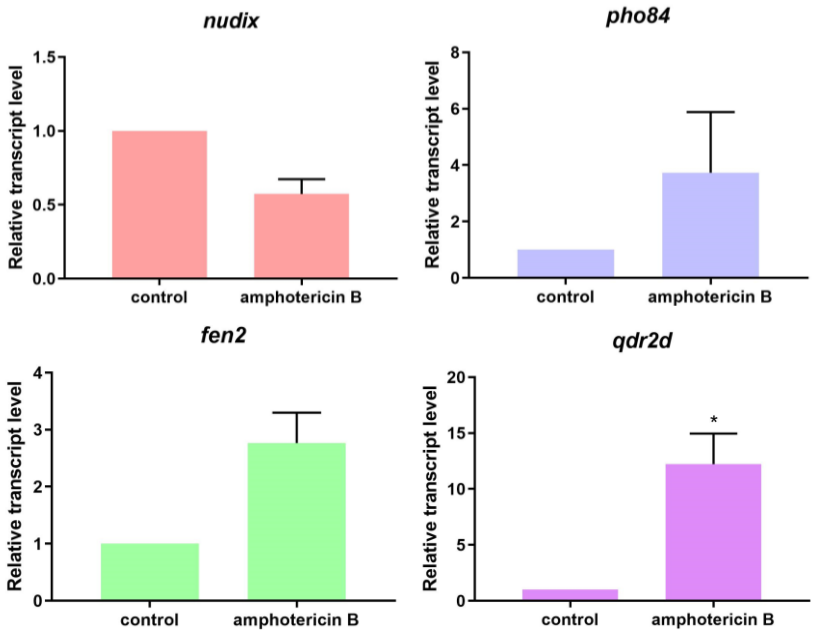

Figure 14. Relative transcript levels of the *nudix*, *pho84*, *fen2* and *qdr2d* genes after amphotericin B treatment under anaerobic condition. MS12 strain was grown in 50 ml RPMI-1640 liquid medium at 25 °C. Transcript level of each gene measured in the untreated control was taken as 1. The presented values are averages of three independent experiments; error bars indicate standard deviation. Relative transcript values followed by asterisk significantly different from the untreated control according to the paired t-test (* $p < 0.05$).

nudix has a role in maintaining cellular integrity by repairing damaged nucleotides. It regulates intracellular levels of toxic metabolites and responds to oxidative stress (**Shimizu et al., 2012; Shimizu and Takaya, 2013**). It regulates sensitivity of *C. neoformans* to antifungals (**Lee et al., 2014**). *pho84* encodes for a phosphate transporter protein involving in ion homeostasis and metabolic processes (**Jensen et al., 2003; Anemaet and van Heusden, 2014; Canadell et al., 2015; Austin and Mayer, 2020**). In *C. albicans*, *pho84* is crucial for signaling cell wall integrity and enhancing resistance against cell wall stress (**Liu et al., 2020**), as well as promoting phosphate-dependent growth and morphogenesis (**Liu et al., 2017**), and virulence (**Liu et al., 2018**). *fen2* encodes for a transmembrane protein involved in iron metabolism and transport. It contributes to resistance to fenpropimorph in *S. cerevisiae* (**Stolz and Sauer, 1999**). *qdr2* encodes a multidrug transporter that pumps out antifungals from fungal cells (**Nunes et al., 2001; Vargas et al., 2004; Tenreiro et al., 2005; Teixeira et al., 2010**). In *C.*

glabrata, overexpression of *qdr2* is associated with increased resistance to miconazole, clotrimazole and ketoconazole (**Costa et al., 2013**; **Widiasih Widiyanto et al., 2019; Santos et al., 2020**). The significant upregulation of *qdr2d* in response to amphotericin B under aerobic and anaerobic conditions suggested its potential role in the antifungal resistance of *M. lusitanicus*. Therefore, *qdr2d* was selected for further studies.

4.3 Transcription analysis of the *qdr2* genes of *M. lusitanicus*

4.3.1 Relative transcript levels of the *qdr2* genes during the cultivation period

The *M. lusitanicus* genome contains four *qdr2* genes encoding Qdr2 proteins, i.e., – *qdr2a* (protein ID: 42380), *qdr2b* (protein ID: 138979), *qdr2c* (protein ID: 152822) and *qdr2d* (protein ID: 160673). Expression of the *qdr2s* was analyzed after 1-, 2-, 3- and 4-days of cultivation (**Figure 15**).

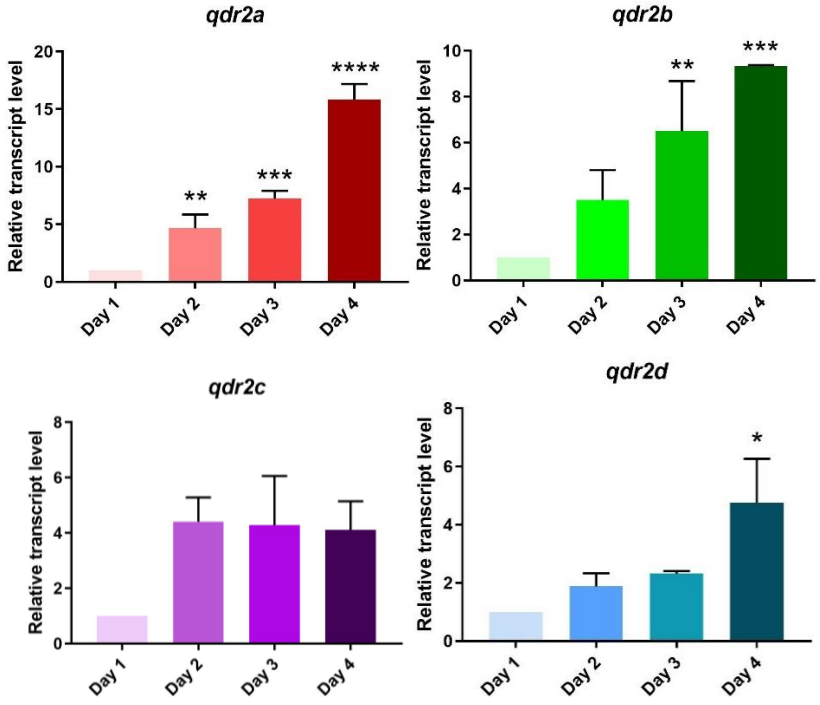

Figure 15. Relative transcript levels of four *qdr2* genes of *M. lusitanicus* during cultivation period at 25°C on YNB medium under aerobic condition. Relative transcript levels of *qdr2* genes measured after 24 h post-inoculation was taken as 1. The presented values are averages of three independent experiments; error bars indicate standard deviation. Values indicated by asterisks significantly differed from the value taken as 1 according to the statistical method one-way ANOVA (* $p < 0.05$; ** $p < 0.01$; *** $p < 0.001$; **** $p < 0.0001$).

qdr2a and *qdr2b* exhibited similar patterns in their expression levels, which increased in parallel with the cultivation time. On the other hand, the expression of *qdr2d* peaked with a 5-fold increase on the fourth day of cultivation.

Relative transcript levels of *qdr2a*, *qdr2b*, *qdr2c* and *qdr2d* genes during the cultivation period were also compared with that of the *qdr2d* gene at 24 h. Relative transcript levels of *qdr2a, qdr2b* and *qdr2d* significantly increased on the fourth day of cultivation. Meanwhile, *qdr2c* demonstrated the highest expression on the third day. These findings suggested that *qdr2* genes are expressed differently throughout the life cycle of *M. lusitanicus* and highlighted the complexity of *qdr2* regulation. It should be also mentioned that *qdr2* genes were predominantly expressed during the hyphal phase of *M. lusitanicus* (**Figure 16**).

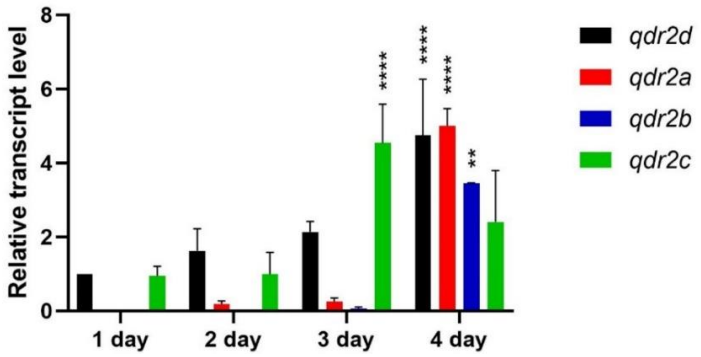

Figure 16. Relative transcript levels of four *qdr2* genes of *M. lusitanicus* during cultivation period at 25 °C on YNB medium under aerobic condition. Transcript levels of *qdr2d* gene measured after 24 h post-inoculation was taken as 1. The presented values are averages of three independent experiments; error bars indicate standard deviation. Values indicated by asterisks significantly differed from the value taken as 1 according to the statistical method two-way ANOVA (** $p < 0.01$; **** $p < 0.0001$).

4.3.2 Relative transcript levels of the *qdr2* genes of *M. lusitanicus* at different temperatures

Analysis of the relative transcript levels of *qdr2* genes under varying cultivation temperatures and aerobic/anaerobic conditions has unveiled a complex pattern of gene expression. Under aerobic conditions, temperature played a significant role in modulating the expression of these genes. At 20 °C, *qdr2a* and *qdr2c* were significantly downregulated, suggesting a potential temperature-sensitive response in these genes. In

contrast, at 15 °C, *qdr2c* and *qdr2d* exhibited significantly higher expression levels, indicating a preference for lower temperatures in their transcription. At 35 °C, *qdr2b* was downregulated, while *qdr2d* was upregulated, suggesting a dynamic response to higher temperatures within the *qdr2* gene family (**Figure 17**).

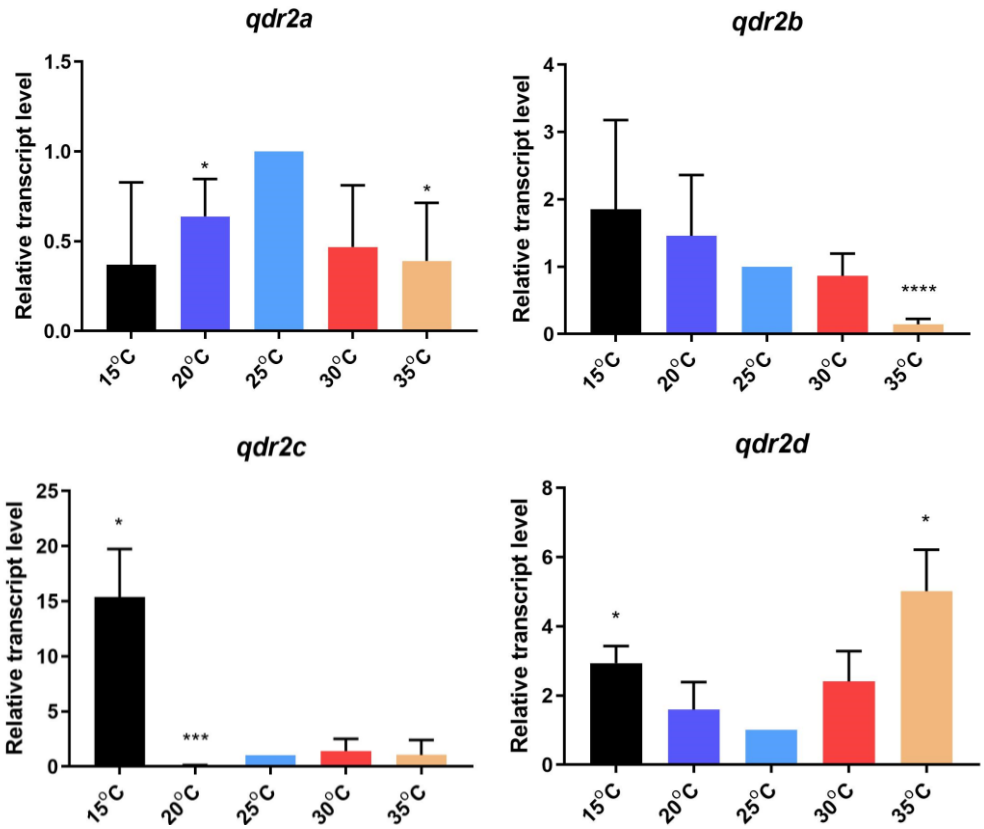

Figure 17. Relative transcript levels of four *qdr2* genes of *M. lusitanicus* at different cultivation temperatures under aerobic condition. MS12 was grown in YNB liquid medium; transcript level of each gene measured at 25 °C was taken as 1. The presented values are averages of three independent experiments; error bars indicate standard deviation. Values indicated by asterisks significantly differed from the value taken as 1 according to the statistical method unpaired t-test (* $p < 0.05$; *** $p < 0.001$; **** $p < 0.0001$).

Under anaerobic conditions, the effect of different temperatures on *qdr2* genes expression was also observed. At 15 °C, all *qdr2* genes showed significant downregulation. At 20 °C, *qdr2a*, *qdr2b*, and *qdr2c* exhibited lower relative transcript levels, while *qdr2d* was significantly upregulated. This indicates that *qdr2d* may play a

distinct role in response to anaerobiosis at this temperature. At 30 and 35 °C, *qdr2a*, *qdr2b*, and *qdr2c* were upregulated under anaerobic conditions, highlighting a temperature-dependent response for these genes (**Figure 18**).

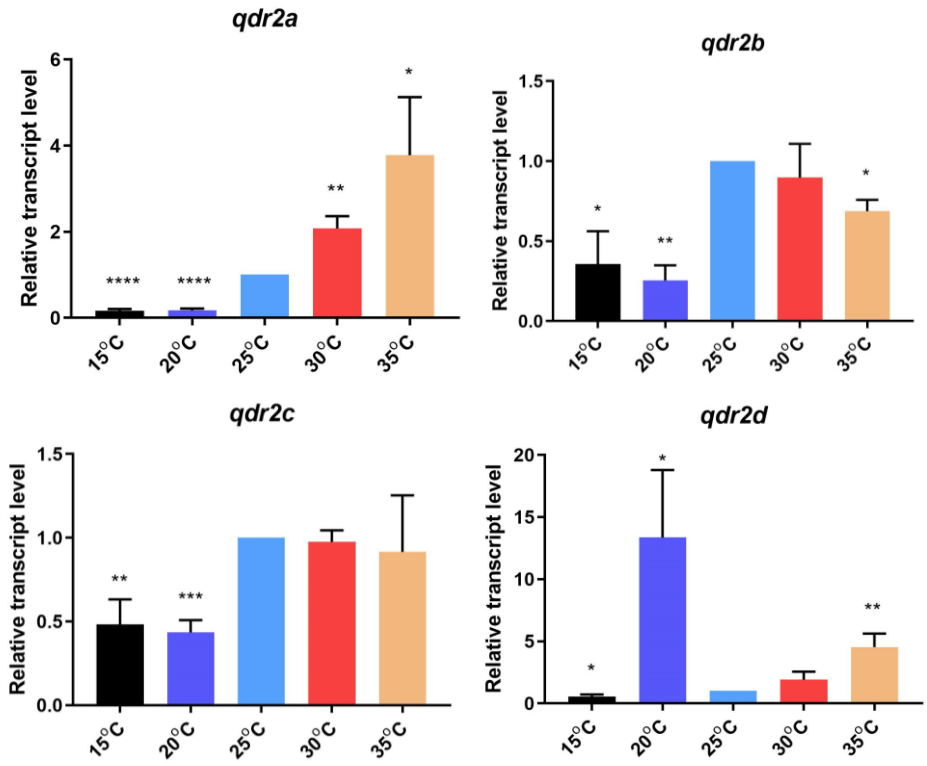

Figure 18. Relative transcript levels of four *qdr2* genes of *M. lusitanicus* at different cultivation temperatures under anaerobic condition. MS12 was grown in YNB liquid medium; transcript level of each gene measured at 25 °C was taken as 1. The presented values are averages of three independent experiments; error bars indicate standard deviation. Values indicated by asterisks significantly differed from the value taken as 1 according to the statistical method unpaired t-test (* $p < 0.05$; ** $p < 0.01$; *** $p < 0.001$; **** $p < 0.0001$).

Heat maps were generated to summarize the transcription patterns of the different *qdr2* genes affected by a range of temperatures and show that some genes had similar expression patterns while others show distinct responses. Under aerobic condition, *qdr2a* and *qdr2b* consistently showed similar expression patterns, being downregulated at 15, 20, 30, and 35 °C. *qdr2c* was downregulated at 20 °C and upregulated at 15 °C. *qdr2d* showed a slightly different pattern, being slightly upregulated at 15, 20, 30, and 35 °C

(**Figure 19A**). In a previous study *qdr2* gene was upregulated at 15 °C in P5 wine strain of *S. cerevisiae* (**García-Ríos et al., 2014**). Under anaerobic conditions, all *qdr2* genes were downregulated at 15 °C. At 20 °C, *qdr2a*, *qdr2b*, and *qdr2c* were downregulated, while *qdr2d* showed increased relative transcript level. At 30 and 35 °C, *qdr2a* and *qdr2d* were slightly upregulated, while *qdr2b* was downregulated. *qdr2b* and *qdr2c* were downregulated at 35 °C (**Figure 19B**).

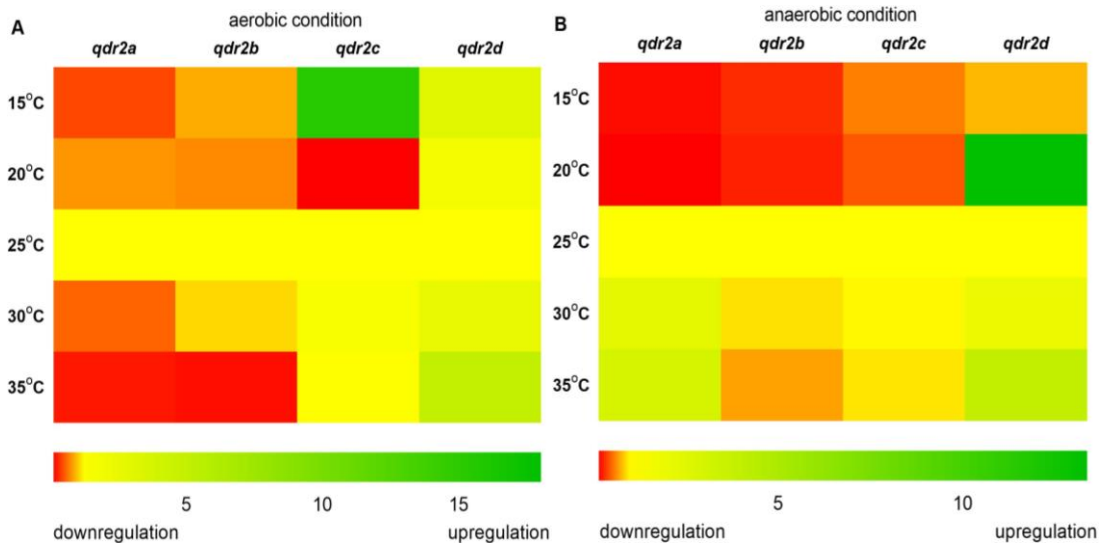

Figure 19. Heat maps of relative transcript levels of four *qdr2* genes in response to different cultivation temperatures under aerobic (A) and anaerobic (B) conditions. Red and green colors indicate down- and upregulation, respectively, while yellow corresponds to the transcription activity measured at 25 °C which was taken as 1.

Changes in temperature affects the fluidity of fungal cell membrane. Qdr2 proteins are members of MFS membrane-integrated transporters. Expression of *qdr2* genes can be affected by changes in membrane characteristics associated to temperature fluctuations. Further investigations into the functional significance of *qdr2*s temperature-mediated expression changes could provide insights into the adaptive mechanisms of *M. lusitanicus*.

4.3.3 Relative transcript levels of the *qdr2* genes after treatment with different antifungal agents

The effect of exposure of *M. lusitanicus* cells to the different antifungal agents on *qdr2* genes transcription was evaluated. The transcript levels of all four *qdr2* genes were

seen to increase upon voriconazole treatment under aerobic condition. Isavuconazole resulted in increased transcript levels for *qdr2a*, *qdr2b*, and *qdr2c*, while amphotericin B treatment led to increased transcript levels for *qdr2a*, *qdr2c*, and *qdr2d*. Ketoconazole treatment significantly elevated transcript levels of *qdr2a*, *qdr2b*, and *qdr2d*. Additionally, *qdr2a* and *qdr2d* were upregulated after the treatment with posaconazole and fluconazole. Interestingly, *qdr2d* showed significant upregulation after itraconazole treatment (**Figure 20**).

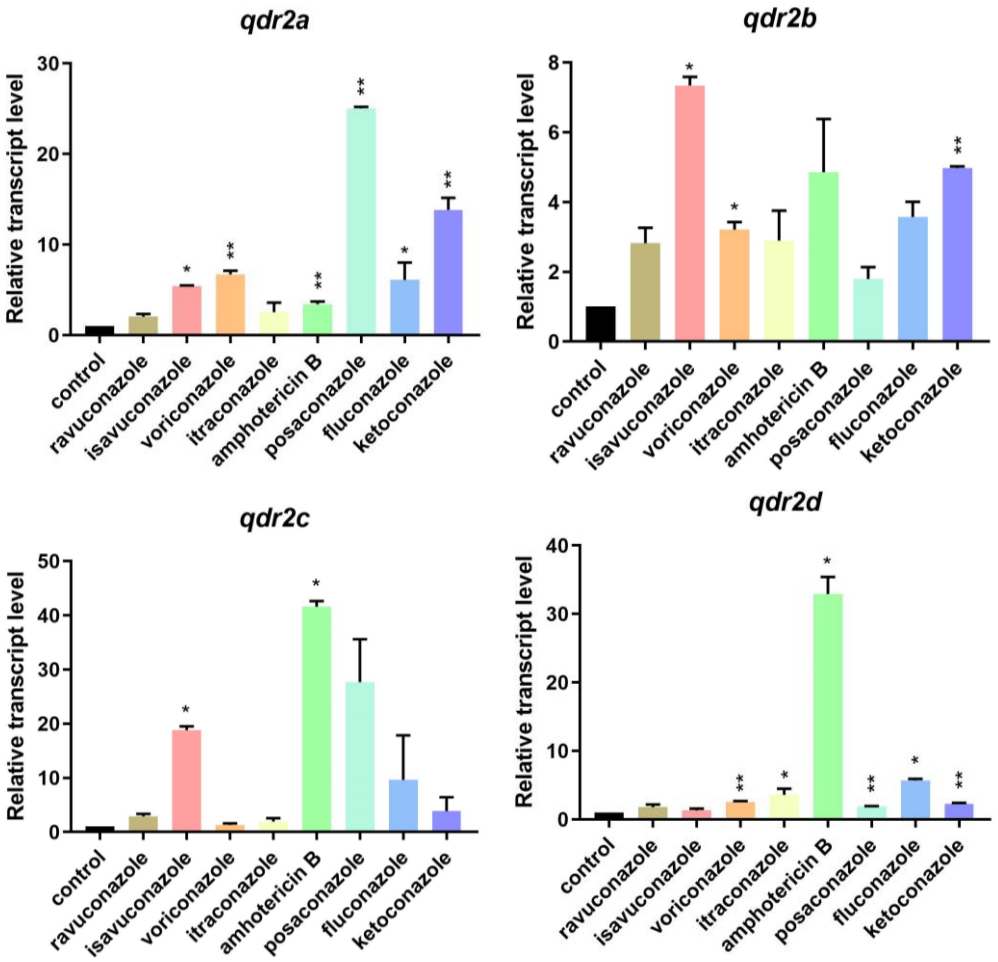

Figure 20. Relative transcript levels of the *qdr2* genes after antifungals treatment under aerobic condition. MS12 was grown in RPMI-1640 liquid medium at 25 °C; transcript level of each gene measured in the untreated control was taken as 1. The presented values are averages of three independent experiments; error bars indicate standard deviation. Values indicated by asterisks significantly differed from the value taken as 1 according to the statistical method paired t-test (* $p < 0.05$; ** $p < 0.01$).

Under anaerobic conditions, the response patterns of the *qdr2*s differed. *qdr2a* was downregulated when exposed to ravuconazole, but it showed significantly higher transcript level after isavuconazole treatment. *qdr2b* showed significantly lower transcript levels in response to treatment with ravuconazole, itraconazole and fluconazole. *qdr2c* demonstrated a significantly decrease in transcript level in response to voriconazole treatment. *qdr2d* was significantly upregulated upon to exposure to ravuconazole and amphotericin B (**Figure 21**).

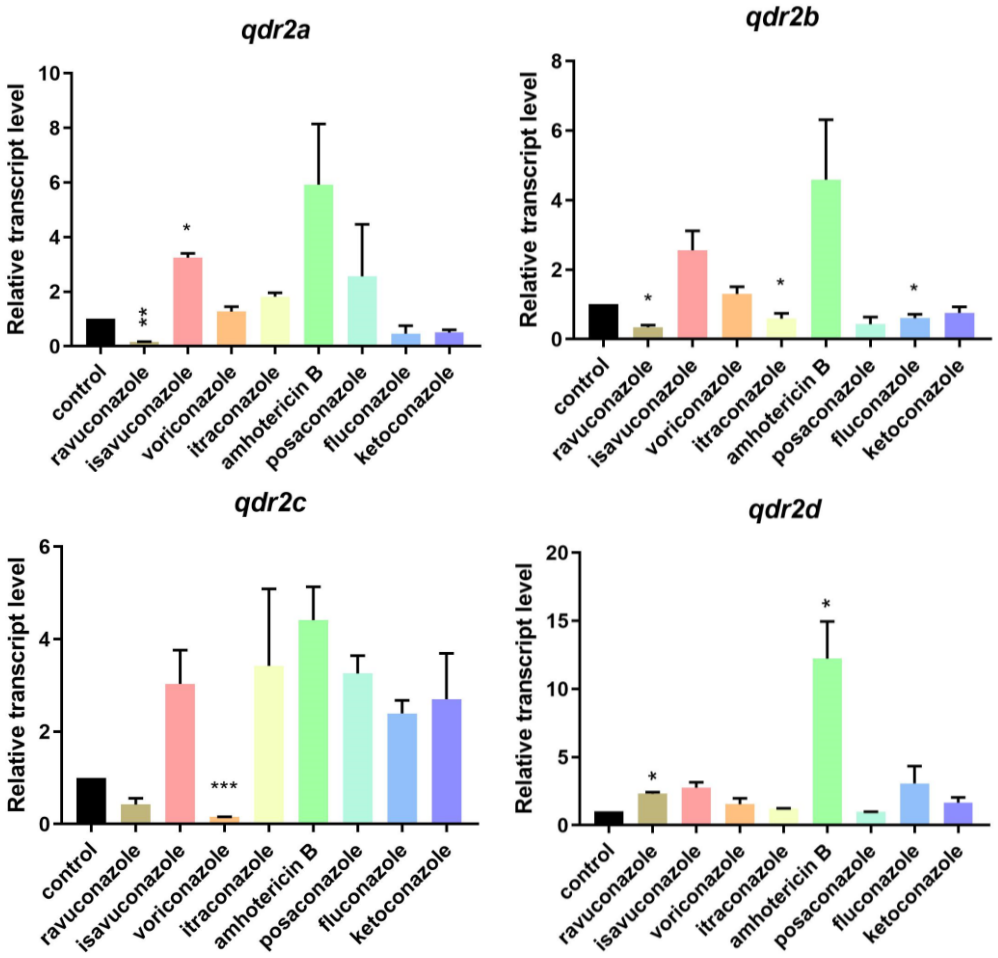

Figure 21. Relative transcript levels of the *qdr2* genes after antifungals treatment under anaerobic condition. MS12 was grown in RPMI-1640 liquid medium at 25 °C; transcript level of each gene measured in the untreated control was taken as 1. The presented values are averages of three independent experiments; error bars indicate standard deviation. Values indicated by asterisks significantly differed from the value taken as 1 according to the statistical method paired t-test (* $p < 0.05$; ** $p < 0.01$; *** $p < 0.001$).

A heat maps were created to summarize the results of the qRT-PCR experiments examining the impact of antifungal treatment on the expression of *qdr2* genes. After antifungal treatment in aerobic conditions, *qdr2* genes were generally upregulated or exhibited similar transcript levels to control sample (**Figure 22A**). Under anaerobic conditions, *qdr2a* had low transcript levels upon exposure to ravuconazole, fluconazole, and ketoconazole, but it was upregulated in the presence of isavuconazole, voriconazole, itraconazole, amphotericin B and posaconazole. *qdr2b* showed downregulation after treatment with ravuconazole, itraconazole, posaconazole, fluconazole and ketoconazole. *qdr2c* was upregulated after treatment with all tested antifungals except voriconazole. *qdr2d* exhibited high transcript levels in the presence of ravuconazole, isavuconazole, voriconazole, amphotericin B, fluconazole, and ketoconazole (**Figure 22B**).

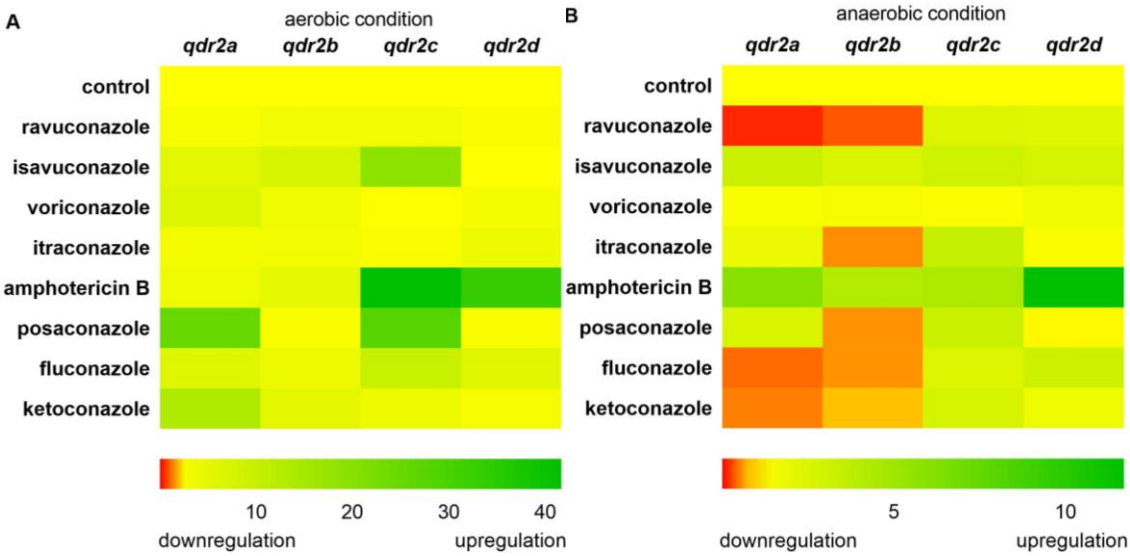

Figure 22. Heat map of relative transcript levels of *qdr2* genes in response to exposure to azoles under aerobic (A) and anaerobic (B) conditions. Red and green colors indicate down- and upregulation, respectively, while yellow corresponds to the transcription activity of the control.

In our experiments, *qdr2* genes showed different responses to antifungal agents under both aerobic and anaerobic cultivation conditions. In *S. cerevisiae*, ketoconazole treatment led to the upregulated expression of the *qdr2* gene (**Vargas et al., 2004**). Similarly, in *C. glabrata*, the expression of *qdr2* was associated with resistance to imidazole drugs, such as miconazole, tioconazole, clotrimazole, and ketoconazole. *qdr2*

was found to be upregulated in azole-resistant strains of *C. glabrata* (**Costa et al., 2013; Costa et al., 2016**). However, it is important to note that in *C. albicans*, the Qdr2 transporters were not observed to have a role in resistance against any known antifungal agents (**Shah et al., 2014**).

4.4 Characterization of the *hsf* and *qdr2* disruption mutants

4.4.1 Characterization of *hsf* disruption mutants

4.4.1.1 Construction of disruption mutants for the *hsf1* and *hsf2* genes using the CRISPR-Cas9 method

Single disruptions of *hsf1* and *hsf2* were carried out by integrating the *pyrG* uracil auxotrophy complementing selection marker gene into the corresponding gene via CRISPR-Cas9 technique (see **disruption cassette**, **Figure 10**), which resulted in the strains MS12+*Δhsf1* and MS12+*Δhsf2*, respectively. The applied technique is an *in vitro* CRISPR-Cas9 genome editing method adapted to *M. lusitanicus* (**Nagy et al., 2017**) and used routinely to construct knock-out mutants in our laboratory (**Nagy et al., 2019; Nagy et al., 2021; Bauer et al., 2023**). Successful gene disruption was proven by PCR amplification of the expected fragments in each case (**Figure 23**).

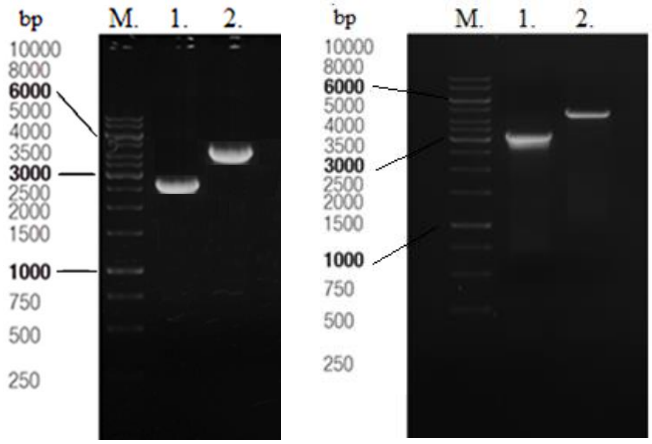

Figure 23. Confirmation of the disruption of the *hsf1* and *hsf2* genes in *M. lusitanicus* transformants. PCR was carried out with the primer pairs Mc123815P7 and Mc123815P8 for *Δhsf1,* Mc125667P1 and Mc125667P6 for *Δhsf2* (**Table S1**). Panel **A**: lane M – GeneRuler 1 kb DNA ladder (Thermo Scientific); lane 1 – MS12 (*hsf1* control), 2693 bp; lane 2 – MS12+*Δhsf1*, 4315 bp. Panel **B**: lane M – Gene Ruler 1 kb DNA ladder; lane 1 – MS12 (*hsf2* control) 3135 bp; lane 2 – MS12+*Δhsf2*, 4604 bp.

Transformation frequency was 1 for *hsf1* and 5 for *hsf2* per 10^5 protoplasts. qRT-PCR analysis proved the absence of the *hsf1* and *hsf2* transcripts in their respective mutants MS12+*Δhsf1* and MS12+*Δhsf2*. We selected one mutant per gene for further analysis. Mutants proved to be mitotically stable retaining the integrated fragment even after 20 cultivation cycles.

4.4.1.2 Colony growth of the *hsf* disruption mutants at different temperatures

Colony growth of the *hsf* mutants was checked at 15, 20, 25, 30 and 35 °C for 4 days. Disruption of *hsf1* and *hsf2* genes had no effect on the colony growth of *M. lusitanicus* at 25 °C. However, the colony diameter of MS12+Δ*hsf1* was significantly decreased at 15 and 20 °C and MS12+Δ*hsf2* showed significantly decreased growth at 15, 20, 30 and 35 °C compared to the control strain (**Figure 24**).

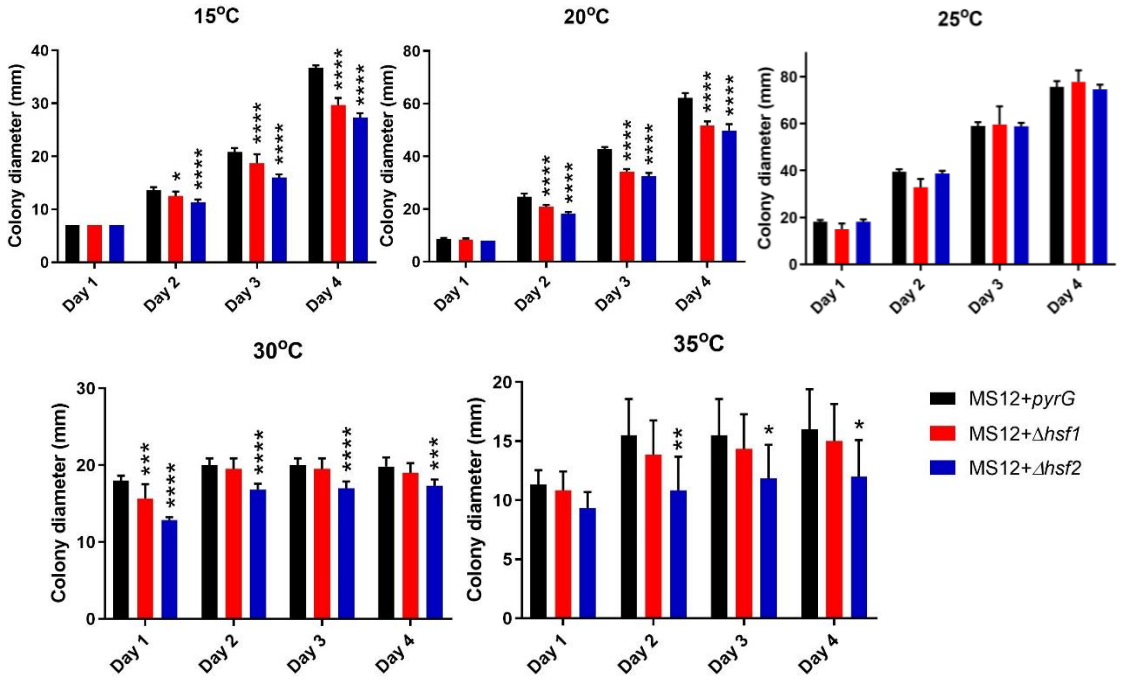

Figure 24. Colony diameter of the *hsf* disruption mutants and the MS12+*pyrG* strain at different temperatures. Strains were grown on YNB medium plates for four days. The presented values are averages; colony diameters were measured during three independent cultivations (error bars indicate standard deviation). Values indicated with asterisks significantly differed from the corresponding value of the MS12+*pyrG* strain according to the statistical method two-way ANOVA (*p < 0.05; **p < 0.01; ***p < 0.001; **** p < 0.0001).

Deletion of *hsf1* leads to lethality in *S. cerevisiae*, *C. albicans*, *A. fumigatus* and *Neurospora crassa* (**Wiederrecht et al., 1988; Bonner et al., 2000; Thompson et al., 2008; Nicholls et al., 2009; Fabri et al., 2021**). In *N. crassa hsf1* is required for the mycelial growth, and *hsf2* has an essential role for the asexual development (**Thompson et al., 2008**). In the mycoparasitic fungus *Coniothyrium minitans, hsf1* was upregulated at 37 and 45 °C, but it was downregulated at lower temperatures, e.g., at 4 and 10 °C (**Hamid et al., 2013**).

The results indicate a role of *hsf* genes in *M. lusitanicus* viability and growth under heat and cold stresses. *hsf1* might be involved in the adaptation to suboptimal temperatures and *hsf2* may have a role in low- and high-temperature adaptation.

4.4.1.3 Sporulation and germination ability of the *hsf* disruption mutants

The ability to sporulate and germinate is an essential trait for fungal growth and survival. Sporulation ability of *hsf1* and *hsf2* disruption mutants was investigated in comparison to the control MS12+*pyrG* strain (**Figure 25**).

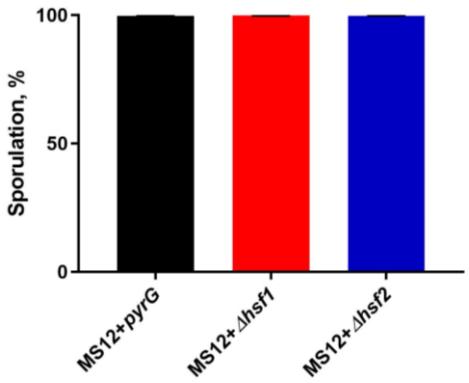

Figure 25. Sporulation of *hsf1* and *hsf2* disruption mutants and MS12+*pyrG* grown on MEA plates for 4 days at 25 °C. The inoculum size was 5×10^4 in each case. The presented values are averages; Spores were counted after three independent cultivations (error bars indicate standard deviation). Values were compared with the corresponding value of the MS12+*pyrG* strain according to the statistical method unpaired t-test.

Results showed that the sporulation ability of both *hsf1* and *hsf2* disruption mutants did not change compared to the control strain, suggesting that these two genes do not play a role in the regulation of the sporulation in *M. lusitanicus*. This finding is consistent with previous reports which indicate that some fungi have multiple pathways

for controlling sporulation, and mutation of one gene may not significantly impact the process if other mechanisms compensate for its loss (**Martinelli and Clutterbuck, 1971; Adams et al., 1998; Ajmal et al., 2022**).

Furthermore, the germination rate of the *hsf* disruption mutants was not significantly different from that of the control strain, suggesting that these mutations do not affect the early stages of fungal growth and development (**Figure 26**). Similarly, in the entomopathogenic fungus *Beauveria bassiana* deletion of *hsf1* did not affect conidial germination percentages at 25 °C compared to wild-type strain (**Zhou et al., 2018**).

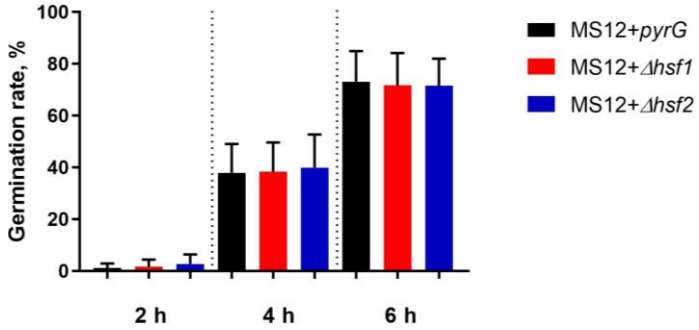

Figure 26. Germination rates of the sporangiospores of the *hsf* mutants and the MS12+*pyrG* strain. Spores (10^6 spores/ml) were incubated in liquid YNB medium for 6 h at 25 °C and then germinated spores were counted. The presented values are averages. Spores were counted after three independent cultivations (error bars indicate standard deviation). Values were compared with the corresponding value of the MS12+*pyrG* strain according to the statistical method one-way ANOVA.

4.4.1.4 Effect of detergents on the growth of the *hsf* mutants

In a study, a conditional Δ*hsf1* mutant of *C. albicans*, in which the expression of *hsf1* was regulated by the TET promoter (tetracycline), was shown to be sensitive to SDS (**Dhamgaye et al., 2014**). *Hsf1* of *C. albicans* responded with a slightly increased activity to SDS treatment (**Nicholls et al., 2009**). Conditional *hsfA* mutant of *A. nidulans*, in which the *hsfA* gene was under the control of the *Penicillium chrysogenum xylP* promoter (xylose), had a decreased colony growth in the presence of SDS (0.01 and 0.015%) (**Fabri et al., 2021**).

To test if the disruption of *hsf* genes affects the sensitivity of *M. lusitanicus* cells to membrane stressors, MS12+Δ*hsf1* and MS12+Δ*hsf2* mutants were grown in the

presence of detergents, such as SDS and Triton X-100. SDS was shown to affect the growth of the *hsf2* disruption mutant. MS12+Δ*hsf2* had a decreased colony growth on the fourth day of cultivation compared to the control MS12+*pyrG* strain (**Figure 27**).

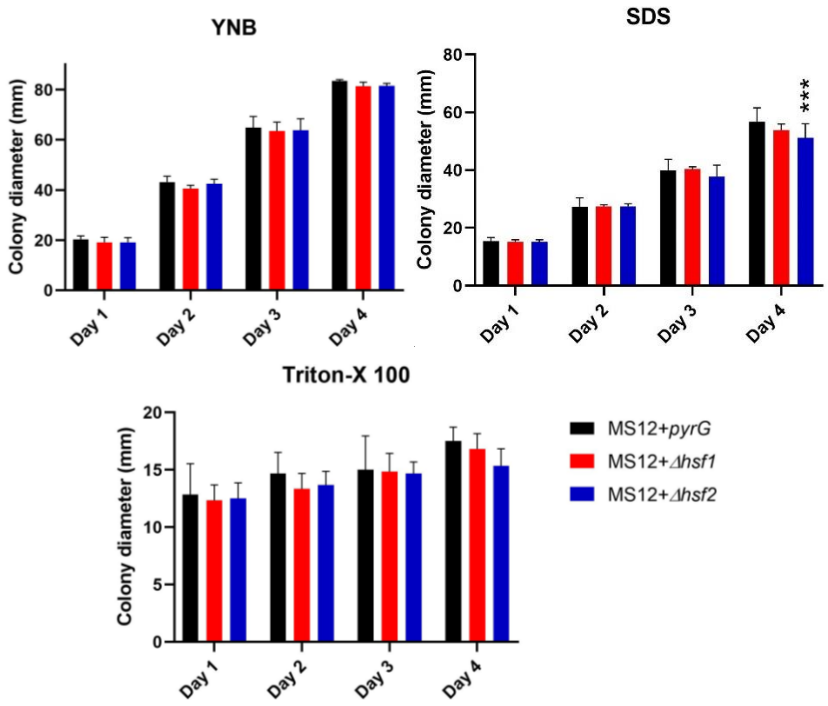

Figure 27. Effect of SDS and Triton X-100 on the colony growth of the *hsf* mutants compared to that of the MS12+*pyrG* strain. Strains were cultivated on YNB supplemented with SDS or Triton X-100 for 4 days at 25 °C. The presented values are from three independent cultivations (error bars indicate standard deviation). Values indicated with asterisks significantly differed from the corresponding value of the MS12+*pyrG* strain according to the statistical method two-way ANOVA (***p < 0.001).

4.4.1.5 Effect of cell wall stressors on the growth of the *hsf* mutants

Hsf1 has a role in maintaining the cell wall integrity of *B. bassiana* since the deletion of the encoding gene caused an increased sensitivity to CR, an increased hyphal cell wall fragility, changes in cell wall composition of the conidia, and less defined cell walls (**Zhou et al., 2018**). In *A. nidulans*, *hsfA* is upregulated in response to CR concentration ranging from 50 µg/ml to 200 µg/ml. Conditional *hsfA* mutant of *A. nidulans* had a decreased colony growth in the presence of CFW (25 and 50 µg/ml). These results indicate that *hsfA* is required to cope with the cell wall stress (**Fabri et al., 2021**). Conditional Δ*hsf1* mutant of *C. albicans* showed susceptibility to CR and CFW

(**Dhamgaye et al., 2014**). Similar results were obtained in case of the disruption of *hsf2* in *M. lusitanicus*. MS12+Δ*hsf2* had significantly decreased colony growth on the second, third and fourth days of cultivation upon to exposure to CFW compared to the control strain. Also, it showed weaker growth on the third and fourth days in the presence of CR. However, the disruption of *hsf1* in *M. lusitanicus* did not affect its sensitivity to cell wall stressors (**Figure 28**).

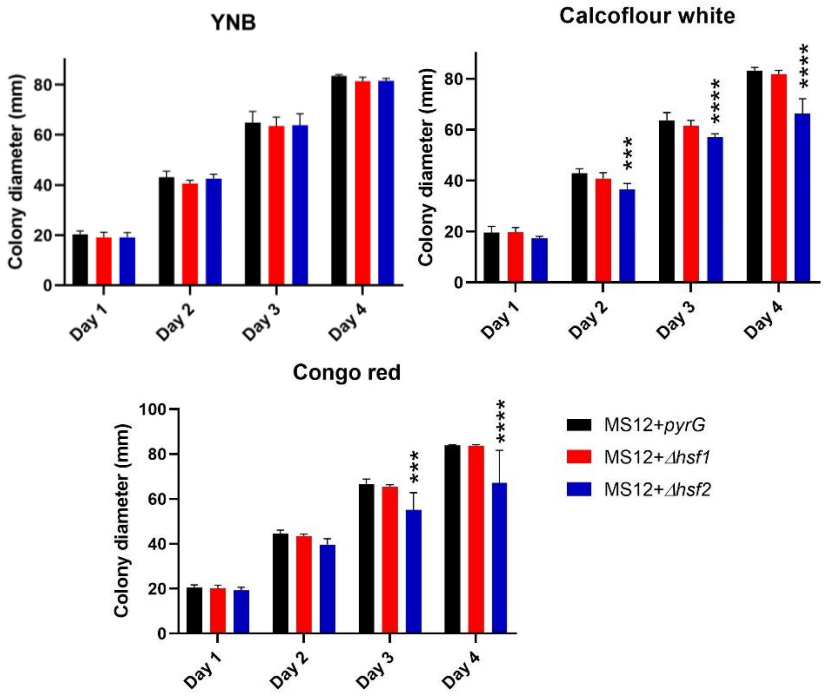

Figure 28. Effect of calcofluor white (CFW) and congo red (CR) on the colony growth of the *hsf* mutants compared to that of the MS12+*pyrG* strain. Strains were cultivated on YNB supplemented with CFW or CR for 4 days at 25 °C. The presented values are from three independent cultivations (error bars indicate standard deviation). Values indicated with asterisks significantly differed from the corresponding value of the MS12+*pyrG* strain according to the statistical method two-way ANOVA (***p < 0.001; ****p < 0.0001).

4.4.1.6 Virulence of the *hsf* mutants in *Galleria mellonella*

To examine whether Hsf has a potential role in the pathogenicity of *M. lusitanicus*, *G. mellonella* (i.e., wax moth larvae) was used as a non-vertebrate animal model. The use of *G. mellonella* has a high correlation with murine models of disseminated infection.

Healthy larvae are active and light colored, while larvae infected and killed by fungi are dark (**Chamilos et al., 2007; Fallon et al., 2012**).

Hsf1 increased virulence of *C. albicans* by binding to virulence, adhesion, and biofilm genes during heat shock (**Nicholls et al., 2011; Leach et al., 2016**). Previous studies showed a role of *hsf1* in the virulence of *B. bassiana* (**Zhou et al., 2018**). *Hsf1* disruption mutant of *C. minitans* showed a decreased parasitic ability compared to the parental strain (**Hamid et al., 2013**).

However, our results showed no significant differences in the survival rate of larvae infected with *hsf* disruption mutants and the MS12+*pyrG* control strain. This suggests that *hsf1* and *hsf2* genes have no role in the pathogenicity of *M. lusitanicus* in *G. mellonella* (**Figure 29**).

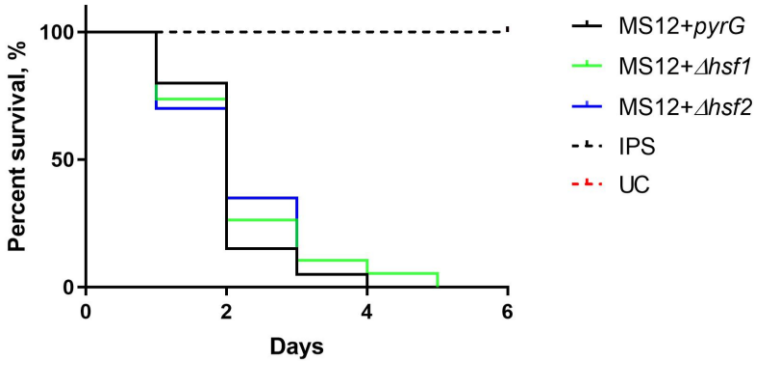

Figure 29. Survival of *G. mellonella* larvae infected with the *hsf1* and *hsf2* mutants and the control *M. lusitanicus* MS12+*pyrG* strains. The presented values are averages of three independent experiments, considering 10 larvae per condition per assay. Values were compared with the corresponding value of the MS12+*pyrG* strain according to the statistical method Gehan-Breslow-Wilcoxon test.

4.4.2 Characterization of *qdr2* disruption mutants

4.4.2.1 Construction of disruption mutants for the *qdr2a, qdr2b, qdr2c* and *qdr2d* genes using the CRISPR-Cas9 method

Single disruptions of *qdr2a*, *qdr2b*, *qdr2c* and *qdr2d* were carried out by integrating the *pyrG* selection marker gene into the corresponding gene via the CRISPR-Cas9 technique (see **disruption cassette, Figure 10**), which resulted in the strains MS12+*Δqdr2a*, MS12+*Δqdr2b,* MS12+*Δqdr2c* and MS12+*Δqdr2d*, respectively. Transformation frequencies were 11 for the disruption of *qdr2a*, 7 for *qdr2b*, 10 for *qdr2c*,

and 8 for *qdr2d* per 10^5 protoplasts. Successful gene disruption was proven by PCR amplifying the expected fragments in each case (**Figure 30**).

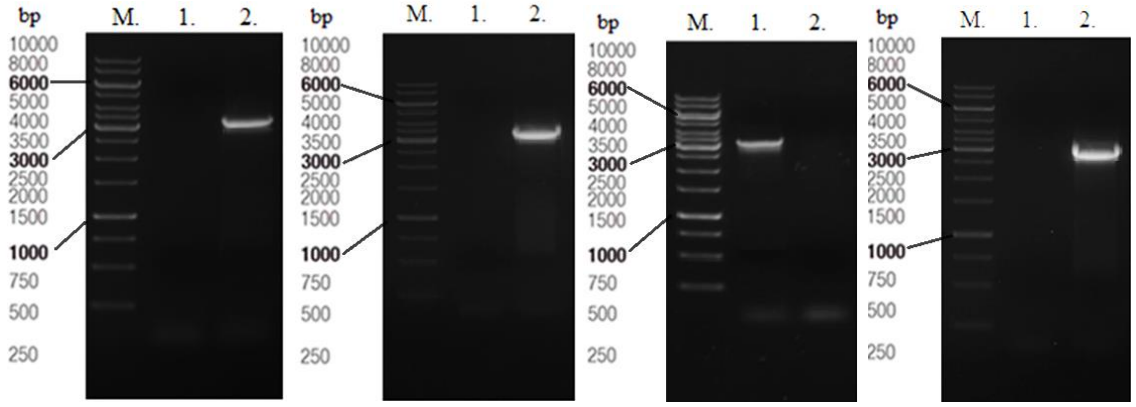

Figure 30. Confirmation of the disruption of the *qdr2a, qdr2b, qdr2c* and *qdr2d* genes in *M. lusitanicus* transformants. PCR was carried out with the primer pairs Mc42380P3 and Mc42380P8 for *Δqdr2a,* Mc138979P3 and Mc138979P8 for *Δqdr2b,* Mc152822P3 and Mc152822P8 for *Δqdr2c,* Mc160673P3 and Mc160673P8 for *Δqdr2d* (**Table S1**). Panel **A**: lane M - Gene Ruler; lane 1 - MS12 (*qdr2a* control), no product; lane 2 - MS12+*Δqdr2a*, 3305 bp. Panel **B**: lane M - Gene Ruler; lane 1 - MS12 (*qdr2b* control), no product; lane 2 - MS12+*Δqdr2b*, 3294 bp. Panel **C**: lane M - Gene Ruler; lane 1 - MS12+*Δqdr2c*, 3223 bp; lane 2 - MS12 (*qdr2c* control) no product. Panel **D**: lane M - Gene Ruler; lane 1 - MS12 (*qdr2d* control), no product; lane 2 - MS12+*Δqdr2d*, 3042 bp.

qRT-PCR analysis proved the absence of the *qdr2a, qdr2b, qdr2c* and *qdr2d* transcripts in their respective mutants, i.e., in MS12+*Δqdr2a,* MS12+*Δqdr2b,* MS12+*Δqdr2c* and MS12+*Δqdr2d*. We selected one mutant per gene for further analysis. Selected mutants proved to be mitotically stable retaining the integrated fragment even after 20 cultivation cycles.

4.4.2.2 Relative transcript levels of *qdr2* genes in the *qdr2* disruption mutants

Relative transcript levels of *qdr2* genes in the *qdr2* disruption mutants and MS12 strains were analyzed. Disruption of the *qdr2* genes led to a complete loss of their expression in their respective disruption mutants under aerobic and anaerobic conditions. At first, the expression of *qdr2* genes were checked under aerobic condition. After the

disruption of the *qdr2a* gene, relative transcript levels of *qdr2c* and *qdr2d* genes proved to be significantly upregulated. The disruption of *qdr2b* gene resulted in significantly increased transcript levels of *qdr2a*, *qdr2c* and *qdr2d* genes. Transcript levels of *qdr2a* and *qdr2b* significantly decreased in *qdr2d* disruption mutants. There might be some regulatory relationship between *qdr2* genes, where the loss of one of *qdr2* genes affects other *qdr2* genes expression. It indicates a compensatory response, where the loss of *qdr2b* function triggers increased expression of other *qdr2* genes to compensate for the missing function. (**Figure 31**).

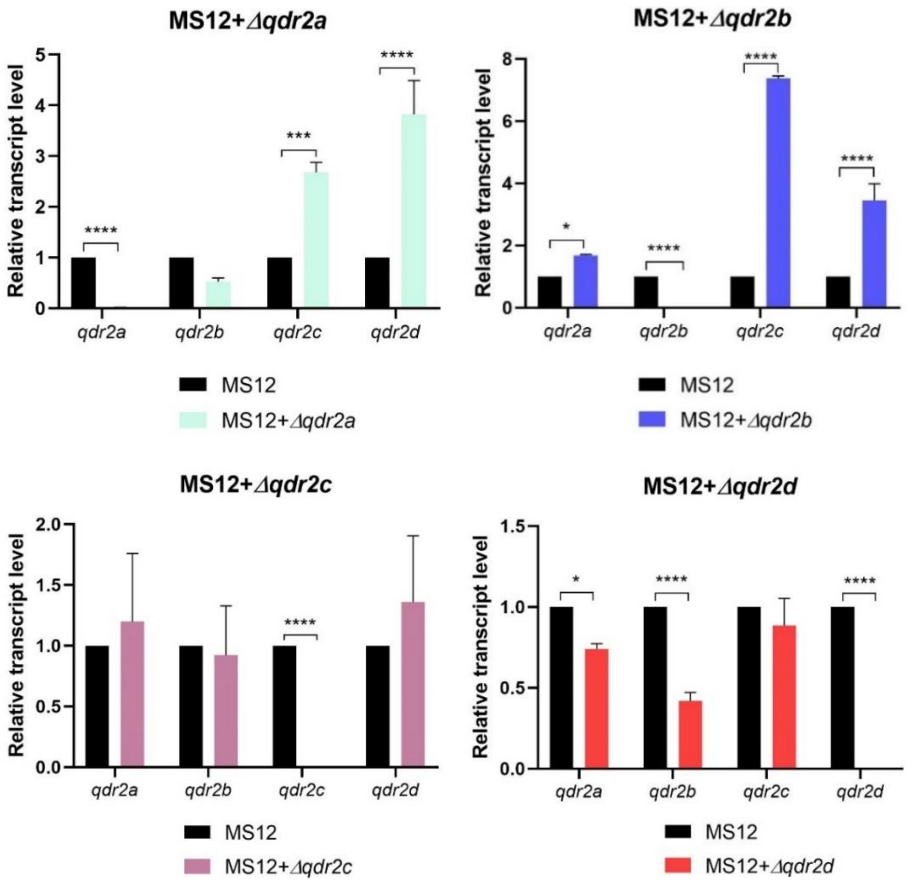

Figure 31. Relative transcript levels of *qdr2a, qdr2b, qdr2c* and *qdr2d* in the MS12+*Δqdr2a*, MS12+*Δqdr2b*, MS12+*Δqdr2c* and MS12+*Δqdr2d* mutants compared to that in the original MS12 strain under aerobic condition. Transcript level of each gene measured in the strain MS12 was taken as 1. The presented values are averages of three independent experiments (error bars indicate standard deviation). Values indicated with asterisks significantly differed from the corresponding value of the MS12 strain according to unpaired t-test (*$p < 0.05$; ***$p < 0.001$; **** $p < 0.0001$).

Under anaerobic conditions, we observed slight upregulation of *qdr2a* and *qdr2c* in the MS12+*Δqdr2b* mutant, suggesting that the absence of *qdr2b* may trigger a compensatory response in the expression of other *qdr2* genes. However, *qdr2b* was downregulated in MS12+*Δqdr2a* mutant, indicating a potential negative impact of the disruption of *qdr2a* gene on transporter function of Qdr2b protein during low oxygen stress. Additionally, *qdr2a* was upregulated in MS12+*Δqdr2d* mutant, showing that the disruption of *qdr2d* led to the activation of a compensatory response in the relative transcript level of the *qdr2a* gene (**Figure 32**).

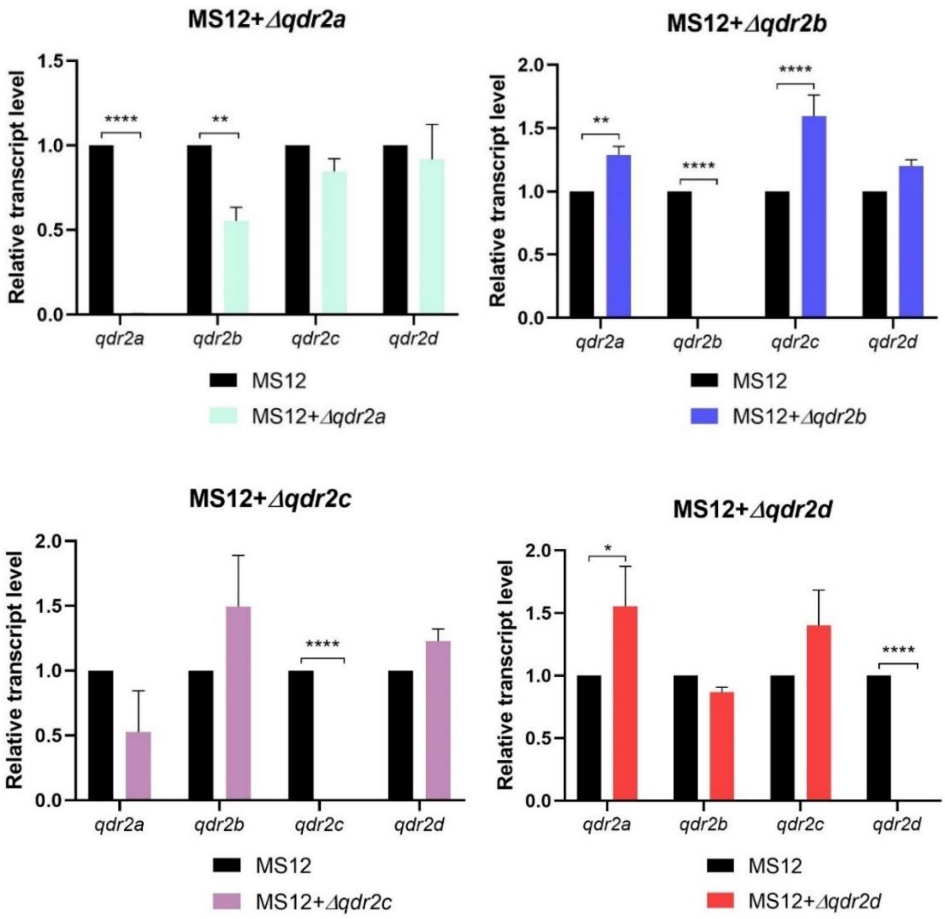

Figure 32. Relative transcript levels of *qdr2a, qdr2b, qdr2c* and *qdr2d* in the MS12+*Δqdr2a*, MS12+*Δqdr2b*, MS12+*Δqdr2c* and MS12+*Δqdr2d* mutants compared to that in the original MS12 strain under anaerobic condition. Transcript level of each gene measured in the strain MS12 was taken as 1. The presented values are averages of three independent experiments (error bars indicate standard deviation). Values indicated with asterisks significantly differed from the corresponding value of the MS12 strain according to unpaired t-test (**$p < 0.01$; **** $p < 0.0001$).

These results suggest that the regulation of the *qdr2* genes is interconnected in *M. lusitanicus*. The disruption of one *qdr2* gene can affect the expression of others. The phenomenon, where the transcription of another gene significantly increases when one gene is knocked out and the cell attempts to compensate for the missing activity, has also been observed in other genes that exist in multiple copies in the genome *M. lusitanicus* (**Nagy et al., 2019; Nagy et al, 2021; Bauer et al., 2023**).

4.4.2.3 Colony growth of the *qdr2* disruption mutants at different temperatures

Since *qdr2* genes differentially responded to temperature changes (**Figure 17 and Figure 18**), colony growth of MS12+*Δqdr2a*, MS12+*Δqdr2b,* MS12+*Δqdr2c* and MS12+*Δqdr2d* mutants at different temperatures were analyzed. Colony growth of mutants was not different compared to the control strain at 20 and 25 °C (**Figure 33**).

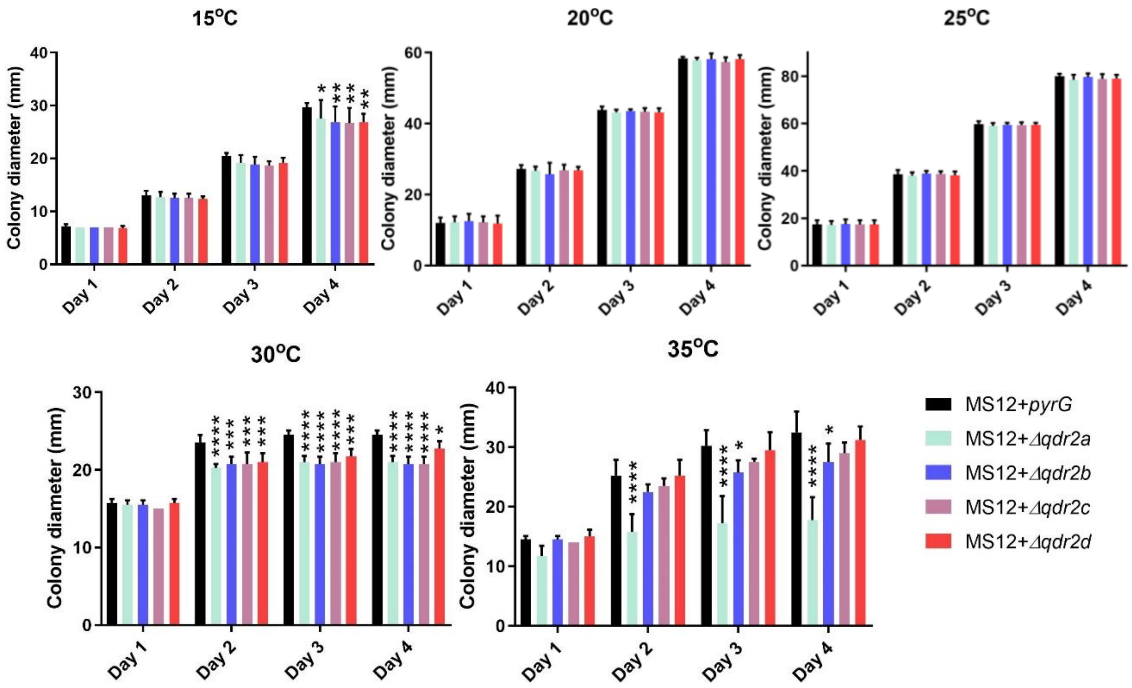

Figure 33. Colony diameter of the *qdr2* disruption mutants and MS12+*pyrG* strains at different temperatures. Strains were grown on YNB plates for four days. The presented values are averages; colony diameters were measured during three independent cultivations (error bars indicate standard deviation). Values indicated with asterisks significantly differed from the corresponding value of the MS12+*pyrG* strain according to the statistical method two-way ANOVA (*p < 0.05; **p < 0.01; ***p < 0.001; **** p < 0.0001).

Disruption of *qdr2* genes significantly affected colony growth of the *M. lusitanicus* at non optimum temperatures. All four mutants showed weaker growth compared to the control strain at 30 °C during the whole cultivation period and at 15 °C on the fourth day of cultivation. MS12+*Δqdr2a* mutant had significantly smaller colony size on the second, third and fourth days and MS12+*Δqdr2b* grew weaker on the third and fourth days of cultivation when strains were cultivated at 35 °C. Deletion of *qdr2* in *C. albicans* did not affect the yeast colony growth at 25 and 42 °C compared to wild-type strain (**Shah et al., 2014; Qadri et al., 2022**).

These results indicate a clear negative impact of the disruption of *qdr2* genes on the ability of *M. lusitanicus* to grow at 15, 30 and 35 °C. It is possible that the disruption of *qdr2* genes leads to changes in membrane transport characteristics, causing an inefficient nutrient exchange, impaired energy generation or increased susceptibility to environmental stressors. These potential factors would explain why the mutants were less competitive than the wild type under unfavorable temperatures.

4.4.2.4 Sporulation and germination ability of *qdr2* disruption mutants

Sporulation is an important process in the life cycle of fungi as it allows them to reproduce and ensure their survival. MS12+*Δqdr2b* and MS12+*Δqdr2d* mutants sporulated significantly less than the control strain (**Figure 34**).

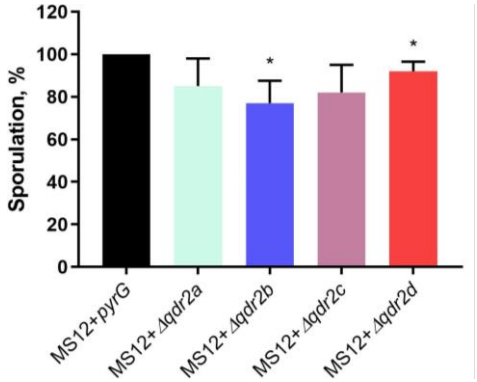

Figure 34. Sporulation of MS12+*pyrG* and the *qdr2* disruption mutants grown on MEA plates for 4 days at 25 °C. The inoculum size was 5×10^4 in each case. The presented values are averages; Spores were counted after three independent cultivations (error bars indicate standard deviation). Values indicated with asterisks significantly differed from the corresponding value of the MS12+*pyrG* strain according to unpaired t-test (* $p < 0.05$).

Germination rate serves as a reliable indicator of fungal growth and viability. Deletion of *qdr2* gene in *Fusarium graminearum* resulted defects in conidial germination (**Ma et al., 2022**). To examine the effect of Qdr2s on the germination ability of *M. lusitanicus*, we compared the germination rates of the *qdr2* disruption mutants with the control MS12+*pyrG* strain. MS12+*Δqdr2a*, MS12+*Δqdr2b* and MS12+*Δqdr2d* mutants showed significantly decreased germination rates after 4 hours of cultivation. However, the germination rates of the *qdr2* disruption mutants were not significantly different than that of the control strain after 6 hours, showing a temporary delay of fungal germination (**Figure 35**).

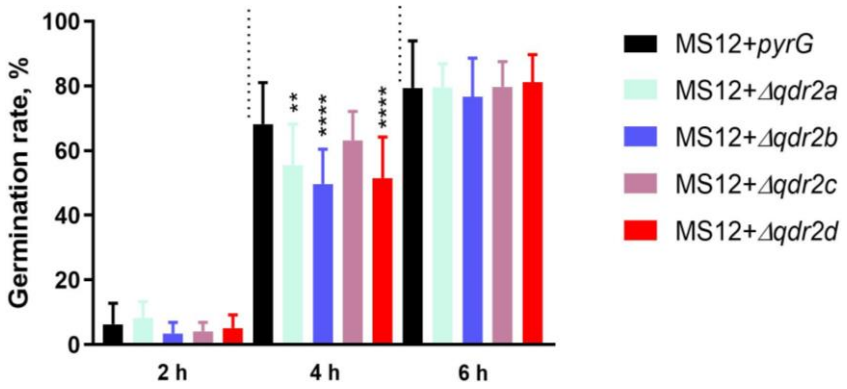

Figure 35. Germination rates of the sporangiospores of the *qdr2* mutants and the MS12+*pyrG* strain. Spores (10^6 spores/ml) were incubated in YNB broth for 6 h at 25 °C and then germinated spores were counted. The presented values are averages. Spores were counted after three independent cultivations (error bars indicate standard deviation). Values indicated with asterisks significantly differed from the corresponding value of the MS12+*pyrG* strain according to the one-way ANOVA (**p < 0.01; ****p < 0.0001).

4.4.2.5 Effect of detergents on the growth of the *qdr2* mutants

SDS and Triton X-100 disrupt fungal cell membrane permeability, activate a stress response, and inhibit cell growth (**Igual et al., 1996; Bickle et al., 1998; Cócera et al., 1999; Klimek-Ochab et al., 2011**). Since Qdr2 proteins are located in the fungal cell membrane (**Vargas et al., 2004**), the effect of these detergents on the growth of *qdr2* disruption mutants were analyzed. Recent research findings indicated that deletion of *qdr2* gene did not alter the growth and viability of the *C. albicans* cells when cultivated in the presence of 0.006% SDS (**Shah et al., 2014; Qadri et al., 2022**).

Similar results were shown in the present studies in case of *M. lusitanicus*. Addition of SDS and Triton X-100 to the cultivation medium did not change the viability and growth ability of the MS12+*Δqdr2a*, MS12+*Δqdr2b*, MS12+*Δqdr2b* and MS12+*Δqdr2d* mutants compared to the control strain (**Figure 36**).

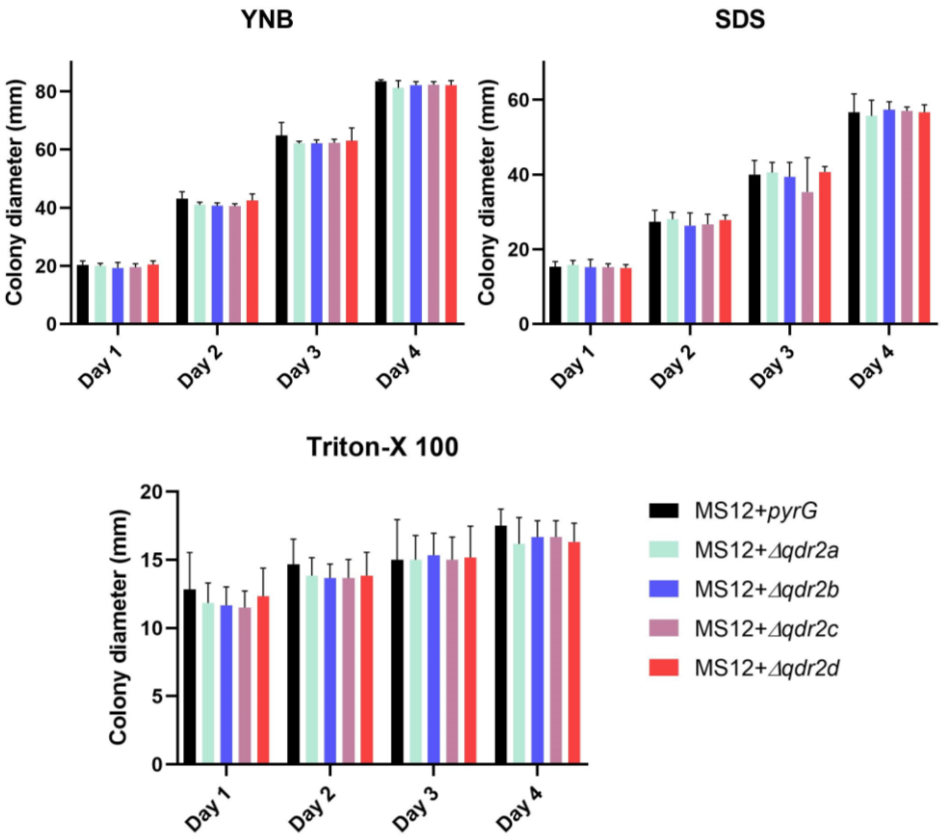

Figure 36. Effect of SDS and Triton X-100 on the colony growth of the *qdr2* mutants compared to that of the MS12+*pyrG* strain. Strains were cultivated on YNB medium supplemented with SDS or Triton X-100 for 4 days at 25 °C. The presented values are from three independent cultivations (error bars indicate standard deviation).

4.4.2.6 Effect of cell wall stressors on the growth of the *qdr2* mutants

Recent studies indicated that cell wall-disrupting agents such as CFW (300 µg/ml) and CR (225µg/ml) did not result in noticeable defects in *qdr2* knockout mutants of *C. albicans* (**Shah et al., 2014; Qadri et al., 2022**).

In the present study, addition of CFW and CR to the cultivation medium did not change the growth of the MS12+*Δqdr2a,* MS12+*Δqdr2b,* MS12+*Δqdr2c* and

MS12+*Δqdr2d* mutants. There were no significant or visible phenotypic changes in *M. lusitanicus* (**Figure 37**).

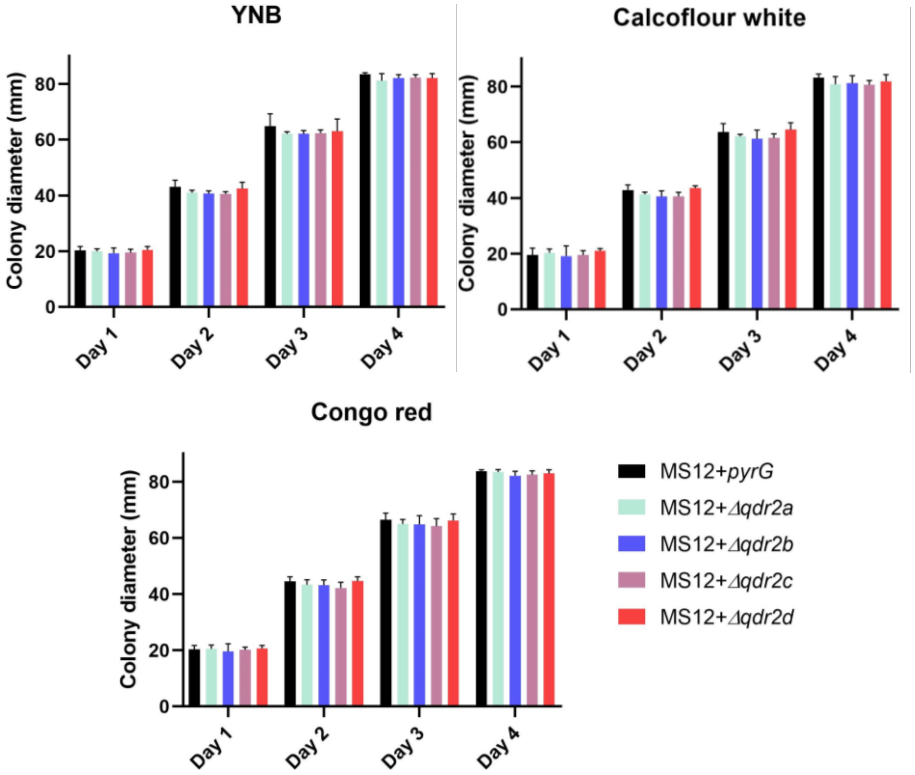

Figure 37. Effect of calcofluor white (CFW) and congo red (CR) on the colony growth of the *qdr2* mutants compared to that of the MS12+*pyrG* strain. Strains were cultivated on YNB supplemented with CFW or CR for 4 days at 25 °C. The presented values are from three independent cultivations (error bars indicate standard deviation).

4.4.2.7 Growth of *qdr2* mutants during the copper and potassium deficiency

Previous studies suggested that Qdr2 is involved in potassium (K^+) uptake in *S. cerevisiae* by potentially acting as an alternative K^+ importer. Qdr2 protein provides a physiological advantage to yeast cells under quinidine-induced stress that inhibits K^+ uptake by acting as a membrane uncoupler. Qdr2 has also an essential role in extruding divalent copper ions (Cu^{2+}) from yeast cells, with Cu^{2+} being the primary physiological substrate for Qdr2 in *S. cerevisiae* (**Vargas et al., 2007; Ríos et al., 2013**). However, *qdr2* in *C. glabrata* does not have the same function as in *S. cerevisiae*. The roles and significance of Qdr*2* homologs may differ among fungal species, indicating some level of species-specific functionality (**Costa et al., 2013**). Therefore, the effect of potassium

and copper deficiency on the colony growth of *M. lusitanicus qdr2* disruption mutants was analyzed. It was shown that potassium and copper deficiency did not affect the colony growth of *qdr2* disruption mutants compared to the control strain (**Figure 38**).

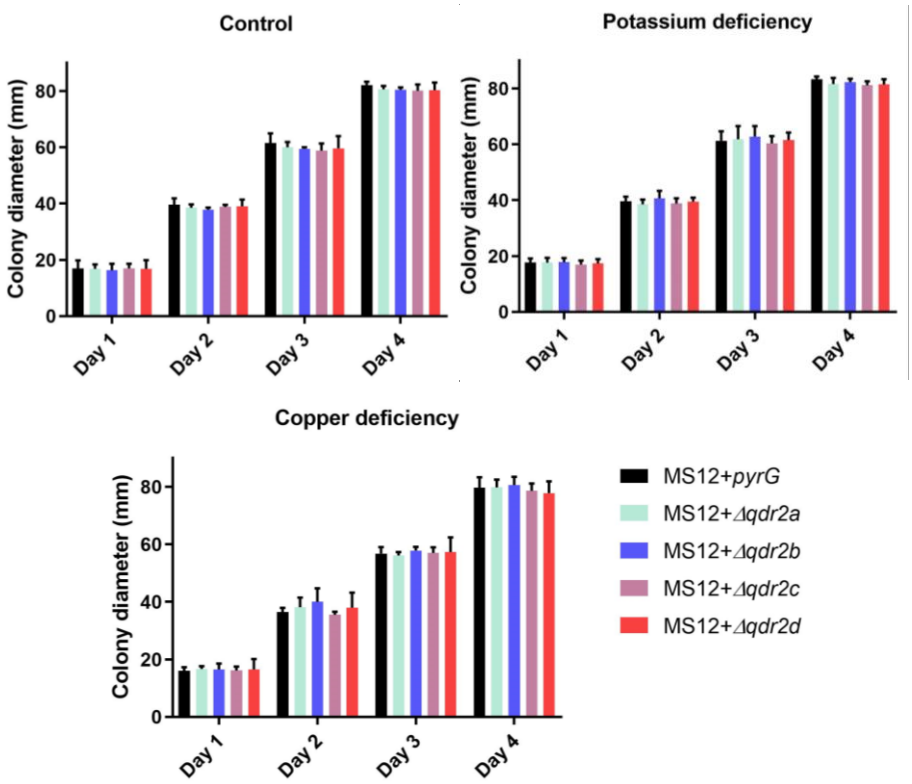

Figure 38. Effect of the copper and potassium deficiency on the colony growth of the *qdr2* mutants compared to the control MS12+*pyrG* strain. Strains were cultivated on Czapek-Dox medium lacking copper or potassium for 4 days at 25 °C. The presented values are from three independent cultivations (error bars indicate standard deviation).

4.4.2.8 Antifungal susceptibility of the *M. lusitanicus qdr2* mutants

In *S. cerevisiae qdr2* was involved in resistance to ketoconazole but not to the amphotericin B and azoles such as itraconazole, miconazole and fluconazole (**Vargas et al., 2004**). In *C. glabrata qdr2* has an essential role in resistance to azoles (**Costa et al., 2013; Costa et al., 2014; Costa et al., 2016; Widiasih Widiyanto et al., 2019; Salazar et al., 2022**). However, in *C. albicans qdr2* is also not involved in antifungal transport (**Shah et al., 2014**).

Susceptibility of the MS12+*Δqdr2a*, MS12+*Δqdr2b,* MS12+*Δqdr2c* and MS12+*Δqdr2d* mutants and the control MS12+*pyrG* strain to different antifungal agents

was analyzed. Broth microdilution method was used to find out the minimal inhibitory concentration (MIC) of the antifungal drugs under aerobic (**Table 2**) and anaerobic (**Table 3**) conditions.

Table 2. Minimal inhibitory concentrations (MIC) of different antifungals against the *qdr2* mutant and the control *M. lusitanicus* MS12+*pyrG* strains under aerobic condition. AMB – amphotericin B; POS – posaconazole; RAV – ravuconazole; VOR – voriconazole; ISA – isavuconazole; KET – ketoconazole; FLU – fluconazole.

Strains	MIC_{90} (μg/ml)							
	AmB	POS	RAV	VOR	ITR	ISA	KET	FLU
MS12+*pyrG*	1	2	>16	>16	>64	>16	>64	>64
MS12+*Δqdr2a*	1	2	>16	>16	>64	>16	>64	>64
MS12+*Δqdr2b*	1	2	>16	>16	>64	>16	>64	>64
MS12+*Δqdr2c*	1	2	>16	>16	>64	>16	>64	>64
MS12+*Δqdr2d*	1	2	>16	>16	>64	>16	>64	>64

Table 3. Minimal inhibitory concentrations (MIC) of different antifungals against the *qdr2* mutant and the control *M. lusitanicus* MS12+*pyrG* strains under anaerobic condition. AMB – amphotericin B; POS – posaconazole; RAV – ravuconazole; VOR – voriconazole; ISA – isavuconazole; KET – ketoconazole; FLU – fluconazole.

Strains	MIC_{90} (μg/ml)							
	AmB	POS	RAV	VOR	ITR	ISA	KET	FLU
MS12+*pyrG*	0.5	>16	>16	>16	>64	>16	>64	>64
MS12+*Δqdr2a*	0.5	>16	>16	>16	>64	>16	>64	>64
MS12+*Δqdr2b*	0.5	>16	>16	>16	>64	>16	>64	>64
MS12+*Δqdr2c*	0.5	>16	>16	>16	>64	>16	>64	>64
MS12+*Δqdr2d*	0.5	>16	>16	>16	>64	>16	>64	>64

The results showed that the sensitivity of *qdr2* disruption mutants did not differ from the MS12+*pyrG* strain in response to amphotericin B, posaconazole, ravuconazole, voriconazole, itraconazole, isavuconazole, ketoconazole and fluconazole across both environmental conditions. These findings appear to contrast with previous studies on yeasts.

These findings suggest that the disruption of *qdr2* genes in *M. lusitanicus* does not affect the effectiveness of commonly used antifungals for treating mucormycosis. The reason for this might be the compensatory effect of other *qdr2* genes in the absence of

one specific *qdr2* gene, variations in the specific pathways to adopt antifungal resistance or existence of alternative resistance mechanisms.

4.4.2.9. Susceptibility of the *M. lusitanicus qdr2* mutants to quinidine, cisplatin, and bleomycin

In *S. cerevisiae* Qdr2 is associated with active export of quinidine and anti-cancer drugs cisplatin, and bleomycin out of the yeast cells (**Vargas et al., 2004**). Therefore, a sensitivity of *M. lusitanicus* after the disruption of *qdr2* genes to these drugs were analyzed. All four *qdr2* disruption mutants did not show the altered susceptibility to tested drugs under aerobic and anaerobic conditions (**Table 4**).

Table 4. Minimal inhibitory concentrations (MIC) of quinidine, cisplatin, and bleomycin against the *qdr2* mutant and the control *M. lusitanicus* MS12+*pyrG* strains.

Strains	MIC_{90} (mg/ml)					
	Aerobic condition			Anaerobic condition		
	Quinidine	Cisplatin	Bleomycin	Quinidine	Cisplatin	Bleomycin
MS12+*pyrG*	4	1	0.1	4	1	0.1
MS12+*Δqdr2a*	4	1	0.1	4	1	0.1
MS12+*Δqdr2b*	4	1	0.1	4	1	0.1
MS12+*Δqdr2c*	4	1	0.1	4	1	0.1
MS12+*Δqdr2d*	4	1	0.1	4	1	0.1

These results suggest that there may be compensatory changes in the expression of *qdr2* genes related to drug resistance in response to the disruption of one of the *qdr2*s, preserving drug susceptibility. Alternatively, it is possible that the tested drugs may not be substrates for Qdr2 proteins in *M. lusitanicus*.

4.4.2.10 Susceptibility of the *qdr2* disruption mutants to different stressors

Qdr2 protein is involved in cation homeostasis and the oxidative stress response in certain fungi. *qdr2* knockout mutant of *S. cerevisiae* showed increased sensitivity to $CuSO_4$ and *qdr2* overexpression mutant displayed tolerance to 1.2 M NaCl (**Ríos et al., 2013**). It was suggested that Qdr2 might be involved in the intracellular regulation of zinc and H_2O_2 levels of *C. glabrata* since deletion of *qdr2* led to increased sensitivity to Zn^{2+} and hydrogen peroxide. But there were no significant changes in the growth of the mutant compared to wild-type strain in the presence of excess NaCl and $CuSO_4$ molecules

(**Widiasih Widiyan et al., 2019**). Deletion of *qdr2* in *C. albicans* did not affect the susceptibility of mutants compared to the wild-type strain on exposure to 10 mM H_20_2, NaCl, 0.1mM $CuSO_4$ (**Qadri et al., 2022**). In *F. graminearum qdr2* has been involved in the sodium and copper transport. *qdr2* deletion mutants showed increased sensitivity towards osmotic stress (**Ma et al., 2022**).

In the current study, the growth of the MS12+*Δqdr2a*, MS12+*Δqdr2b,* MS12+*Δqdr2c* and MS12+*Δqdr2d* mutants along with the control MS12+*pyrG* strain in the presence of different abiotic stressors was tested. Strains were exposed to different stress inducers such as osmotic stress (sodium chloride and D-sorbitol), oxidative stress (hydrogen peroxide) and metal ions (Cu^{2+}, Zn^{2+}, Fe^{2+} and Mg^{2+}). *qdr2* disruption mutants of *M. lusitanicus* did not show any significant changes in the susceptibility compared to the control strain in the presence of any of the tested stressors (**Table 5**), suggesting that *qdr2* genes may not have a role in coping with these specific abiotic stressors.

Table 5. Minimal inhibition concentration (MIC_{90}) of abiotic stressors against the *qdr2* mutant and the control MS12+*pyrG* strains.

Strain	MIC_{90} (µg/ml)					
	H_2O_2	D-sorbitol	NaCl	$FeSO_4$	$CuSO_4$	$ZnSO_4$
MS12+*pyrG*	8 mM	2.25 M	1.5 M	3 mM	2 mM	3 mM
MS12+*Δqdr2a*	8 mM	2.25 M	1.5 M	3 mM	2 mM	3 mM
MS12+*Δqdr2b*	8 mM	2.25 M	1.5 M	3 mM	2 mM	3 mM
MS12+*Δqdr2c*	8 mM	2.25 M	1.5 M	3 mM	2 mM	3 mM
MS12+*Δqdr2d*	8 mM	2.25 M	1.5 M	3 mM	2 mM	3 mM

4.4.2.11 Virulence of the *qdr2* mutants in *Galleria mellonella*

Qdr2 was also found to play a role in the pathogenesis of *C. albicans*. Deletion of *qdr2* gene has shown to attenuate the virulence of yeast cells in mice (**Shah et al., 2014**). Qdr2 protein has a significant role in the pathogenesis of the plant pathogen *F. graminearum.* Its *qdr2* knockout mutant showed reduced virulence on wheat coleoptiles and corn silks (**Ma et al., 2022**).

In the present study, MS12+Δ*qdr2a*, MS12+Δ*qdr2b*, MS12+Δ*qdr2c* and MS12+Δ*qdr2d* disruption mutants of *M. lusitanicus* proved to be less virulent compared to the control MS12+*pyrG* strain. *G. mellonella* larvae infected with the *qdr2* disruption mutants survived up to 6 days post-infection compared to larvae infected with the control

strain succumbed to infection within 5 days (**Figure 39)**. These findings highlight the role importance of *qdr2* genes in the pathogenesis of *M. lusitanicus*.

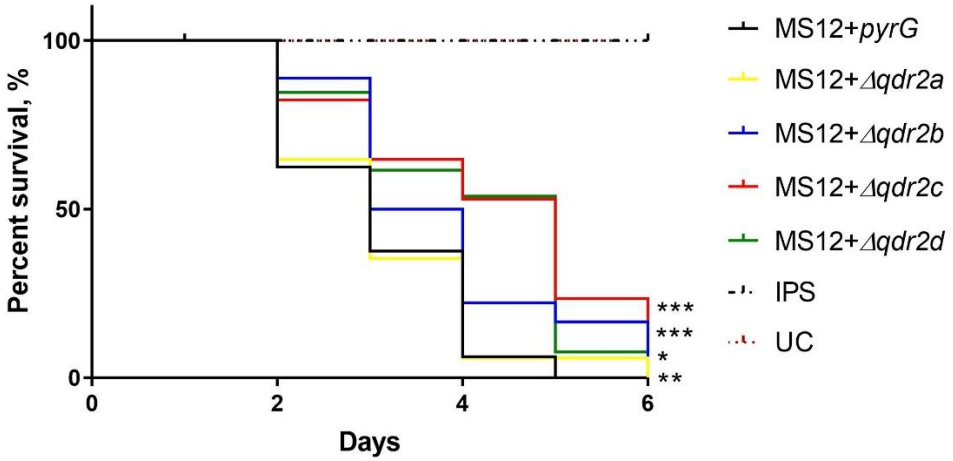

Figure 39. Survival of *G. mellonella* larvae infected with the *qdr2* disruption mutants and the control MS12+*pyrG* strain. The results represent the average of three independent experiments. Survival curve followed by asterisk was significantly differed from the control strain according to the Gehan-Breslow-Wilcoxon test (*p < 0.05; **p < 0.01; ***p < 0.001).

4.4.2.12 Lipid composition of *M. lusitanicus qdr2* disruption mutants

Several studies showed the coordinate control between multidrug resistance and membrane lipid metabolism (**Panwar et al., 2008**; **Shahi and Moye-Rowley, 2009; Beccaccioli et al., 2019**). In *C. albicans* deletion of *qdr2* led to the accumulation of phosphatidylinositol, phosphatidylserine, and sphingolipids, indicating involvement in lipid homeostasis (**Shah et al., 2014**).

Studies indicated involvement of sphingolipids in several cellular processes such as heat stress response and azole resistance (**Liu et al., 2005; Chen et al., 2013; Gao et al., 2018; Zhai et al., 2019**). Therefore, we decided to analyze the cellular lipid homoeostasis in *qdr2* disruption mutants of *M. lusitanicus*.

The amount of the main components of sphingolipid biosynthesis such as ceramide (d18:1:16), dihydroceramide (d18:16), dihydrosphingosine, phytoceramide (cer(d18:1/16:0(2OH)), and phytosphingosine (**Gault et al., 2010; Rhome et al., 2010**) was not altered in the created mutant strains. Results of the lipidome analysis revealed clearly different amount and presence of 75 lipid species significantly altered in the

created mutant strains. There were significant changes in phospholipid, sphingolipid, glycerolipid, and ceramide content (**Figure 40**).

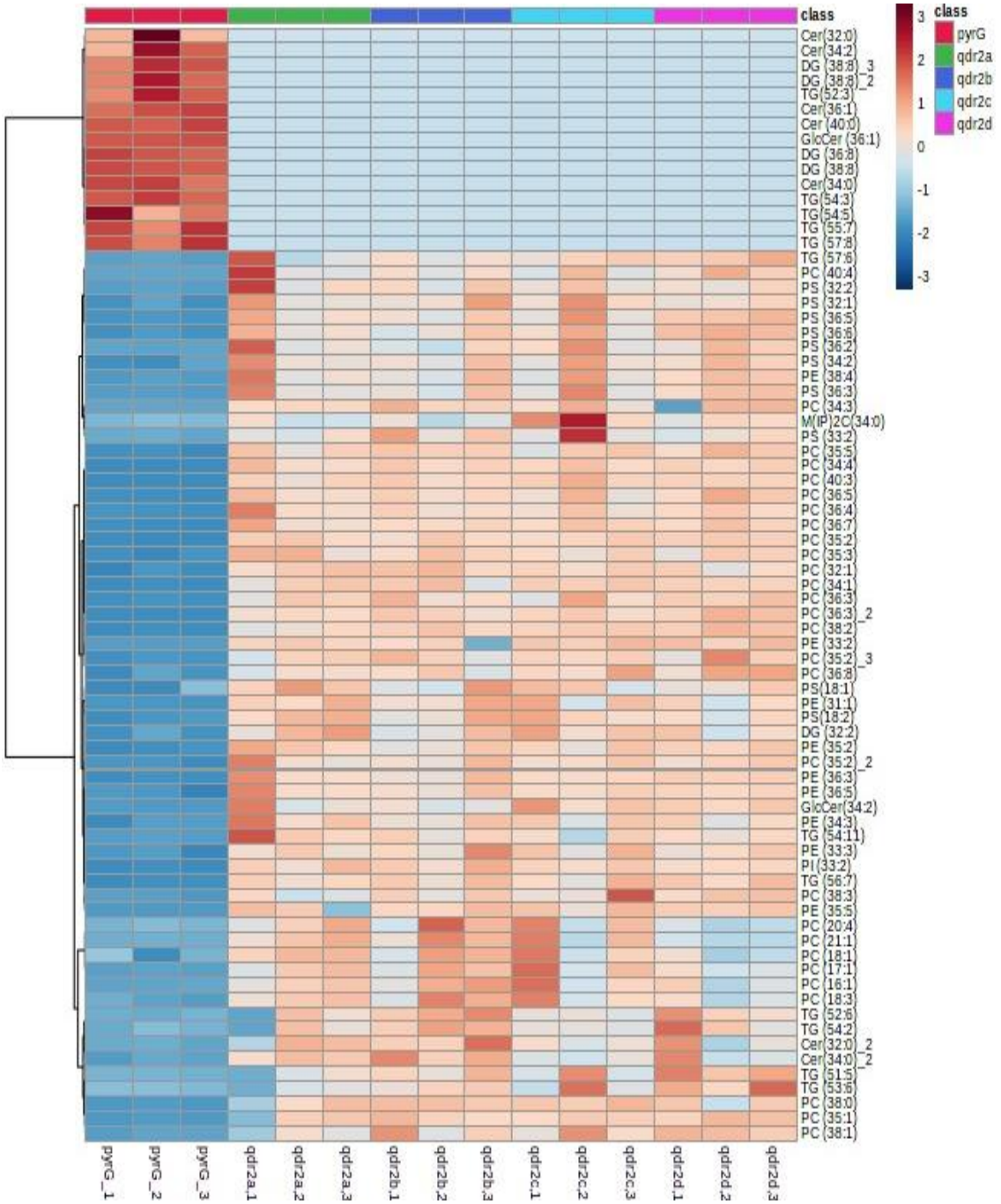

Figure 40. Molecular lipid species composition of *qdr2* disruption mutants and control MS12+*pyrG* strain of *M. lusitanicus*. Data is represented as % of peak area to lipid mass. Blue and red color depict the highest and lowest values respectively. pyrG – MS12+*pyrG*, qdr2a – MS12+Δ*qdr2a*, qdr2b – MS12+Δ*qdr2b*, qdr2c – MS12+Δ*qdr2c*, qdr2d – MS12+Δ*qdr2c*, qdr2d – MS12+Δ*qdr2d*.

Several phospholipid classes, including PC (phosphatidylcholine), PS (phosphatidylserine), PE (phosphatidylethanolamine), PI (phosphatidylinositol); glycerolipids including diglyceride – DG (32:2) and triglycerides - TG (54:11), TG (56:7), TG (57:6), TG (54:11), TG (56:7), TG (52:6), TG (54:2), TG (51:5), TG (53:6); sphingolipids including mannosyldiinositolphosphoceramide (MIP2C), glucosylceramide - GlcCer (34:2); and ceramides - Cer (32:0)_2, Cer (34:0)_2 were accumulated in *qdr2* disruption mutants. At the same time, Cer (32:0), Cer (34:2), Cer (36:1), Cer (40:0), Cer (34:0), DG (38:8)_3, DG (38:8)_2, DG (36:8), DG (38:8), TG (52:3), TG (54:3), TG (54:5), TG (55:7), TG (57:8), GlCer (36:1) were depleted in the *qdr2* disruption mutants.

Overall, these findings suggest that *qdr2* genes play a significant role in regulating lipid metabolism and maintenance of lipid balance in *M. lusitanicus*. Disruption of these genes leads to changes in the cellular lipid profile.

5. CONCLUSION

After anaerobic cultivation of *Mucor lusitanicus*, 539 differentially expressed genes were detected by RNA-sequencing analysis. Among these, 190 genes were upregulated, and 349 were downregulated. We focused our study on two key groups of differentially expressed genes, the heat shock transcription factors (i.e., Hsf1 and Hsf2) and quinidine drug resistance 2 transporters (i.e., Qdr2a, Qdr2b, Qdr2c and Qdr2d).

Hsf proteins play essential roles in regulating stress response genes under different stress conditions, including heat shock, oxidative stress, and glucose starvation (**Sugiyama et al., 2000; Zahringer et al., 2000; Hahn and Thiele, 2004; Albrecht et al., 2010; Nicholls et al., 2011; Brandman et al., 2012; Sueiro-Olivares et al., 2015; Nair et al., 2017; Barna et al., 2018; Gomez-Pastor et al., 2018; Fabri et al., 2021; Xiao et al., 2022**). The Qdr2 transporters, on the other hand, are known for their involvement in resistance to antiarrhythmic drug quinidine and anticancer drugs bleomycin and cisplatin (**Nunes et al., 2001; Vargas et al., 2004; Tenreiro et al., 2005**).

Our study revealed distinct temperature and oxygen tension related expression patterns for *hsf1*, *hsf2* and four *qdr2* genes, suggesting their significance in adapting to temperature and oxygen level changes. *qdr2*s responded differently to antifungal treatments under aerobic and anaerobic conditions. All four *qdr2* genes were generally upregulated in response to different antifungal drugs under aerobic condition. However, *qdr2a* and *qdr2b* were mostly downregulated and *qdr2c* and *qdr2d* were upregulated upon exposure to antifungals under anaerobic condition.

To further understand the functions of two *hsf* and four *qdr2* genes, we used the CRISPR-Cas9 method to disrupt them by inserting the *pyrG* selection marker. Successful gene disruptions and the absence of transcripts of the disrupted genes were proven by molecular analysis.

hsf1 disruption mutants showed weaker growth at temperatures below 25 °C, while *hsf2* disruption mutant displayed weaker growth at higher temperatures. This suggests that *hsf1* gene is involved in adaptation to lower temperatures, whereas *hsf2* plays a role in both low and high-temperature adaptation. Disruption of *hsf1* and *hsf2* did not affect sporulation, germination, and pathogenicity of *M. lusitanicus*.

Disruption of one of the *qdr2* genes often resulted in changes in the expression of others, suggesting a genetic compensation in response to a disruption of a gene. All four *qdr2* mutants had weaker growth at 15, 30, and 35 °C, suggesting that *qdr2* genes are essential for adaptation of *M. lusitanicus* to temperature stress. Qdr2b and Qdr2d were

found to be involved in regulation of sporulation. Although there were some initial delays in germination of *qdr2* disruption mutants, compensatory mechanisms restored normal germination rate. However, *qdr2* genes have not been found involving in the regulation of cell membrane integrity, drug resistance, susceptibility to specific stressors, or viability under potassium and copper deficiency. Surprisingly, *qdr2* disruption mutants did not exhibit altered resistance to antifungals, suggesting the compensatory effect of the other *qdr2* genes in the absence of one of them, or limited role in antifungal drug transport. *qdr2* disruption mutants showed reduced virulence in *Galleria mellonella*, indicating their importance in the pathogenicity of *M. lusitanicus*. Lipidome analysis revealed significant changes in the lipid composition of *qdr2* mutants, suggesting their role in lipid homeostasis.

For further functional analysis of the Hsf and Qdr2 proteins, the development of *hsf* and *qdr2* double knockout mutants is suggested.

In conclusion, the results of current study provide insights into the roles of *hsf1*, *hsf2* and *qdr2s* genes in adaptation of *M. lusitanicus* to environmental changes. Hsf1 and Hsf2 proteins are heat shock transcription factors that have a role in temperature adaptation, maintenance of cell membrane and cell wall integrity. Qdr2 proteins are multidrug transporters that are involved in temperature adaptation, sporulation, germination, pathogenesis, and lipid homeostasis in *M. lusitanicus*. This study showed a complex regulatory network among *qdr2* genes.

6. SUMMARY

Mucor lusitanicus is an opportunistic fungal pathogen that has an ability to switch between yeast and filamentous growth in response to environmental changes. It has multi-budded yeast growth form in the presence of a fermentable hexose under anaerobic conditions, while filamentous growth is triggered under aerobic conditions or upon nutrient limitation. The presence of the genes that have adaptive potential for fungal pathogens poses a significant challenge for antifungal therapy, as it can potentially result in treatment failure and disease relapse.

The aim of the study was to identify and characterize differentially expressed genes in *M. lusitanicus* under anaerobic conditions, determine their functions, and investigate their role in pathogenicity.

The objectives of the presented research were the following:

1. Identification of differentially expressed genes under anaerobiosis in *M. lusitanicus* via transcriptomic analysis.
2. Validation and selection of genes for further characterization based on transcription analysis under various cultivation conditions, such as oxygen tension, cultivation time, different temperatures, and antifungal treatments.
3. Functional characterization of the selected genes:

   a) Disruption of the selected genes by using a plasmid-free CRISPR-Cas9 method.

   b) Morphological and physiological characterization of the disruption mutants (growth under different conditions, pathogenicity test).

Results:

1. Identification of differentially expressed genes under anaerobiosis in *M. lusitanicus* via transcriptomic analysis.

After RNA-sequencing analysis, 539 genes were found to be differentially expressed. Genes that were differentially upregulated under anaerobic conditions include *hsf1*, *hsf2*, *nudix*, and *qdr2d*, while genes that were differentially downregulated include *fen2* and *pho84*.

2. Validation and selection of genes for further characterization based on transcription analysis under various cultivation conditions, such as oxygen tension, cultivation time, different temperatures, and antifungal treatments.

The results of the RNA-sequencing analysis were validated through qRT-PCR. Following the RNA-sequencing analysis and qRT-PCR heat shock transcription factors (*hsf1* and *hsf2*) and quinidine drug resistance 2 transporters (*qdr2a, qdr2b, qdr2c and qdr2d*) were chosen to further investigations. Selected *hsf1*, *hsf2* and four *qdr2* genes play roles in adaptation to temperature and oxygen level changes. *qdr2*s responded differently to antifungal treatments under aerobic and anaerobic conditions, with all *qdr2* genes upregulated after exposure antifungals under aerobic condition; *qdr2a* and *qdr2b* downregulated, and *qdr2c* and *qdr2d* upregulated in response to antifungal treatment under anaerobic condition.

3. Functional characterization of the selected genes:

a) Disruption of the selected genes by using a plasmid-free CRISPR-Cas9 method.

hsf1, hsf2, qdr2a, qdr2b, qdr2c and *qdr2d* genes were disrupted by applying the CRISPR-Cas9 technique.

b) Morphological and physiological characterization of the disruption mutants (growth at different conditions, pathogenicity test).

hsf1 has a role in adaptation to temperatures below optimal, while *hsf2* is involved in low and high-temperature response. Disruption of *hsf1* and *hsf2* did not affect sporulation, germination, and virulence of *M. lusitanicus*. Disruption of one of *qdr2* genes tended to lead to changes in the expression of others, suggesting the existence of genetic compensation phenomenon that regulates the expression of *qdr2* genes in *M. lusitanicus*. Results showed that *qdr2* genes are involved in the temperature adaptation. Qdr2b and Qdr2d transporters were found to be important for sporulation. Despite the previous studies on other fungal species, disruption of *qdr2* genes in *M. lusitanicus* did not affect cell membrane integrity, susceptibility to abiotic stressors, and potassium and copper sensitivity. *qdr2* genes were differentially expressed in response to antifungals. However, *qdr2* disruption mutants did not exhibit altered susceptibility to antifungals, indicating their limited role in antifungal resistance or the effect of genetic compensatory mechanisms. *qdr2s* disruption attenuated fungal virulence in *G. mellonella*, suggesting their role in the pathogenicity of *M. lusitanicus*. Results showed altered lipid content of *qdr2* mutants, indicating that *qdr2* genes are involved in the regulation of the lipid homeostasis.

7. ÖSSZEFOGLALÓ

A *Mucor lusitanicus* egy opportunista humánpatogén gomba, amely egyes környezeti hatásokra képes átváltani az élesztő és a fonalas növekedés között. Anaerob körülmények között és fermentálható hexóz jelenlétében élesztő növekedést mutat, míg a fonalas növekedés aerob körülmények között indul el. A patogén gombák adaptációs potenciálja és a megfelelő genetikai háttért biztosító gének jelenléte jelentős kihívást jelent a gombaellenes terápia számára, mivel potenciálisan a kezelés sikertelenségét eredményezheti.

A vizsgálat célja a *M. lusitanicus*ban anaerob körülmények között eltérően expresszálódó egyes gének azonosítása és jellemzése, funkcióik meghatározása, valamint patogenitásban betöltött szerepük vizsgálata volt.

A bemutatott kutatás konkrét céljai ennek megfelelően a következők voltak:

1. Anaerobiózis esetén eltérően expresszálódó gének azonosítása *M. lusitanicus*ban transzkriptom analízissel.

2. Egyes kiválasztott gének felhasználása a transzkriptom analízis validálására, valamint további transzkripciós analízisre eltérő tenyésztési körülmények esetén, pl. eltérő oxigéntenzió, tenyésztési idő, hőmérséklet és gombaellenes kezelések során.

3. A kiválasztott gének funkcionális jellemzése:

a) A kiválasztott gének kiütése plazmidmentes CRISPR-Cas9 módszerrel.

b) Az előállított mutánsok morfológiai és fiziológiai jellemzése (pl. növekedési tesztek eltérő körülmények esetén, patogenitási tesztek).

Eredmények:

1. Anaerobiózis esetén eltérően expresszálódó gének azonosítása *M. lusitanicus*ban transzkriptom analízissel.

Az RNS-szekvenálás elemzése után 539 gént találtunk eltérően expresszálódónak. Anaerob körülmények között a felülszabályozott gének közé tartozott a *hsf1*, *hsf2*, *nudix* és *qdr2d*, míg az alulszabályozott gének közé tartozott a *fen2* és a *pho84*.

2. Egyes kiválasztott gének felhasználása a transzkriptom analízis validálására, valamint további transzkripciós analízisre.

Az RNS-szekvenálási analízis eredményeit qRT-PCR segítségével validáltuk. A transzkriptom és qRT-PCR elemzés alapján, *hsf1* és *hsf2* hősokk transzkripciós faktor, valamint a kinidin drogrezisztencia 2 transzporter (*qdr2a*, *qdr2b*, *qdr2c* és *qdr2d*) géneket

választottuk ki a további vizsgálatokhoz. A kiválasztott *hsf1*, *hsf2* és négy *qdr2* gén szerepet játszik a hőmérséklet- és oxigénszint-változásokhoz való alkalmazkodásban. A *qdr2* gének eltérő transzkripciót mutattak aerob és anaerob körülmények között végzett gombaellenes kezelések esetén. Az összes *qdr2* gén felülszabályozottnak bizonyult a gombaellenes szerekkel való kezelés után aerob körülmények között. A *qdr2a* és *qdr2b* kifejeződése csökkent, a *qdr2c* és *qdr2d* géneké pedig növekedett anaerob körülmények között végzett gombaellenes kezelés hatására.

3. A kiválasztott gének funkcionális jellemzése

a) A kiválasztott gének kiütése plazmidmentes CRISPR-Cas9 módszerrel.

A *hsf1*, *hsf2*, *qdr2a*, *qdr2b*, *qdr2c* és *qdr2d* génekre nézve diszrupciós mutánsokat hoztunk létre a CRISPR-Cas9 technika alkalmazásával.

b) Az előállított mutánsok morfológiai és fiziológiai jellemzése.

A géndiszrupciós mutánsok vizsgálatával megállapítottuk, hogy a *hsf1* szerepet játszik az optimálisnál alacsonyabb hőmérsékletekhez való alkalmazkodásban, míg a *hsf2* részt vesz az alacsony és magas hőmérséklethez történő adaptációban. A *hsf1* és a *hsf2* elrontása nem befolyásolta a *M. lusitanicus* sporulációját, csírázását és virulenciáját.

Az egyes *qdr2* gének kiütése a többi *qdr2* gén kifejeződésének megváltozását okozta, ami arra utal, hogy a hiányzó génműködést a többi gén kifejeződése kompenzálhatja *M. lusitanicus*ban. Az eredmények azt mutatták, hogy a *qdr2* gének részt vesznek a hőmérséklet-adaptációban. A Qdr2b és Qdr2d transzportereket fontosnak bizonyultak a sporuláció szempontjából. A más gombafajokon végzett korábbi vizsgálatokkal ellentétben a *qdr2* gének elrontása *M. lusitanicus*ban nem befolyásolta a sejtmembrán integritását, az abiotikus stresszorokra való érzékenységet, valamint a kálium- és réz érzékenységet. A *qdr2* gének eltérően expresszálódtak gombaellenes szerek hatására, ugyanakkor a mutánsok érzékenysége nem változott a gombaellenes szerek iránt a kontroll törzshöz képest, ami arra utal, hogy korlátozott szerepük van a gombaellenes rezisztenciában, vagy hiányukat más mechanizmusok (pl. egyéb *qdr* vagy más transzporterek) kompenzálhatják. A *qdr2*-k kiütése csökkentette a gomba virulenciáját *G. mellonellá*ban, ami arra utal, hogy ezek gének szerepet játszhatnak a *M. lusitanicus* patogenitásában. Eredményeink azt mutatták, hogy a *qdr2* mutánsok lipidösszetétele alapvetően megváltozott, ami arra utal, hogy a *qdr2* gének részt vesznek a lipid homeosztázis szabályozásában.

8. ACKNOWLEDGEMENT

To begin with, I express my sincere appreciation to Prof. Dr. Csaba Vágvölgyi for providing me with the opportunity to pursue my PhD thesis at the department of Microbiology, Faculty of Science and Informatics, University of Szeged. Furthermore, I am grateful to the Tempus Public Foundation, Hungary for awarding me the Stipendium Hungaricum scholarship and the Stipendium Hungaricum Dissertation scholarship.

I would like to acknowledge the tremendous support and guidance provided by my supervisors Prof. Dr. Tamás Papp and Dr. Gábor Nagy over the course of my PhD journey. Their unwavering dedication, expertise, and encouragement have been pivotal in shaping my academic trajectory, honing my critical thinking abilities, and fostering a passion for research.

I wish to express my gratitude to Dr. Amanda Grace Vaz, Dr. Tünde Márki-Kartali, Dr. Csilla Szebenyi, Olivér Jáger and all my colleagues in laboratory 309 who have offered valuable assistance, advice, and support on numerous occasions. I especially want to thank Amanda for her indispensable help and for being a true friend. Moreover, I appreciate my dear friend Dr. Anuar Zhumakayev for his patience, help and useful advice regarding PhD studies and exams. I am also thankful to all my colleagues at the Department of Microbiology who have helped my work in any way.

I appreciate Dr. Mónika Varga for her guidance in the lipid extraction process and lipid composition data analysis. Additionally, I express gratitude to Dr. Mónika Homa from the Department of Microbiology and Dr. László Bodai, Dr. Nóra Zsindely and Gábor Nagy from the Department of Biochemistry and Molecular Biology for RNA sequencing and the analysis of RNA sequencing data.

I extend my utmost gratitude to the members of my thesis committee, whose valuable feedback and constructive criticism have significantly enhanced the quality of my research work.

I am indebted to my parents Amangeldy Ibragimov and Manshuk Ibragimova, siblings Ulan Ibragimov, Nurasyl Ibragimov, Dana Ibragimova, sister-in-law Aigerim Baibusinova and two nephews Amangeldy Akan and Amangeldy Zhanarys who are still waiting for me, despite my long “absence”, constant encouraging, love, and support that kept me going during challenging times. To all my friends, I want to thank for keeping me as “emotionally healthy” as possible.

The study was supported by the grants GINOP-2.3.2.-15-2016-00035, NKFI K131796, HUN-REN 2001007 and TKP-2021-EGA-28.

9. REFERENCES

Adams, T. H., Wieser, J. K., & Yu, J. H. (1998). Asexual sporulation in *Aspergillus nidulans*. *Microbiology and Molecular Biology Reviews*, *62*(1), 35-54.

Ajmal, M., Hussain, A., Ali, A., Chen, H., & Lin, H. (2022). Strategies for controlling the sporulation in *Fusarium* spp. *Journal of Fungi*, *9*(1), 10.

Albrecht, D., Guthke, R., Brakhage, A. A., & Kniemeyer, O. (2010). Integrative analysis of the heat shock response in *Aspergillus fumigatus*. *BMC Genomics*, *11*, 32.

Almyroudis, N. G., Sutton, D. A., Fothergill, A. W., Rinaldi, M. G., & Kusne, S. (2007). *In vitro* susceptibilities of 217 clinical isolates of Zygomycetes to conventional and new antifungal agents. *Antimicrobial Agents and Chemotherapy*, *51*(7), 2587-2590.

Andrade, V. S., Sarubbo, L. A., Fukushima, K., Miyaji, M., Nishimura, K., & Campos-Takaki, G. M. D. (2002). Production of extracellular proteases by *Mucor circinelloides* using D-glucose as carbon source/substrate. *Brazilian Journal of Microbiology*, *33*(2), 106-110.

Anemaet, I. G., & van Heusden, G. P. (2014). Transcriptional response of *Saccharomyces cerevisiae* to potassium starvation. *BMC Genomics*, *15*(1), 1040.

Austin, S., & Mayer, A. (2020). Phosphate homeostasis – a vital metabolic equilibrium maintained through the INPHORS signaling pathway. *Frontiers in Microbiology*, *11*, 1367.

Baberwal, P., Singh, A., Adarsh, A., & Kumar, Y. (2022). Key molecules of Mucorales for COVID-19-associated mucormycosis: a narrative review. *Journal of Bio-X Research, 5*(3), 104-111.

Barna, J., Csermely, P., & Vellai, T. (2018). Roles of heat shock factor 1 beyond the heat shock response. *Cellular and Molecular Life Sciences*, *75*(16), 2897-2916.

Bauer, K., Rafael, B., Vágó, B., Kiss-Vetráb, S., Molnár, A., Szebenyi, C., et al. (2023). Characterization of the sterol 24-C-methyltransferase genes reveals a network of alternative sterol biosynthetic pathways in *Mucor lusitanicus*. *Microbiology Spectrum*, *11*(3), e0031523.

Beccaccioli, M., Reverberi, M., & Scala, V. (2019). Fungal lipids: biosynthesis and signalling during plant-pathogen interaction. *Frontiers in Bioscience, 24*(1), 172-185.

Bickle, M., Delley, P. A., Schmidt, A., & Hall, M. N. (1998). Cell wall integrity modulates RHO1 activity via the exchange factor ROM2. *The EMBO Journal*, *17*(8), 2235-2245.

Bielawski, J., Pierce, J. S., Snider, J., Rembiesa, B., Szulc, Z. M., & Bielawska, A. (2009). Comprehensive quantitative analysis of bioactive sphingolipids by high-

performance liquid chromatography-tandem mass spectrometry. *Methods in Molecular Biology (Clifton, N.J.)*, *579*, 443-467.

Binder, U., Navarro-Mendoza, M. I., Naschberger, V., Bauer, I., Nicolas, F. E., Pallua, J. D., et al. (2018). Generation of a *Mucor circinelloides* reporter strain – a promising new tool to study antifungal drug efficacy and mucormycosis. *Genes*, *9*(12), 613.

Bleackley, M. R., & MacGillivray, R. T. A. (2011). Transition metal homeostasis: from yeast to human disease. *BioMetals*, *24*(5), 785-809.

Bonner, J. J., Carlson, T., Fackenthal, D. L., Paddock, D., Storey, K., & Lea, K. (2000). Complex regulation of the yeast heat shock transcription factor. *Molecular Biology of the Cell*, *11*(5), 1739-1751.

Borges-Walmsley, M. I., & Walmsley, A. R. (2000). cAMP signalling in pathogenic fungi: control of dimorphic switching and pathogenicity. *Trends in Microbiology*, *8*(3), 133-141.

Borman, A. M., Fraser, M., Patterson, Z., Palmer, M. D., & Johnson, E. M. (2021). *In vitro* antifungal drug resistance profiles of clinically relevant members of the Mucorales (Mucoromycota) especially with the newer triazoles. *Journal of Fungi*, *7*(4), 271.

Botha, A., & du Preez, J. C. (1999). MUCOR. In R. K. Robinson (Ed.), Encyclopedia of Food Microbiology (pp. 1493-1500).

Brandman, O., Stewart-Ornstein, J., Wong, D., Larson, A., Williams, C. C., Li, G. W., et al. (2012). A ribosome-bound quality control complex triggers degradation of nascent peptides and signals translation stress. *Cell*, *151*(5), 1042-1054.

Brown, J. (2005). Zygomycosis: an emerging fungal infection. *American Journal of Health-System Pharmacy*, *62*(24), 2593-2596.

Bulent Ertugrul, M., & Arikan-Akdagli, S. (2014). Mucormycosis. In Ö. Ergönül, F. Can, L. Madoff, & M. Akova (Eds.), *Emerging Infectious Diseases* (pp. 309-321).

Cannon, R. D., Lamping, E., Holmes, A. R., Niimi, K., Baret, P. V., Keniya, M. V., et al. (2009). Efflux-mediated antifungal drug resistance. *Clinical Microbiology Reviews*, *22*(2), 291-321.

Canadell, D., González, A., Casado, C., & Ariño, J. (2015). Functional interactions between potassium and phosphate homeostasis in *Saccharomyces cerevisiae*. *Molecular Microbiology*, *95*(3), 555-572.

Carvalho, A. K. F., Faria, E. L. P., Rivaldi, J. D., Andrade, G. S. S., Oliveira, P. C. de, & Castro, H. F. de. (2015). Performance of whole-cells lipase derived from *Mucor*

circinelloides as a catalyst in the ethanolysis of non-edible vegetable oils under batch and continuous run conditions. *Industrial Crops and Product*s, *67*, 287-294.

Cavalheiro, M., Pais, P., Galocha, M., & Teixeira, M.C. (2018). Host-pathogen interactions mediated by MDR transporters in fungi: as pleiotropic as it gets! *Genes*, *9*(7), 332.

Chamilos, G., Lionakis, M. S., Lewis, R. E., & Kontoyiannis, D. P. (2007). Role of mini-host models in the study of medically important fungi. *Lancet. Infectious Diseases*, *7*(1),42-55.

Chang, Z., & Heitman, J. (2019). Drug-resistant epimutants exhibit organ-specific stability and induction during murine infections caused by the human fungal pathogen *Mucor circinelloides*. *MBio*, *10*(6), e02579-19.

Chayakulkeeree, M., Ghannoum, M. A., & Perfect, J. R. (2006). Zygomycosis: the re-emerging fungal infection. *European Journal of Clinical Microbiology and Infectious Diseases*, *25*(4), 215-229.

Chen, P. W., Fonseca, L. L., Hannun, Y. A., & Voit, E. O. (2013). Coordination of rapid sphingolipid responses to heat stress in yeast. *PLoS Computational Biology*, *9*(5), e1003078.

Clinical and Laboratory Standards Institute (CLSI) (2008) Reference method for broth dilution antifungal susceptibility testing of filamentous fungi; approved standard-2nd ed., M38-A2. Wayne, PA: CLSI.

Corrochano, L.M., Kuo, A., Marcet-Houben, M., Polaino, S., Salamov, A., Villalobos-Escobedo, J.M., et al. (2016). Expansion of signal transduction pathways in fungi by extensive genome duplication. *Current Biology*, *26*(12), 1577-1584.

Costa, C., Pires, C., Cabrito, T. R., Renaudin, A., Ohno, M., Chibana, H., et al. (2013). *Candida glabrata* drug:H+ antiporter CgQdr2 confers imidazole drug resistance, being activated by transcription factor CgPdr1. *Antimicrobial Agents and Chemotherapy*, *57*(7), 3159-3167.

Costa, C., Dias, P. J., Sá-Correia, I., & Teixeira, M. C. (2014). MFS multidrug transporters in pathogenic fungi: Do they have real clinical impact? *Frontiers in Physiology*. *5*, 197.

Costa, C., Ribeiro, J., Miranda, I. M., Silva-Dias, A., Cavalheiro, M., Costa-de-Oliveira, S., et al. (2016). Clotrimazole drug resistance in *Candida glabrata* clinical isolates correlates with increased expression of the drug:H(+) antiporters CgAqr1, CgTpo1_1, CgTpo3, and CgQdr2. *Frontiers in Microbiology*, *7*, 526.

Cócera, M., Lopez, O., Coderch, L., Parra, J. L., & de la Maza, A. (1999). Influence of the level of ceramides on the permeability of stratum corneum lipid

liposomes caused by a C12-betaine/sodium dodecyl sulfate mixture. *International Journal of Pharmaceutics*, *183*(2), 165-173.

Cui Z, Zhang X, Yang H, & Sun L. (2017) Bioremediation of heavy metal pollution utilizing composite microbial agent of *Mucor circinelloides*, *Actinomucor* sp. and *Mortierella* sp. *Journal of Environmental Chemical Engineering*, *5*(4), 3616-3621.

Dhamgaye, S., Devaux, F., Vandeputte, P., Khandelwal, N. K., Sanglard, D., Mukhopadhyay, G., & Prasad, R. (2014). Molecular mechanisms of action of herbal antifungal alkaloid berberine, in *Candida albicans*. *PloS one*, *9*(8), e104554.

Dikicioglu, D., Oc, S., Rash, B. M., Dunn, W. B., Pir, P., Kell, D. B., et al. (2014). Yeast cells with impaired drug resistance accumulate glycerol and glucose. *Molecular BioSystems*, *10*(1), 93-102.

Dotsenko, A. S., Dotsenko, G. S., Senko, O. V., Stepanov, N. A., Lyagin, I. V., Efremenko, E. N., et al. (2018). Complex effect of lignocellulosic biomass pretreatment with 1-butyl-3-methylimidazolium chloride ionic liquid on various aspects of ethanol and fumaric acid production by immobilized cells within SSF. *Bioresource Technology*, *250*, 429-438.

Drogari-Apiranthitou, M., Mantopoulou, F. D., Skiada, A., Kanioura, L., Grammatikou, M., Vrioni, G., et al. (2012). *In vitro* antifungal susceptibility of filamentous fungi causing rare infections: synergy testing of amphotericin B, posaconazole and anidulafungin in pairs. *The Journal of Antimicrobial Chemotherapy*, *67*(8), 1937-1940.

Dumont F. J. (2000). FK506, an immunosuppressant targeting calcineurin function. *Current Medicinal Chemistry*, *7*(7), 731-748.

Elkhateeb, W. A., & Daba, G. M. (2022). Insight into secondary metabolites of *Circinella*, *Mucor* and *Rhizopus* the three musketeers of order Mucorales. *Journal of Biomedical Science*, *41*(2), 32534-32540.

Fabri, J. H. T. M., Rocha, M. C., Fernandes, C. M., Persinoti, G. F., Ries, L. N. A., da Cunha, A. F., et al. (2021). The heat shock transcription factor HsfA is essential for thermotolerance and regulates cell wall integrity in *Aspergillus fumigatus*. *Frontiers in Microbiology*, *12*, 656548.

Fallon, J., Kelly, J., & Kavanagh, K. (2012). *Galleria mellonella* as a model for fungal pathogenicity testing. *Methods in Molecular Biology*, *845*, 469-485.

Feder, M. E., & Hofmann, G. E. (1999). Heat-shock proteins, molecular chaperones, and the stress response: evolutionary and ecological physiology. *Annual Review of Physiology*, *61*, 243-282.

Galocha, M., Costa, I. V., & Teixeira, M. C. (2020). Carrier-mediated drug uptake in fungal pathogens. *Genes*, *11*(11), 1324.

Gao, J., Wang, H., Li, Z., Wong, A. H., Wang, Y. Z., Guo, Y., et al. (2018). *Candida albicans* gains azole resistance by altering sphingolipid composition. *Nature Communications*, *9*(1), 4495.

Gao, X., Fu, Y., Sun, S., Gu, T., Li, Y., & Ding, C. (2022). Cryptococcal Hsf3 controls intramitochondrial ROS homeostasis by regulating the respiratory process. *Nature Communications*, *13*(1), 5407.

García-Ríos, E., López-Malo, M., & Guillamón, J. M. (2014). Global phenotypic and genomic comparison of two *Saccharomyces cerevisiae* wine strains reveals a novel role of the sulfur assimilation pathway in adaptation at low temperature fermentations. *BMC genomics*, *15*(1), 1059.

Gault, C. R., Obeid, L. M., & Hannun, Y. A. (2010). An overview of sphingolipid metabolism: from synthesis to breakdown. *Advances in Experimental Medicine and Biology*, *688*, 1-23.

Gbelska, Y., Krijger, J. J., & Breunig, K. D. (2006). Evolution of gene families: the multidrug resistance transporter genes in five related yeast species. *FEMS Yeast Research*, *6*(3), 345-355.

Gomez-Pastor, R., Burchfiel, E. T., & Thiele, D. J. (2018). Regulation of heat shock transcription factors and their roles in physiology and disease. *Nature Reviews. Molecular Cell Biology*, *19*(1), 4-19.

Hahn, J. S., & Thiele, D. J. (2004). Activation of the *Saccharomyces cerevisiae* heat shock transcription factor under glucose starvation conditions by Snf1 protein kinase. *The Journal of Biological Chemistry*, *279*(7), 5169-5176.

Hamid, M. I., Zeng, F., Cheng, J., Jiang, D., & Fu, Y. (2013). Disruption of heat shock factor 1 reduces the formation of conidia and thermotolerance in the mycoparasitic fungus *Coniothyrium minitans*. *Fungal Genetics and Biology*, *53*, 42-49.

Harris, S. D. (2006). Cell polarity in filamentous fungi: shaping the mold. *International Review of Cytology*, *251*, 41-77.

Hassan, M. I. A., & Voigt, K. (2019). Pathogenicity patterns of mucormycosis: epidemiology, interaction with immune cells and virulence factors. *Medical Mycology*, *57*(2), 245-256.

He, Q., Rajendran, A., Gan, J., Lin, H., Felt, C. A., & Hu, B. (2019). Phosphorus recovery from dairy manure wastewater by fungal biomass treatment. *Water and Environment Journal*, *33*(4), 508-517.

Homa, M., Ibragimova, S., Szebenyi, C., Nagy, G., Zsindely, N., Bodai, L., et al. (2022). Differential gene expression of *Mucor lusitanicus* under aerobic and anaerobic conditions. *Journal of Fungi*, *8*(4), 404.

Hossain, S., Lash, E., Veri, A. O., & Cowen, L. E. (2021). Functional connections between cell cycle and proteostasis in the regulation of *Candida albicans* morphogenesis. *Cell Reports*, *34*(8), 108781.

Huang, Y., Busk, P. K., Grell, M. N., Zhao, H., & Lange, L. (2014). Identification of a β-glucosidase from the *Mucor circinelloides* genome by peptide pattern recognition. *Enzyme and Microbial Technology*, *67*, 47-52.

Hussain, M. K., Ahmed, S., Khan, A., Siddiqui, A. J., Khatoon, S., & Jahan, S. (2023). Mucormycosis: A hidden mystery of fungal infection, possible diagnosis, treatment and development of new therapeutic agents. *European Journal of Medicinal Chemistry*, *246*, 115010.

Ibrahim, A. S., Spellberg, B., Avanessian, V., Fu, Y., & Edwards, J. E., Jr (2005). *Rhizopus oryzae* adheres to, is phagocytosed by, and damages endothelial cells *in vitro*. *Infection and Immunity*, *73*(2), 778-783.

Ibrahim, A. S., & Kontoyiannis, D. P. (2013). Update on mucormycosis pathogenesis. *Current Opinion in Infectious Diseases*, *26*(6), 508-515.

Igual, J. C., Johnson, A. L., & Johnston, L. H. (1996). Coordinated regulation of gene expression by the cell cycle transcription factor Swi4 and the protein kinase C MAP kinase pathway for yeast cell integrity. *The EMBO journal*, *15*(18), 5001-5013.

Jaeger, A. M., Pemble, C. W., 4th, Sistonen, L., & Thiele, D. J. (2016). Structures of HSF2 reveal mechanisms for differential regulation of human heat-shock factors. *Nature Structural & Molecular Biology*, *23*(2), 147-154.

Jakab, Á., Balla, N., Ragyák, Á., Nagy, F., Kovács, F., Sajtos, Z., et al. (2021). Transcriptional profiling of the *Candida auris* response to exogenous farnesol exposure. *mSphere*, *6*(5), e0071021.

Jensen, L. T., Ajua-Alemanji, M., & Culotta, V. C. (2003). The *Saccharomyces cerevisiae* high affinity phosphate transporter encoded by PHO84 also functions in manganese homeostasis. *The Journal of Biological Chemistry*, *278*(43), 42036-42040.

Jeong, W., Keighley, C., Wolfe, R., Lee, W. L., Slavin, M. A., Kong, D. C. M., et al. (2019). The epidemiology and clinical manifestations of mucormycosis: a systematic review and meta-analysis of case reports. *Clinical Microbiology and Infection*, *25*(1), 26-34.

Jestin, M., Azoulay, E., Pène, F., Bruneel, F., Mayaux, J., Murgier, M., et al. (2021). Poor outcome associated with mucormycosis in critically ill hematological patients: results of a multicenter study. *Annals of Intensive Care, 11*(1), 31.

Jones, S., Jedd, G., Kahn, R. A., Franzusoff, A., Bartolini, F., & Segev, N. (1999). Genetic interactions in yeast between Ypt GTPases and Arf guanine nucleotide exchangers. *Genetics, 152*(4), 1543-1556.

Juvvadi, P. R., Lee, S. C., Heitman, J., & Steinbach, W. J. (2017). Calcineurin in fungal virulence and drug resistance: Prospects for harnessing targeted inhibition of calcineurin for an antifungal therapeutic approach. *Virulence, 8*(2), 186-197.

Kahn, R. A., Cherfils, J., Elias, M., Lovering, R. C., Munro, S., & Schurmann, A. (2006). Nomenclature for the human Arf family of GTP-binding proteins: ARF, ARL, and SAR proteins. *The Journal of Cell Biology, 172*(5), 645-650.

Katragkou, A., Walsh, T. J., & Roilides, E. (2014). Why is mucormycosis more difficult to cure than more common mycoses? *Clinical Microbiology and Infection, 20*(6), 74-81.

Kennedy, K. J., Daveson, K., Slavin, M. A., van Hal, S. J., Sorrell, T. C., Lee, A., et al. (2016) Mucormycosis in Australia: contemporary epidemiology and outcomes. *Clinical Microbiology and Infection, 22*(9), 775-781.

Klimek-Ochab, M., Brzezińska-Rodak, M., Zymańczyk-Duda, E., Lejczak, B., & Kafarski, P. (2011). Comparative study of fungal cell disruption – scope and limitations of the methods. *Folia Microbiologica, 56*(5), 469-475.

Kubo, H., & Mihara, H. (2007). cAMP promotes hyphal branching in *Mucor globosus*. *Mycoscience, 48*(3), 187-189.

Lanthaler, K., Bilsland, E., Dobson, P. D., Moss, H. J., Pir, P., Kell, D. B., et al. (2011). Genome-wide assessment of the carriers involved in the cellular uptake of drugs: a model system in yeast. *BMC Biology, 9*, 70.

Lax, C., Pérez-Arques, C., Navarro-Mendoza, M. I., Cánovas-Márquez, J. T., Tahiri, G., Pérez-Ruiz, J. A., et al. (2020). Genes, pathways, and mechanisms involved in the virulence of Mucorales. *Genes, 11*(3), 317.

Law, C. J., Maloney, P. C., & Wang, D. N. (2008). Ins and outs of major facilitator superfamily antiporters. *Annual Review of Microbiology, 62*, 289-305.

Leach, M. D., Budge, S., Walker, L., Munro, C., Cowen, L. E., & Brown, A. J. (2012a). Hsp90 orchestrates transcriptional regulation by Hsf1 and cell wall remodelling by MAPK signaling during thermal adaptation in a pathogenic yeast. *PLoS Pathogens, 8*(12), e1003069.

Leach, M. D., Tyc, K. M., Brown, A. J., & Klipp, E. (2012b). Modelling the regulation of thermal adaptation in *Candida albicans*, a major fungal pathogen of humans. *PloS One*, *7*(3), e32467.

Leach, M. D., & Cowen, L. E. (2013). Surviving the heat of the moment: a fungal pathogens perspective. *PLoS Pathogens*, *9*(3), e1003163.

Leach, M. D., & Cowen, L. E. (2014). Membrane fluidity and temperature sensing are coupled via circuitry comprised of Ole1, Rsp5, and Hsf1 in *Candida albicans*. *Eukaryotic Cell*, *13*(8), 1077-1084.

Leach, M. D., Farrer, R. A., Tan, K., Miao, Z., Walker, L. A., Cuomo, C. A., et al. (2016). Hsf1 and Hsp90 orchestrate temperature-dependent global transcriptional remodelling and chromatin architecture in *Candida albicans*. *Nature Communications*, *7*, 11704.

Lee, S. C., Li, A., Calo, S., & Heitman, J. (2013). Calcineurin plays key roles in the dimorphic transition and virulence of the human pathogenic zygomycete *Mucor circinelloides*. *PLoS Pathogens*, *9*(9), e1003625.

Lee, K. T., Kwon, H., Lee, D., & Bahn, Y. S. (2014). A Nudix hydrolase protein, Ysa1, regulates oxidative stress response and antifungal drug susceptibility in *Cryptococcus neoformans*. *Mycobiology*, *42*(1), 52-58.

Lee, S. C., Li, A., Calo, S., Inoue, M., Tonthat, N. K., Bain, J. M., et al. (2015). Calcineurin orchestrates dimorphic transitions, antifungal drug responses and host-pathogen interactions of the pathogenic mucoralean fungus *Mucor circinelloides*. *Molecular Microbiology*, *97*(5), 844-865.

Li, C. H., Cervantes, M., Springer, D. J., Boekhout, T., Ruiz-Vazquez, R. M., Torres-Martinez, S. R., et al. (2011). Sporangiospore size dimorphism is linked to virulence of *Mucor circinelloides*. *PLoS Pathogens*, *7*(6), e1002086.

Liu, K., Zhang, X., Sumanasekera, C., Lester, R. L., & Dickson, R. C. (2005). Signaling functions for sphingolipid long-chain bases in *Saccharomyces cerevisiae*. *Biochemical Society Transactions*, *33*(5), 1170-1173.

Liu, N. N., Flanagan, P. R., Zeng, J., Jani, N. M., Cardenas, M. E., Moran, G. P., et al. (2017). Phosphate is the third nutrient monitored by TOR in *Candida albicans* and provides a target for fungal-specific indirect TOR inhibition. *Proceedings of the National Academy of Sciences of the United States of America*, *114*(24), 6346-6351.

Liu, N. N., Uppuluri, P., Broggi, A., Besold, A., Ryman, K., Kambara, H., et al. (2018). Intersection of phosphate transport, oxidative stress and TOR signaling in *Candida albicans* virulence. *PLoS Pathogens*, *14*(7), e1007076.

Liu, N. N., Acosta-Zaldívar, M., Qi, W., Diray-Arce, J., Walker, L. A., Kottom, T. J., et al. (2020). Phosphoric metabolites link phosphate import and polysaccharide biosynthesis for *Candida albicans* cell wall maintenance. *mBio*, *11*(2), e03225-19.

Livak, K.J., & Schmittgen, T.D. (2001). Analysis of relative gene expression data using real-time quantitative PCR and the 2-ΔΔct method. *Methods, 25*(4), 402-408.

López-Fernández, L., Sanchis, M., Navarro-Rodríguez, P., Nicolás, F. E., Silva-Franco, F., Guarro, J., et al. (2018). Understanding *Mucor circinelloides* pathogenesis by comparative genomics and phenotypical studies. *Virulence*, *9*(1), 707-720.

Lübbehüsen, T., Polo, V. G., Rossi, S., Nielsen, J., Moreno, S., McIntyre, M., et al. (2004). Protein kinase A is involved in the control of morphology and branching during aerobic growth of *Mucor circinelloides*. *Microbiology*, *150*(1), 143-150.

Ma, T., Li, Y., Lou, Y., Shi, J., Sun, K., Ma, Z., et al. (2022). The drug H^+ antiporter FgQdr2 is essential for multiple drug resistance, ion homeostasis, and pathogenicity in *Fusarium graminearum*. *Journal of Fungi*, *8*(10), 1009.

Madhavan, Y., Sai, K. V., Shanmugam, D. K., Manimaran, A., Guruviah, K., Mohanta, Y. K., et al. (2022). Current treatment options for COVID-19 associated mucormycosis: present status and future perspectives. *Journal of Clinical Medicine*, *11*(13), 3620.

Martinelli, S. D., & Clutterbuck, A. J. (1971). A quantitative survey of conidiation mutants in *Aspergillus nidulans*. *Journal of General Microbiology*, *69*(2), 261-268.

Masser, A. E., Ciccarelli, M., & Andréasson, C. (2020). Hsf1 on a leash – controlling the heat shock response by chaperone titration. *Experimental Cell Research*, *396*(1), 112246.

McIntyre, M., Breum, J., Arnau, J., & Nielsen, J. (2002). Growth physiology and dimorphism of *Mucor circinelloides (syn. racemosus)* during submerged batch cultivation. *Applied Microbiology and Biotechnology*, *58*(4), 495-502.

Mitra, D., Rasmussen, M. L., Chand, P., Chintareddy, V. R., Yao, L., Grewell, D., et al. (2012). Value-added oil and animal feed production from corn-ethanol stillage using the oleaginous fungus *Mucor circinelloides*. *Bioresource Technology*, *107*, 368-375.

Morace, G., & Borghi, E. (2012). Invasive mold infections: virulence and pathogenesis of Mucorales. *International Journal of Microbiology*, *2012*, 349278.

Morin-Sardin, S., Nodet, P., Coton, E., & Jany, J. L. (2017). A Janus-faced fungal genus with human health impact and industrial applications. *Fungal Biology Reviews*. *31*(1), 12-32.

Moriwaki-Takano, M., Iwakura, R., & Hoshino, K. (2021). Dimorphic mechanism on cAMP mediated signal pathway in *Mucor circinelloides*. *Applied Biochemistry and Biotechnology*, *193*(5), 1252-1265.

Muszewska, A., Pawłowska, J., & Krzyściak, P. (2014). Biology, systematics, and clinical manifestations of Zygomycota infections. *European Journal of Clinical Microbiology & Infectious Diseases*, *33*(8), 1273-1287.

Muthu, V., Agarwal, R., Dhooria, S., Sehgal, I. S., Prasad, K. T., Aggarwal, A. N., et al. (2021). Has the mortality from pulmonary mucormycosis changed over time? A systematic review and meta-analysis. *Clinical Microbiology and Infection, 27*(4), 538-549.

Nagy, G., Farkas, A., Csernetics, Á., Bencsik, O., Szekeres, A., Nyilasi, I., et al. (2014). Transcription of the three HMG-CoA reductase genes of *Mucor circinelloides. BMC Microbiology*, *14*, 93.

Nagy, G., Szebenyi, C., Csernetics, Á., Vaz, A. G., Tóth, E. J., Vágvölgyi, C., et al. (2017). Development of a plasmid free CRISPR-Cas9 system for the genetic modification of *Mucor circinelloides*. *Scientific Reports, 7*(1), 16800.

Nagy, G., Vaz, A. G., Szebenyi, C., Takó, M., Tóth, E. J., Csernetics, Á., et al. (2019). CRISPR-Cas9-mediated disruption of the HMG-CoA reductase genes of *Mucor circinelloides* and subcellular localization of the encoded enzymes. *Fungal Genetics and Biology*, *129*, 30-39.

Nagy, G., Kiss, S., Varghese, R., Bauer, K., Szebenyi, C., Kocsubé, S., et al. (2021). Characterization of three pleiotropic drug resistance transporter genes and their participation in the azole resistance of *Mucor circinelloides*. *Frontiers in Cellular and Infection Microbiology*, *11*, 660347.

Nair, R., Shariq, M., Dhamgaye, S., Mukhopadhyay, C. K., Shaikh, S., & Prasad, R. (2017). Non-heat shock responsive roles of HSF1 in *Candida albicans* are essential under iron deprivation and drug defense. *Biochimica et Biophysica Acta. Molecular Cell Research, 1864*(2), 345-354.

Navarro, E., Lorca-Pascual, J. M., Quiles-Rosillo, M. D., Nicolás, F. E., Garre, V., Torres-Martínez, S., et al. (2001). A negative regulator of light-inducible carotenogenesis in *Mucor circinelloides*. *Molecular Genetics and Genomics, 266*(3), 463-470.

Navarro-Mendoza, M. I., Pérez-Arques, C., Murcia, L., Martínez-García, P., Lax, C., Sanchis, M., et al. (2018). Components of a new gene family of ferroxidases involved in virulence are functionally specialized in fungal dimorphism. *Scientific Reports*, *8*(1), 7660.

Navarro-Mendoza, M. I., Pérez-Arques, C., Panchal, S., Nicolás, F. E., Mondo, S. J., Ganguly, P., et al. (2019). Early diverging fungus *Mucor circinelloides* lacks centromeric histone CENP-A and displays a mosaic of point and regional centromeres. *Current Biology: CB*, *29*(22), 3791-3802.e6.

Naz, T., Nosheen, S., Li, S., Nazir, Y., Mustafa, K., Liu, Q., et al. (2020). Comparative analysis of β-carotene production by *Mucor circinelloides* strains CBS 277.49 and WJ11 under light and dark conditions. *Metabolites*, *10*(1), 38.

Neef, D. W., Jaeger, A. M., Gomez-Pastor, R., Willmund, F., Frydman, J., & Thiele, D. J. (2014). A direct regulatory interaction between chaperonin TRiC and stress-responsive transcription factor HSF1. *Cell Reports*, *9*(3), 955-966.

Neudegger, T., Verghese, J., Hayer-Hartl, M., Hartl, F. U., & Bracher, A. (2016). Structure of human heat-shock transcription factor 1 in complex with DNA. *Nature Structural & Molecular Biology*, *23*(2), 140-146.

Nicholls, S., Leach, M. D., Priest, C. L., & Brown, A. J. (2009). Role of the heat shock transcription factor, Hsf1, in a major fungal pathogen that is obligately associated with warm-blooded animals. *Molecular Microbiology*, *74*(4), 844-861.

Nicholls, S., MacCallum, D. M., Kaffarnik, F. A., Selway, L., Peck, S. C., & Brown, A. J. (2011). Activation of the heat shock transcription factor Hsf1 is essential for the full virulence of the fungal pathogen *Candida albicans*. *Fungal Genetics and Biology*, *48*(3), 297-305.

Nicolás, F. E., Torres-Martínez, S., & Ruiz-Vázquez, R. M. (2003). Two classes of small antisense RNAs in fungal RNA silencing triggered by non-integrative transgenes. *The EMBO Journal*, *22*(15), 3983-3991.

Nicolás, F. E., Calo, S., Murcia-Flores, L., Garre, V., Ruiz-Vázquez, R. M., & Torres-Martínez, S. (2008). A RING-finger photocarotenogenic repressor involved in asexual sporulation in *Mucor circinelloides*. *FEMS Microbiology Letters*, *280*(1), 81-88.

Nover, L., Bharti, K., Döring, P., Mishra, S. K., Ganguli, A., & Scharf, K. D. (2001). Arabidopsis and the heat stress transcription factor world: how many heat stress transcription factors do we need? *Cell Stress & Chaperones*, *6*(3), 177-189.

Nunes, P. A., Tenreiro, S., & Sá-Correia, I. (2001). Resistance and adaptation to quinidine in *Saccharomyces cerevisiae*: role of QDR1 (YIL120w), encoding a plasma membrane transporter of the major facilitator superfamily required for multidrug resistance. *Antimicrobial Agents and Chemotherapy*, *45*(5), 1528-1534.

Ocampo, J., Fernandez Nuñez, L., Silva, F., Pereyra, E., Moreno, S., Garre, V., & Rossi, S. (2009). A subunit of protein kinase a regulates growth and differentiation in the fungus *Mucor circinelloides*. *Eukaryotic Cell*, *8*(7), 933-944.

Ocampo, J., McCormack, B., Navarro, E., Moreno, S., Garre, V., & Rossi, S. (2012). Protein kinase A regulatory subunit isoforms regulate growth and differentiation in *Mucor circinelloides*: essential role of PKAR4. *Eukaryotic cell*, *11*(8), 989-1002.

Orlowski M. (1991). *Mucor* dimorphism. *Microbiological Reviews*, *55*(2), 234-258.

Panwar, S. L., Pasrija, R., & Prasad, R. (2008). Membrane homoeostasis and multidrug resistance in yeast. *Bioscience Reports*, *28*(4), 217-228.

Patiño-Medina, J. A., Maldonado-Herrera, G., Pérez-Arques, C., Alejandre-Castañeda, V., Reyes-Mares, N. Y., Valle-Maldonado, M. I., et al. (2018). Control of morphology and virulence by ADP-ribosylation factors (Arf) in *Mucor circinelloides*. *Current Genetics*, *64*(4), 853-869.

Patiño-Medina, J. A., Reyes-Mares, N. Y., Valle-Maldonado, M. I., Jácome-Galarza, I. E., Pérez-Arques, C., Nuñez-Anita, R. E., et al. (2019a). Heterotrimeric G-alpha subunits Gpa11 and Gpa12 define a transduction pathway that control spore size and virulence in *Mucor circinelloides*. *PloS One*, *14*(12), e0226682.

Patiño-Medina, J. A., Valle-Maldonado, M. I., Maldonado-Herrera, G., Pérez-Arques, C., Jácome-Galarza, I. E., Díaz-Pérez, C., et al. (2019b). Role of Arf-like proteins (Arl1 and Arl2) of *Mucor circinelloides* in virulence and antifungal susceptibility. *Fungal genetics and biology: FG & B*, *129*, 40-51.

Paulsen, I. T., Brown, M. H., & Skurray, R. A. (1996). Proton-dependent multidrug efflux systems. *Microbiological Reviews*, *60*(4), 575-608.

Petrikkos, G., Skiada, A., Lortholary, O., Roilides, E., Walsh, T. J., & Kontoyiannis, D. P. (2012). Epidemiology and clinical manifestations of mucormycosis. *Clinical Infectious Diseases*, *54*(1), 23-34.

Pérez-Arques, C., Navarro-Mendoza, M. I., Murcia, L., Lax, C., Martínez-García, P., Heitman, J., et al. (2019). *Mucor circinelloides* thrives inside the phagosome through an Atf-mediated germination pathway. *mBio*, *10*(1), e02765-18.

Pincus, D., Anandhakumar, J., Thiru, P., Guertin, M. J., Erkine, A. M., & Gross, D. S. (2018). Genetic and epigenetic determinants establish a continuum of Hsf1 occupancy and activity across the yeast genome. *Molecular Biology of the Cell*, *29*(26), 3168-3182.

Pirkkala, L., Nykänen, P., & Sistonen, L. (2001). Roles of the heat shock transcription factors in regulation of the heat shock response and beyond. *FASEB Journal: Official Publication of the Federation of American Societies for Experimental Biology*, *15*(7), 1118-1131.

Qadri, H., Haseeb Shah, A., Ahmad Mir, M., Fazal Qureshi, M., & Prasad, R. (2022). Quinidine drug resistance transporter knockout *Candida* cells modulate glucose transporter expression and accumulate metabolites leading to enhanced azole drug resistance. *Fungal Genetics and Biology: FG & B, 161*, 103713.

Redhu, A. K., Shah, A. H., & Prasad, R. (2016). MFS transporters of *Candida* species and their role in clinical drug resistance. *FEMS Yeast Research*, *16*(4), fow043.

Rhome, R., & Del Poeta, M. (2010). Sphingolipid signaling in fungal pathogens. *Advances in Experimental Medicine and Biology*, *688*, 232-237.

Richardson M. (2009). The ecology of the Zygomycetes and its impact on environmental exposure. *Clinical Microbiology and Infection*, *15(5)*, 2-9.

Riley, T. T., Muzny, C. A., Swiatlo, E., & Legendre, D. P. (2016). Breaking the mold: a review of mucormycosis and current pharmacological treatment options. *The Annals of Pharmacotherapy*, *50*(9), 747-757.

Rinaldi, J., Ocampo, J., Rossi, S., & Moreno, S. (2008). A novel activating effect of the regulatory subunit of protein kinase A on catalytic subunit activity. *Archives of Biochemistry and Biophysics*, *480*(2), 95-103.

Rintala, E., Jouhten, P., Toivari, M., Wiebe, M. G., Maaheimo, H., Penttilä, M., et al. (2011). Transcriptional responses of *Saccharomyces cerevisiae* to shift from respiratory and respirofermentative to fully fermentative metabolism. *OMICS: A Journal of Integrative Biology*, 15(7-8), 461-476.

Ríos, G., Cabedo, M., Rull, B., Yenush, L., Serrano, R., & Mulet, J. M. (2013). Role of the yeast multidrug transporter Qdr2 in cation homeostasis and the oxidative stress response. *FEMS Yeast Research*, *13*(1), 97-106.

Rodaki, A., Bohovych, I. M., Enjalbert, B., Young, T., Odds, F. C., Gow, N. A., et al. (2009). Glucose promotes stress resistance in the fungal pathogen *Candida albicans*. *Molecular Biology of the Cell*, *20*(22), 4845-4855.

Roden, M. M., Zaoutis, T. E., Buchanan, W. L., Knudsen, T. A., Sarkisova, T. A., Schaufele, R. L., et al. (2005). Epidemiology and outcome of zygomycosis: a review of 929 reported cases. *Clinical infectious diseases: an official publication of the Infectious Diseases Society of America*, *41*(5), 634-653.

Rodríguez-Frómeta, R. A., Gutiérrez, A., Torres-Martínez, S., & Garre, V. (2013). Malic enzyme activity is not the only bottleneck for lipid accumulation in the oleaginous fungus *Mucor circinelloides*. *Applied Microbiology and Biotechnology*, *97*(7), 3063-3072.

Sakurai, H., & Enoki, Y. (2010). Novel aspects of heat shock factors: DNA recognition, chromatin modulation and gene expression. *The FEBS journal*, *277*(20), 4140-4149.

Salazar, S. B., Pinheiro, M. J. F., Sotti-Novais, D., Soares, A. R., Lopes, M. M., Ferreira, T., Rodrigues, V., et al. (2022). Disclosing azole resistance mechanisms in resistant *Candida glabrata* strains encoding wild-type or gain-of-function CgPDR1 alleles through comparative genomics and transcriptomics. *G3: Genes|Genomes|Genetics*, *12*(7), jkac110.

Sambrook, J., & Russel, D. W. (2001). Molecular cloning: a laboratory manual, 3rd ed., Cold Spring Harbor Laboratory Press, Cold Spring Harbor, N.Y. *Zool. Res.*, Vol. 1.

Sankaran, S., Khanal, S. K., Jasti, N. V. K., Jin, B., Pometto, A. L., & van Leeuwen, J. H. (2010). Use of filamentous fungi for wastewater treatment and production of high value fungal byproducts: a review. *Critical Reviews in Environmental Science and Technology*, *40*, 400-449.

Santos, R., Cavalheiro, M., Costa, C., Takahashi-Nakaguchi, A., Okamoto, M., Chibana, H., et al. (2020). Screening the drug:H^+ antiporter family for a role in biofilm formation in *Candida glabrata*. *Frontiers in Cellular and Infection Microbiology*, *10*, 29.

Sathya, R., Pradeep, B. V., Angayarkanni, J., & Palaniswamy, M. (2009). Production of milk clotting protease by a local isolate of *Mucor circinelloides* under SSF using agro-industrial wastes. *Biotechnology and Bioprocess Engineering*, *14*(6), 788-794.

Sá-Correia, I., dos Santos, S. C., Teixeira, M. C., Cabrito, T. R., & Mira, N. P. (2009). Drug:H+ antiporters in chemical stress response in yeast. *Trends in Microbiology*, *17*(1), 22-31.

Serrano, I., Lopes da Silva, T., & Carlos Roseiro, J. (2001). Ethanol-induced dimorphism and lipid composition changes in *Mucor fragilis* CCMI 142. *Letters in Applied Microbiology*, *33*(1), 89-93.

Shah, A. H., Singh, A., Dhamgaye, S., Chauhan, N., Vandeputte, P., Suneetha, K. J., et al. (2014). Novel role of a family of major facilitator transporters in biofilm development and virulence of *Candida albicans*. *The Biochemical Journal*, *460*(2), 223-235.

Shahi, P., & Moye-Rowley, W. S. (2009). Coordinate control of lipid composition and drug transport activities is required for normal multidrug resistance in fungi. *Biochimica et Biophysica Acta*, *1794*(5), 852-859.

Shimizu, M., Masuo, S., Fujita, T., Doi, Y., Kamimura, Y., & Takaya, N. (2012). Hydrolase controls cellular NAD, sirtuin, and secondary metabolites. *Molecular and Cellular Biology*, *32*(18), 3743-3755.

Shimizu, M., & Takaya, N. (2013). Nudix hydrolase controls nucleotides and glycolytic mechanisms in hypoxic *Aspergillus nidulans*. *Bioscience, Biotechnology, and Biochemistry*, *77*(9), 1888-1893.

Shimonaka, A., Koga, J., Baba, Y., Nishimura, T., Murashima, K., Kubota, H., et al. (2006). Specific characteristics of family 45 endoglucanases from Mucorales in the use of textiles and laundry. *Bioscience, Biotechnology, and Biochemistry*, *70*(4), 1013-1016.

Schwartze, V. U., Winter, S., Shelest, E., Marcet-Houben, M., Horn, F., Wehner, S., et al. (2014). Gene expansion shapes genome architecture in the human pathogen *Lichtheimia corymbifera*: an evolutionary genomics analysis in the ancient terrestrial Mucorales (Mucoromycotina). PLoS genetics, 10(8), e1004496.

Silva, F., Torres-Martínez, S., & Garre, V. (2006). Distinct white collar-1 genes control specific light responses in *Mucor circinelloides*. *Molecular Microbiology*, *61*(4), 1023-1037.

Silva, F., Navarro, E., Peñaranda, A., Murcia-Flores, L., Torres-Martínez, S., & Garre, V. (2008). A RING-finger protein regulates carotenogenesis via proteolysis-independent ubiquitylation of a white collar-1-like activator. *Molecular Microbiology*, *70*(4), 1026-1036.

Skiada, A., Lass-Floerl, C., Klimko, N., Ibrahim, A., Roilides, E., & Petrikkos, G. (2018). Challenges in the diagnosis and treatment of mucormycosis. *Medical Mycology*, *56*(1), 93-101.

Smith, C., & Lee, S. C. (2022). Current treatments against mucormycosis and future directions. *PLoS Pathogens*, *18*(10), e1010858.

Solís, E. J., Pandey, J. P., Zheng, X., Jin, D. X., Gupta, P. B., Airoldi, E. M., et al. (2016). Defining the essential function of yeast Hsf1 reveals a compact transcriptional program for maintaining eukaryotic proteostasis. *Molecular Cell*, *63*(1), 60-71.

Spatafora, J. W., Chang, Y., Benny, G. L., Lazarus, K., Smith, M. E., Berbee, M. L., et al. (2016). A phylum-level phylogenetic classification of zygomycete fungi based on genome-scale data. *Mycologia*, *108*(5), 1028-1046.

Spellberg, B., Edwards, J., Jr, & Ibrahim, A. (2005). Novel perspectives on mucormycosis: pathophysiology, presentation, and management. *Clinical Microbiology Reviews*, *18*(3), 556-569.

Stolz, J., & Sauer, N. (1999). The fenpropimorph resistance gene FEN2 from *Saccharomyces cerevisiae* encodes a plasma membrane H+-pantothenate symporter. *The Journal of Biological Chemistry, 274*(26), 18747-18752.

Sueiro-Olivares, M., Fernandez-Molina, J. V., Abad-Diaz-de-Cerio, A., Gorospe, E., Pascual, E., Guruceaga, X., et al. (2015). *Aspergillus fumigatus* transcriptome response to a higher temperature during the earliest steps of germination monitored using a new customized expression microarray. *Microbiology*, *161*(3), 490-502.

Sugiyama, K., Izawa, S., & Inoue, Y. (2000). The Yap1p-dependent induction of glutathione synthesis in heat shock response of *Saccharomyces cerevisiae*. *The Journal of Biological Chemistry*, *275*(20), 15535-15540.

Szczęsna-Antczak, M., Antczak, T., Piotrowicz-Wasiak, M., Rzyska, M., Binkowska, N., & Bielecki, S. (2006). Relationships between lipases and lipids in mycelia of two *Mucor* strains. *Enzyme and Microbial Technology*, 39(6), 1214-1222.

Szczęsna-Antczak, M., Szeląg, J., Stańczyk, Ł., Borowska, A., & Antczak, T. (2016). Engineering of lipase-catalyzed transesterification reaction media using water and diethylamine. *Biocatalysis and Biotransformation*, *34*(6), 253-264.

Tahiri, G., Lax, C., Cánovas-Márquez, J. T., Carrillo-Marín, P., Sanchis, M., Navarro, E., et al. (2023). Mucorales and mucormycosis: recent insights and prospects. *Journal of Fungi*, *9*(3), 335.

Takano, M., & Hoshino, K. (2012). Direct ethanol production from rice straw by coculture with two high-performing fungi. *Frontiers of Chemical Science and Engineering*, *6*, 139-145.

Taylor, S. S., Knighton, D. R., Zheng, J., Ten Eyck, L. F., & Sowadski, J. M. (1992). Structural framework for the protein kinase family. *Annual Review of Cell Biology*, *8*, 429-462.

Teixeira, M. C., Cabrito, T. R., Hanif, Z. M., Vargas, R. C., Tenreiro, S., & Sá-Correia, I. (2011). Yeast response and tolerance to polyamine toxicity involving the drug:H+ antiporter Qdr3 and the transcription factors Yap1 and Gcn4. *Microbiology*, *157*(4), 945-956.

Tenreiro, S., Vargas, R. C., Teixeira, M. C., Magnani, C., & Sá-Correia, I. (2005). The yeast multidrug transporter Qdr3 (Ybr043c): localization and role as a determinant of resistance to quinidine, barban, cisplatin, and bleomycin. *Biochemical and Biophysical Research Communications*, *327*(3), 952-959.

Thanh, V. N., Mai, leT., & Tuan, D. A. (2008). Microbial diversity of traditional Vietnamese alcohol fermentation starters (banh men) as determined by PCR-mediated DGGE. *International Journal of Food Microbiology*, *128*(2), 268-273.

Thompson, S., Croft, N. J., Sotiriou, A., Piggins, H. D., & Crosthwaite, S. K. (2008). *Neurospora crassa* heat shock factor 1 is an essential gene; a second heat shock factor-like gene, *hsf2*, is required for asexual spore formation. *Eukaryotic Cell*, *7*(9), 1573-1581.

Tiwari, S., Thakur, R., & Shankar, J. (2015). Role of heat-shock proteins in cellular function and in the biology of fungi. *Biotechnology Research International*, *2015*, 132635.

Torres-Martínez, S., & Ruiz-Vázquez, R. M. (2016). RNAi pathways in *Mucor*: A tale of proteins, small RNAs and functional diversity. *Fungal Genetics and Biology: FG & B*, *90*, 44-52.

Trieu, T. A., Calo, S., Nicolás, F. E., Vila, A., Moxon, S., Dalmay, T., et al. (2015). A non-canonical RNA silencing pathway promotes mRNA degradation in basal Fungi. *PLoS Genetics*, *11*(4), e1005168.

Trieu, T. A., Navarro-Mendoza, M. I., Pérez-Arques, C., Sanchis, M., Capilla, J., Navarro-Rodriguez, P., et al. (2017). RNAi-based functional genomics identifies new virulence determinants in mucormycosis. *PLoS Pathogens*, *13*(1), e1006150.

Valle-Maldonado, M. I., Jácome-Galarza, I. E., Díaz-Pérez, A. L., Martínez-Cadena, G., Campos-García, J., Ramírez-Díaz, M. I., et al. (2015). Phylogenetic analysis of fungal heterotrimeric G protein-encoding genes and their expression during dimorphism in *Mucor circinelloides*. *Fungal Biology*, *119*(12), 1179-1193.

Valle-Maldonado, M. I., Patiño-Medina, J. A., Pérez-Arques, C., Reyes-Mares, N. Y., Jácome-Galarza, I. E., Ortíz-Alvarado, R., et al. (2020). The heterotrimeric G-protein beta subunit Gpb1 controls hyphal growth under low oxygen conditions through the protein kinase A pathway and is essential for virulence in the fungus *Mucor circinelloides*. *Cellular Microbiology*, *22*(10), e13236.

van Heeswijck, R., & Roncero, M. I. G. (1984). High frequency transformation of *Mucor* with recombinant plasmid DNA. *Carlsberg Research Communications*, *49*, 691-702.

Vargas, R. C., Tenreiro, S., Teixeira, M. C., Fernandes, A. R., & Sá-Correia, I. (2004). *Saccharomyces cerevisiae* multidrug transporter Qdr2p (Yil121wp): localization and function as a quinidine resistance determinant. *Antimicrobial Agents and Chemotherapy*, *48*(7), 2531-2537.

Vargas, R. C., García-Salcedo, R., Tenreiro, S., Teixeira, M. C., Fernandes, A. R., Ramos, J., et al. (2007). *Saccharomyces cerevisiae* multidrug resistance transporter Qdr2 is implicated in potassium uptake, providing a physiological advantage to quinidine-stressed cells. *Eukaryotic Cell*, *6*(2), 134-142.

Vellanki, S., Garcia, A. E., & Lee, S. C. (2020). Interactions of FK506 and rapamycin with FK506 binding protein 12 in opportunistic human fungal pathogens. *Frontiers in Molecular Biosciences, 7*, 588913.

Verghese, J., Abrams, J., Wang, Y., & Morano, K. A. (2012). Biology of the heat shock response and protein chaperones: budding yeast (*Saccharomyces cerevisiae*) as a model system. *Microbiology and Molecular Biology Reviews, 76*(2), 115-158.

Veri, A. O., Robbins, N., & Cowen, L. E. (2018). Regulation of the heat shock transcription factor Hsf1 in fungi: implications for temperature-dependent virulence traits. *FEMS Yeast Research, 18*(5), foy041.

Vicente, G., Bautista, L. F., Rodríguez, R., Gutiérrez, F. J., Sádaba, I., Ruiz-Vázquez, R. M., et al. (2009). Biodiesel production from biomass of an oleaginous fungus. *Biochemical Engineering Journal, 48*.

Walther, G., Wagner, L., & Kurzai, O. (2019). Updates on the taxonomy of Mucorales with an emphasis on clinically important taxa. *Journal of Fungi, 5*(4), 106.

Watkins, T. N., Gebremariam, T., Swidergall, M., Shetty, A. C., Graf, K. T., Alqarihi, A., et al. (2018). Inhibition of EGFR signaling protects from mucormycosis. *mBio, 9*(4), e01384-18.

Widiasih Widiyanto, T., Chen, X., Iwatani, S., Chibana, H., & Kajiwara, S. (2019). Role of major facilitator superfamily transporter Qdr2p in biofilm formation by *Candida glabrata*. *Mycoses, 62*(12), 1154-1163.

Wiederrecht, G., Seto, D., & Parker, C. S. (1988). Isolation of the gene encoding the *S. cerevisiae* heat shock transcription factor. *Cell, 54*(6), 841-853.

Wolff, A. M., Appel, K. F., Petersen, J. B., Poulsen, U., & Arnau, J. (2002). Identification and analysis of genes involved in the control of dimorphism in *Mucor circinelloides* (syn. *racemosus*). *FEMS Yeast Research, 2*(2), 203-213.

Xiao, W., Zhang, J., Huang, J., Xin, C., Li, M. J., & Song, Z. (2022). Response and regulatory mechanisms of heat resistance in pathogenic fungi. *Applied Microbiology and Biotechnology, 106*(17), 5415-5431.

Yamamoto, A., Mizukami, Y., & Sakurai, H. (2005). Identification of a novel class of target genes and a novel type of binding sequence of heat shock transcription factor in *Saccharomyces cerevisiae*. *The Journal of Biological Chemistry, 280*(12), 11911-11919.

Yang, D. H., Jung, K. W., Bang, S., Lee, J. W., Song, M. H., Floyd-Averette, A., et al. (2017). Rewiring of signaling networks modulating thermotolerance in the human pathogen *Cryptococcus neoformans*. *Genetics, 205*(1), 201-219.

Ye, Y., Gan, J., & Hu, B. (2015). Screening of phosphorus-accumulating fungi and their potential for phosphorus removal from waste streams. *Applied Biochemistry and Biotechnology, 177*(5), 1127-1136.

Zan, X., Tang, X., Chu, L., Zhao, L., Chen, H., Chen, Y. Q., et al. (2016a). Lipase genes in *Mucor circinelloides*: identification, sub-cellular location, phylogenetic analysis and expression profiling during growth and lipid accumulation. *Journal of Industrial Microbiology & Biotechnology, 43*(10), 1467-1480.

Zan, X., Tang, X., Zhao, L., Chu, L., Chen, H., Chen, W., et al. (2016b). Bioinformatical analysis and preliminary study of the role of lipase in lipid metabolism in *Mucor circinelloides*. *RSC Advances, 6*(65), 60673-60682.

Zähringer, H., Thevelein, J. M., & Nwaka, S. (2000). Induction of neutral trehalase Nth1 by heat and osmotic stress is controlled by STRE elements and Msn2/Msn4 transcription factors: variations of PKA effect during stress and growth. *Molecular Microbiology, 35*(2), 397-406.

Zhai, P., Song, J., Gao, L., & Lu, L. (2019). A sphingolipid synthesis-related protein OrmA in *Aspergillus fumigatus* is responsible for azole susceptibility and virulence. *Cellular Microbiology, 21*(12), e13092.

Zhang, Y., Navarro, E., Cánovas-Márquez, J. T., Almagro, L., Chen, H., Chen, Y. Q., et al. (2016). A new regulatory mechanism controlling carotenogenesis in the fungus *Mucor circinelloides* as a target to generate β-carotene over-producing strains by genetic engineering. *Microbial Cell Factories, 15*, 99.

Zhang, X., Yang, H., & Cui, Z. (2017). *Mucor circinelloides*: efficiency of bioremediation response to heavy metal pollution. *Toxicology Research, 6*(4), 442-447.

Zhao, L., Cánovas-Márquez, J. T., Tang, X., Chen, H., Chen, Y. Q., Chen, W., et al. (2016). Role of malate transporter in lipid accumulation of oleaginous fungus *Mucor circinelloides*. *Applied Microbiology and Biotechnology, 100*(3), 1297-1305.

Zheng, X., Krakowiak, J., Patel, N., Beyzavi, A., Ezike, J., Khalil, A. S., et al. (2016). Dynamic control of Hsf1 during heat shock by a chaperone switch and phosphorylation. *eLife, 5*, e18638.

Zhou, G., Ying, S. H., Hu, Y., Fang, X., Feng, M. G., & Wang, J. (2018). Roles of three HSF domain-containing proteins in mediating heat-shock protein genes and sustaining asexual cycle, stress tolerance, and virulence in *Beauveria bassiana*. *Frontiers in Microbiology, 9*, 1677.

10. LIST OF PUBLICATIONS

Full papers

Homa, M., **Ibragimova, S.,** Szebenyi, C., Nagy, G., Zsindely, N., Bodai, L., et al. (2022). Differential gene expression of *Mucor lusitanicus* under aerobic and anaerobic conditions. *Journal of Fungi*, *8*(4), 404.

Ibragimova, S., Szebenyi, C., Sinka, R., Alzyoud, E. I., Homa, M., Vágvölgyi, C., et al. (2020). CRISPR-Cas9-based mutagenesis of the mucormycosis-causing fungus *Lichtheimia corymbifera. International Journal of Molecular Sciences*, *21*(10), 3727.

Abstracts

Ibragimova, S., Vágvölgyi, C., Nagy, G., Papp, T. (2023). Characterization of the *qdr2* multidrug transporter genes of *Mucor lusitanicus.* 16th European Conference on Fungal Genetics programme & abstracts book, 854-855.

Ibragimova, S. (2021). Development of a novel method for genetic modification of *Lichtheimia corymbifera*. In K., Márialigeti; O., Dobay, Eds., *Acta Microbiol et Immunol Hung Budapest, Hungary: Akadémiai Kiadó,* 72.

Nagy, G., Kiss, S., Szebenyi, C., Verghase, R., Vaz, A. G., Jáger, O., **Ibragimova, S.,** Gu, Y., Ibrahim, A. D., Vágvölgyi, C, et al. (2020). Construction of a mutant library to examine the pathogenicity of *Mucor circinelloides* using CRISPR/Cas9 system. *Fungal Genetics, Host Pathogen Interaction and Evolutionary Ecology*, 289-290.

Nagy, G., Szebenyi, C., Vaz, A. G., Jáger, O., **Ibragimova, S.,** Gu, Y., Ibrahim, A. S., Vágvölgyi, C., et al. (2019). Development of a plasmid free CRISPR/Cas9 system for the genetic modification of opportunistic pathogenic Mucormycotina species. In K., Márialigeti; O., Dobay, Eds., *Acta Microbiol Immunol Hung Budapest, Hungary: Akadémiai Kiadó*, 169.

Vágvölgyi, C., **Ibragimova, S.,** Szebenyi, C., Nagy, G., Papp, T. (2018). Construction of an uracil auxotrophic mutant of the opportunistic pathogen *Lichtheimia corymbifera* using an *in vitro* CRISPR/Cas9 method. *Romanian Journal of Laboratory Medicine*. *26*(3), 57.

11. SUPPLEMENTARY MATERIALS

Table S1: Primers used in the experiments. Primer names, sequences, usage, and the expected size of amplicons are shown in the table.

Name of the primer	Sequence 5'-3'	Length of the amplicon (bp)	Used for
Mc123815P1 (promoter)	TTGCCGTTTCTCAACAATCTC	1338	Primers to construct the disruption cassette for *hsf1*
Mc123815P2 (promoter)	TTTGCTGATGAATGTGCTGAC		
Mc123815P3 (*pyrG*)	CTGCCAAGAGAGGTGTCAGCACATTCA TCAGCAAATGCCTCAGCATTGGTACTTG	2005	
Mc123815P4 (*pyrG*)	CCATGGCAAATGAAGCATGGATATCAC CAGTTTCGGTACACTGGCCATGCTATCG		
Mc123815P5 (terminator)	CGAAACTGGTGATATCCATGCT	1337	
Mc123815P6 (terminator)	CGTATTGCCTAAAGATGAGAAACC		
Mc123815P7 (nested)	CATTGGATACCTGCAAAGTG	4315	
Mc123815P8 (nested)	GATTTCAAGGTGATTAGAGCAG		
Mc125667P1 (promoter)	TGTTCATACTTGGTCTCATCCTACC	1358	Primers to construct the disruption cassette for *hsf2*
Mc125667P2 (promoter)	GTAGTCTTCTTGCCTGTTGTG		
Mc125667P3 (*pyrG*)	TCACTGCCCAAGCCCACAACAGGCAAG AAGACTACTGCCTCAGCATTGGTACTTG	2075	
Mc125667P4 (*pyrG*)	TCCATTGGATGCTTTGTGATGAAGTGTA GGCGAGGGTACACTGGCCATGCTATCG		
Mc125667P5 (terminator)	CCTCGCCTACACTTCATCAC	1241	
Mc125667P6 (terminator)	GAACAATGCTTCTCCAGTATGTC		
Mc125667P7 (nested)	GTTGCTGAACTTTATTGGACTCTC	4422	
Mc125667P8 (nested)	GTGTAAGTGAGTCATATCGCCTG		
Mc42380P1 (promoter)	CTTGTGCTCGGAATGATGAATAGTC	1328	Primers to construct the disruption
Mc42380P2 (promoter)	GATGTTGCCTGCTTGTCGTG		

Mc42380P3 (*pyrG*)	CCCTGGATATTCATGCACGACAAGCAG GCAACATCTGCCTCAGCATTGGTACTTG	2075	cassette for *qdr2a*
Mc42380P4 (*pyrG*)	GTAAGCAAACCTCCGTAGTAGATACAT GGTACTCGGTACACTGGCCATGCTATCG		
Mc42380P5 (terminator)	CGAGTACCATGTATCTACTACGG	1439	
Mc42380P6 (terminator)	GTTGCATGTCTCCATACTTACCA		
Mc42380P7 (nested)	GTATCGAAACACCCAAGGAG	4373	
Mc42380P8 (nested)	ATCTGAACGAACAACCAATGTC		
Mc138979P1 (promoter)	CATACGAGCAGGGAAGACAG	1421	Primers to construct the disruption cassette for *qdr2b*
Mc138979P2 (promoter)	TGAAATATAGCCAAAGAAACCCACC		
Mc138979P3 (*pyrG*)	ATGTCTTTTTGGTGGGTTTCTTTGGCTA TATTTCATGCCTCAGCATTGGTACTTG	2075	
Mc138979P4 (*pyrG*)	GTTTGACAATTATCAGAAAGAAAGCGTA AATGTCGGTACACTGGCCATGCTATCG		
Mc138979P5 (terminator)	CGACATTTACGCTTTCTTTCTG	1346	
Mc138979P6 (terminator)	CATGTATGGGATCGGTTGGT		
Mc138979P7 (nested)	GAAGAGCCATACCTACCACAC	4471	
Mc138979P8 (nested)	TATAGTAATTTGCTGATCGCTCCTG		
Mc152822P1 (promoter)	AATCCAAACCGCCAATCATCC	1305	Primers to construct the disruption cassette for *qdr2c*
Mc152822P2 (promoter)	GCTGTTCAACATCAACATCGT		
Mc152822P3 (*pyrG*)	CACAATGACAGCCTACGATGTTGATGT TGAACAGCTGCCTCAGCATTGGTACTTG	2075	
Mc152822P4 (*pyrG*)	TCAATCTCACAAGCAGACTAATACAAG GCACTCAAGTACACTGGCCATGCTATCG		
Mc152822P5 (terminator)	TTGAGTGCCTTGTATTAGTCTG	1315	
Mc152822P6 (terminator)	ACACAATAACCCTCTCACAC		

Mc152822P7 (nested)	ATACATCAGCATCGTCCGTC	4388	
Mc152822P8 (nested)	ACCCTCACTACTATACATTAACCC		
Mc160673P1 (promoter)	TGCCTTCTATTACAAGACCAG	1346	Primers to construct the disruption cassette for *qdr2d*
Mc160673P2 (promoter)	CATATCACAGCTTCAAGACGA		
Mc160673P3 (*pyrG*)	GTCTTTTTTTCATCTCGTCTTGAAGCTG TGATATGTGCCTCAGCATTGGTACTTG	2075	
Mc160673P4 (*pyrG*)	TTTTATTTTACCCTCGATAATGAACAGA TCTAGCCGTACACTGGCCATGCTATCG		
Mc160673P5 (terminator)	GGCTAGATCTGTTCATTATCGAGG	1120	
Mc160673P6 (terminator)	AGATGACCAAGATGAAGATGAAGAC		
Mc160673P7 (nested)	GGCTTCCATATCGTTTACCAC	4167	
Mc160673P8 (nested)	CAACAACAGACTCAATTTAGCC		
Mc123815rtfw	CCTGAACACTTCAAGCATTCC	123	Primers for qRT-PCR analysis
Mc123815rtrev	CTCCCAGATTTCGTTCTCGT		
Mc125667rtfw	CAAAGTCGATTCTTCCAAAGCA	121	
Mc125667rtrev	CCATACAGTTTATTGGTTTCATCGG		
Mc154932rtfw	AACAAGGTGCTGATGCTCTC	142	
Mc154932rtrev	TGACATTCTCGACCTCAACAC		
Mc155237rtfw	TGCTGTCTTCCGTACTTGTG	263	
Mc155237rtrev	CGATGAAGGTGGTAGTGTTGG		
Mc156313rtfw	TTTGTCCTGCCTGATTTCCC	114	
Mc156313rtrev	GTTCAATCCAGAGACCACACC		
Mc42380rtfw	ACCATACCAAAGAGACCATCC	141	
Mc42380rtrev	CAATACCCACAATCACAGCC		
Mc138979rtfw	CTGCGACCAATACATTACTCGT	244	
Mc138979rtrev	GTAAACAGCCATCCTACACCC		
Mc152822rtfw	AGAAACACCAAGAGCAACCT	287	
Mc152822rtrev	ACAATAACTACCCAAGATACAGCC		
Mc160673rtfw	GCACCGTTCATCTACTTGACAG	192	
Mc160673rtrev	GACAAACGATCCAATGATAGAGCC		
McActinF	CACTCCTTCACTACCACCGCTGA		
McActinR	GAGAGCAGAGGATTGAGCAGCAG		

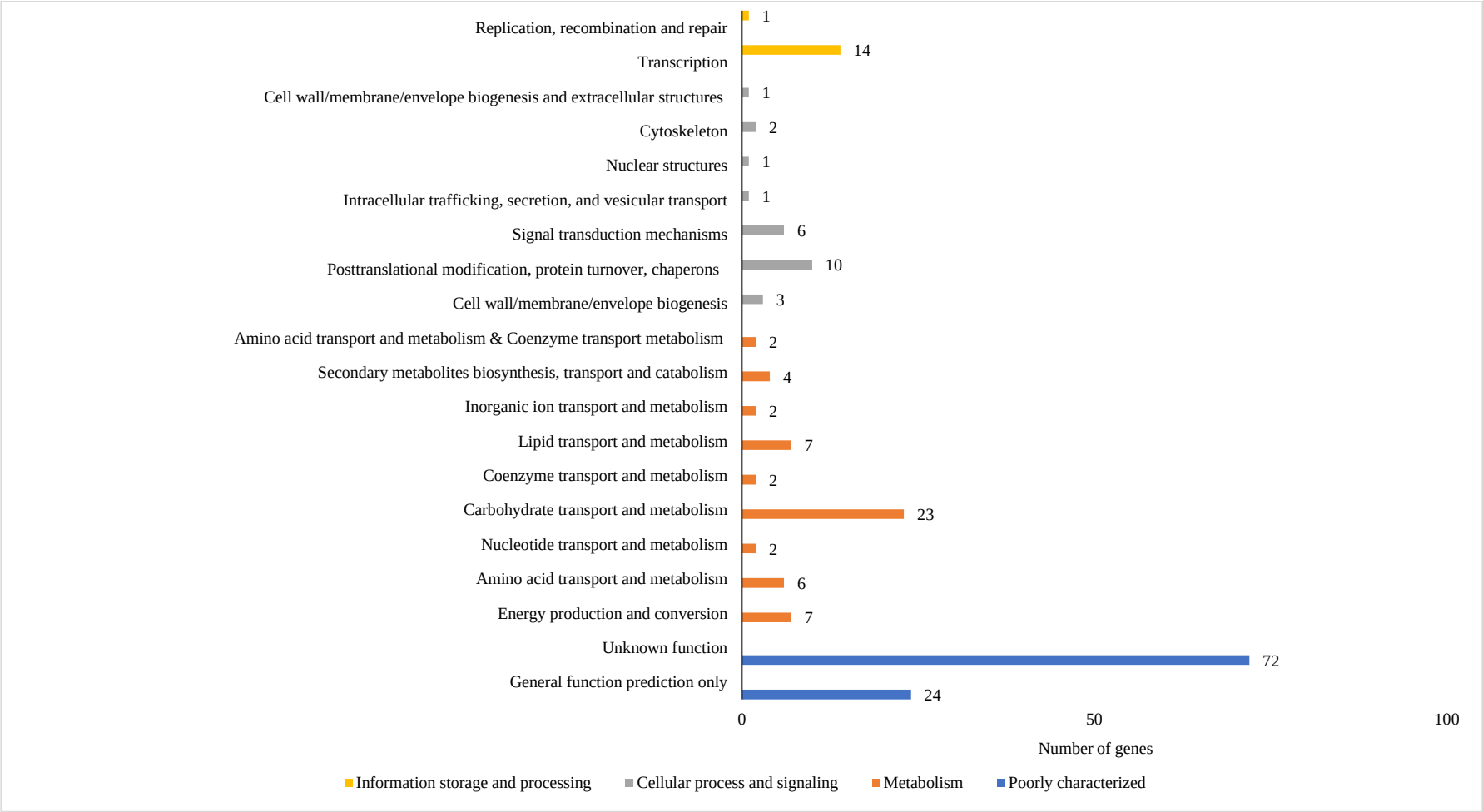

Figure S1. Differentially upregulated genes of *M. lusitanicus* grown anaerobically and their distribution among the main functional categories of the genes.

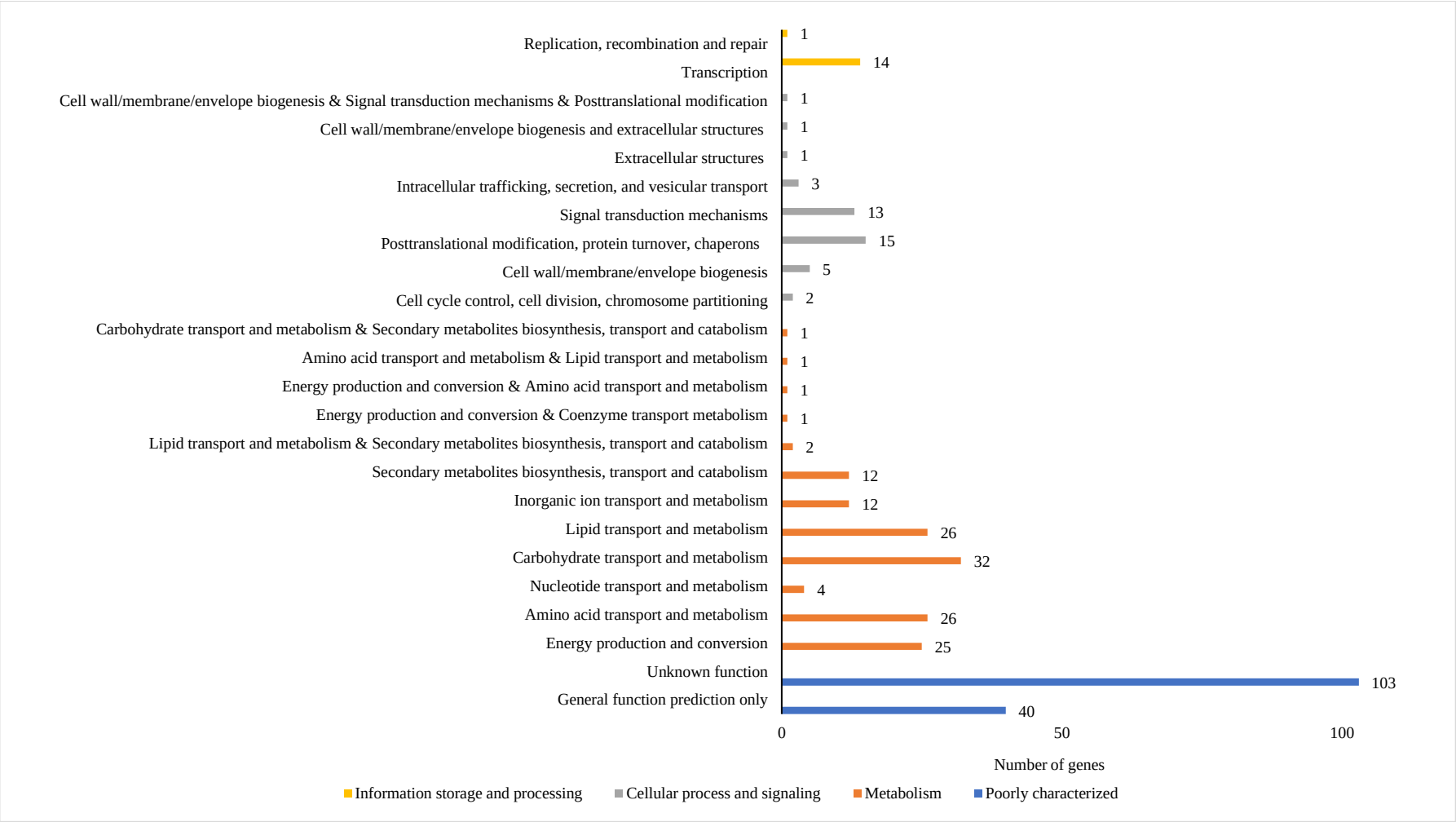

Figure S2. Differentially downregulated genes of *M. lusitanicus* grown anaerobically and their distribution among the main functional categories of the genes.